Electrochemical Degradation of GenX – Study on the Contribution of Electrooxidation and Electroreduction

Presented by

Kara A. Hughes

A thesis submitted to McGill University in partial fulfillment of the requirements of the degree of Doctor of Philosophy

Department of Chemical Engineering

McGill University

Montreal, Quebec, Canada

November 2024

Table of Contents

List of Figures

List of Tables

Abstract

Per- and polyfluoro alkylated substances (PFAS) are well known for their recalcitrant nature caused by the abundance of C-F bonds. It has been proven for some PFAS that electrochemical degradation is a potentially suitable technique for their treatment; however, most studies solely focus on electrochemical oxidation, with limited attention given to electrochemical reduction, and the relative contribution of the two towards the total PFAS degradation has not yet been elucidated.

The aim of this thesis was to investigate the electrodegradation of a target PFAS, hexafluoropropylene oxide dimer acid (HFPO-DA or GenX), and the contribution of electroreduction to the overall removal. Commercial boron doped diamond (BDD) was used as an anode. Several different cathode materials were screened (stainless steel, copper, tin, gold, titanium, graphite and BDD), and copper was determined to be the best-performing one. The oxidation and reduction reactions were successfully decoupled from each other and studied simultaneously using a divided cell in which the two electrolyte/electrode compartments were separated by a membrane.

The experiments demonstrated that GenX can be degraded to concentrations below limits of detection (<7.5 µg/L) in both the divided and undivided cells. It was determined that reduction plays a significant role in the overall degradation of GenX for all of the current densities studied. The general trend of the contribution of reduction decreased with increasing current density up to 50 mA/cm^2, and then again increased at 100 mA/cm^2 (48.4% at 13.5 mA/cm^2, 37.7% at 20 mA/cm^2, 6.8% at 50 mA/cm^2 and 21.9% at 100 mA/cm^2).

Studies into the electrolyte anion influence in the degradation experiments showed that there is no statistical difference when Na_2SO_4, NaCl or both salts are present in the electrolyte when reducing GenX in a divided cell. However, in the oxidation compartment, 0.22 M of Na_2SO_4 and 0.22 M NaCl individually led to slightly better GenX degradation than 0.10 M Na_2SO_4 and 0.12 M NaCl together. Furthermore, electrooxidation of GenX was lower in 0.12 M NaCl compared to 0.10 M Na_2SO_4, the latter of which was the same as when both salts were used. These results indicated that GenX degradation is driven by direct electron transfer on the anode and that active chlorine species produced from chloride oxidation on the anode do not affect the oxidation of GenX

Furthermore, degradation experiments were performed using real water matrices (surface water, wastewater and drinking water) spiked with GenX. The experiments showed that GenX could be electrochemically degraded in these more complex water matrices even at a faster rate than when using an electrolyte consisting of aqueous 0.10 M Na_2SO_4 and 0.12 M NaCl.

Potential transformation products were also investigated in order to assess if GenX electrochemical degradation mechanisms proposed in literature are applicable to what was observed in this thesis work. Several products reported in literature were identified from the divided and undivided cell, which supported the mechanisms proposed. Acute toxicity measurements assessed by Microtox BioAssay before treatment indicated an EC50 value of 2338 mg/L for GenX. In order to eliminate background toxicity from the oxidation of the ions from the salts in the electrolyte, NaCl was removed and the experiments were conducted in 0.10 M Na_2SO_4. Additionally, the samples taken from the oxidation compartment in the divided cell were quenched with 2000 mg/L $Na_2S_2O_3$. After treatment, the measurements indicated that in the undivided cell and in the reduction compartment of the divided cell, there was no toxicity measured. However, in the oxidation compartment of the divided cell, there was some toxicity measured, with an EC50 of 23% of the initial concentration after 2 hours of treatment. This indicated that the processes of electrooxidation of GenX produces some toxicity while the electroreduction and overall electrodegradation do not.

Since the electrochemical redox treatment of GenX requires concentrations higher than environmentally relevant levels, electrochemical coagulation experiments were conducted with the view to use it as a technique to preconcentrate the PFAS for subsequent treatment with electrochemical degradation. The preliminary experiments indicated that GenX could be removed from the liquid phase employing this method and concentrated in flocs. Zn was found to be the most effective electrode in removing GenX, among Zn, Fe and Al.

This PhD work evidences the viability of electrochemical approaches for the treatment of water containing GenX.

Résumé

Les substances per- et polyfluoroalkylées (PFAS) sont bien connues pour leur nature récalcitrante causée par l'abondance de leurs liaisons C-F. Il a été prouvé pour certaines PFAS que la dégradation électrochimique est une technique potentiellement appropriée pour leur traitement ; cependant, la plupart des études se concentrent uniquement sur l'oxydation électrochimique, avec une attention limitée accordée à la réduction électrochimique, et la contribution relative des deux à la dégradation totale des PFAS n'a pas encore été élucidée.

L'objectif de cette thèse était d'étudier le potentiel d'électrodégradation d'une PFAS cible, l'acide dimère d'oxyde d'hexafluoropropylène (HFPO-DA ou GenX) et la contribution de l'électroréduction à son élimination globale. Une anode commerciale composée de diamant dopé au bore (BDD) a été utilisée. Plusieurs matériaux de cathode différents ont été examinés (acier inoxydable, cuivre, étain, or, titane, graphite et BDD), et le cuivre s'est avéré le plus performant. Les réactions d'oxydation et de réduction ont été découplées l'une de l'autre et étudiées simultanément à l'aide d'une cellule divisée dans laquelle les deux compartiments électrolyte/électrode étaient séparés par une membrane.

Les expériences ont démontré que le GenX peut être dégradé à des concentrations inférieures aux limites de détection (< 7,5 µg/L) dans les cellules divisées et non divisées. Il a été déterminé que la réduction joue un rôle significatif dans la dégradation globale du GenX pour toutes les densités de courant étudiées. La tendance générale de la contribution de la réduction a d'abord diminué avec l'augmentation de la densité de courant jusqu'à 50 mA/cm^2, puis a de nouveau augmenté à 100 mA/cm^2 (48,4% à 13,5 mA/cm^2, 37,7% à 20 mA/cm^2, 6,8% à 50 mA/cm^2 et 21,9% à 100 mA/cm^2).

Des études sur l'influence de l'anion électrolytique dans les expériences de dégradation ont montré qu'il n'y a pas de différence statistique lorsque Na_2SO_4, NaCl ou les deux sels sont présents dans l'électrolyte lors de la réduction de GenX dans une cellule divisée. Cependant, dans le compartiment d'oxydation, 0,22 M de Na_2SO_4 et 0,22 M de NaCl ont conduit individuellement à une dégradation du GenX légèrement meilleure qu'avec 0,10 M de Na_2SO_4 et 0,12 M de NaCl ensemble. De plus, l'électrooxydation de GenX était plus faible dans 0,12 M de NaCl par rapport à 0,10 M de Na_2SO_4, ce dernier étant le même que lorsque les deux sels étaient utilisés. Ces résultats ont indiqué que la dégradation de GenX est entraînée par un transfert direct d'électrons

sur l'anode et que les espèces de chlore actif produites par l'oxydation du chlorure sur l'anode n'affectent pas l'oxydation de GenX. De plus, des expériences de dégradation ont été réalisées en utilisant de vraies matrices d'eau (eau de surface, eaux usées et eau potable) enrichies en GenX. Les expériences ont montré que GenX pouvait être dégradé électrochimiquement dans ces matrices aqueuses plus complexes, même plus efficacement que lors de l'utilisation d'un électrolyte composé de Na_2SO_4 aqueux 0,10 M et de NaCl 0,12 M.

Les produits de transformation potentiels ont également été étudiés afin d'évaluer si les mécanismes de dégradation électrochimique de GenX proposés dans la littérature sont applicables à ce qui a été observé dans ce travail de thèse. Plusieurs produits rapportés dans la littérature ont été détectés dans des échantillons des cellules divisée et non divisée, ce qui a soutenu les mécanismes proposés. Les mesures de toxicité aiguë évaluées par Microtox BioAssay avant traitement ont indiqué une valeur CE50 de 2338 mg/L pour GenX. Afin d'éliminer la toxicité de fond due à l'oxydation des ions des sels dans l'électrolyte, le NaCl a été éliminé et les expériences ont été menées dans 0,10 M Na_2SO_4. De plus, les échantillons prélevés dans le compartiment d'oxydation de la cellule divisée ont été traités avec 2000 mg/L de $Na_2S_2O_3$. Après traitement, les mesures ont indiqué que dans la cellule non divisée et dans le compartiment de réduction de la cellule divisée, aucune toxicité n'a été mesurée. Cependant, dans le compartiment d'oxydation de la cellule divisée, une certaine toxicité a été mesurée, avec une CE50 de 23 % de la concentration initiale après 2 heures de traitement. Cela indique que les processus d'électrooxydation de GenX produisent une certaine toxicité alors que l'électroréduction et l'électrodégradation globale ne le font pas.

Étant donné que le traitement redox électrochimique de GenX nécessite des concentrations supérieures aux niveaux pertinents pour l'environnement, des expériences de coagulation électrochimique ont été menées en vue de l'utiliser comme technique de préconcentration du PFAS en vue d'un traitement ultérieur par dégradation électrochimique. Les expériences préliminaires ont indiqué que le GenX pouvait être récupéré de la phase liquide en utilisant cette méthode en les conentrant en flocs. Le Zn s'est avéré être l'électrode la plus efficace pour éliminer le GenX, parmi le Zn, le Fe et l'Al.

Ce travail de doctorat démontre la viabilité des approches électrochimiques pour le traitement de l'eau contenant du GenX.

Acknowledgements

I would like to firstly acknowledge my supervisors, Prof. Sasha Omanovic and Prof. Viviane Yargeau. You two have inspired me beyond what I can express so I would like to thank you for the resources provided for me to conduct my research, your guidance in during graduate school and your wisdom and patience as they oversaw my academic journey. I began this journey at an inconvenient time in McGill history, however, you two have always provided me with the encouragement I needed even when I did not know how to communicate it.

Being a part of both the Laboratory of Electrochemistry and Corrosion and the Laboratory of Controlling Contaminants of Concern, I had great experiences collaborating with others and above all, learning more about my research field. I am appreciative of past and present members of these laboratories and our time spent doing our own independent research while also helping each other. I would like to thank Marco Pineda Castro in particular for his help in navigating the analysis of PFAS, specifically developing and elucidating the methods in publications, and providing insight in my laboratory experiments. I am grateful for the help of undergraduate students such as Maya and Vicky. I hope that you found working with me as great as an experience as I did. Your contributions to my research were substantial and I could not have done it without your help. Other members of the McGill community such as Frank, Andrew and Ranjan have contributing in helping me figuring out analysis solutions using the departmental equipment in Wong. I would also like to acknowledge Prof. Jinxia Liu for providing guidance on my Ph.D. progress reports.

Moreover, grateful acknowledgement is given to Les and Judy Vadasz for faithfully providing engineering students with the opportunity to pursue graduate studies in engineering through their scholarship of which I was a recipient of in 2020 – 2024. I, as well as many of my peers in McGill, have greatly benefitted from this and I appreciate their continued and vested interest in the students and their projects.

Furthermore, I would like to acknowledge my friends that have encouraged me along the way. To members of the Graduate Christian Fellowship of McGill, our discussions and shared experiences helped me have a space to explore my faith with others in a similar stage in life. Other friends such as Reanne, Bintou, Rachelle, who helped me with French abstract, and Chrys, who also helped me

with data analysis, you guys have been there for me in person and over the phone and I love you all dearly.

To members of my community in Anguilla, I would like to thank you for your prayers for my success and concern for my well being. I receive all of your salutations through my family and I thank you for keeping me in mind. To the Department of Education in Anguilla, I would like to thank you for providing for part of my graduate education. The contribution was invaluable to me to completing this degree and to my overall experience.

And at last, but certainly not least, my family. To my parents, Lowell and Liesel, siblings, Amber, Kemba and Kheri, and my extended family I would like to express my sincerest gratitude. All of you have encouraged me and supported me physically, emotionally, financially and spiritually. You have given me a solid foundation to ground myself and wings to soar to the heights of my dreams. Each of you have ambitions and dreams that have served as benchmark of what is possible to achieve when you put your mind to it. So once again, thank you all.

And to all those I have not mentioned who have helped me on this journey, I am truly grateful.

Chapter 1 Introduction

1.1 Project Motivation

Water is an important natural resource both to humans and the environment. With over eight billion people relying on this resource for daily life, it is imperative that water sources are of a sufficient quality to sustain human life and for the wellbeing of the natural environment. As the population continues to increase, so does the demand for clean water in various aspects of society such as agriculture, industry, recreation and the household [1]. Although over 70% of the earth surface is covered in water, it is well known that 96% of that is saline, and most of the freshwater remaining is unavailable for use, being found in glaciers and icecaps [2], [3]. When the limited amount of water available to humans becomes contaminated, this becomes one of the factors which leads to water scarcity, which is a major problem that many people today are facing [1].

Pollution is one of the major causes of potable water scarcity, which is expected to affect 1.8 billion people by the middle of this decade. Contaminated water can lead to food shortage, health problems, destruction of ecosystems and habitat loss for species [4]. Pollutants can change the chemistry of the water by altering the pH, temperature, conductivity and concentration of nutrients and dissolved gases which can reduce its capacity to support and sustain life [5]. Organic chemicals are common pollutants that affect surface water and several of these thousands of chemicals make their way into the water system from the use of various products such as cleaning agents, pharmaceuticals, and materials from other industries, etc. [6]. Several organic pollutants tend to be difficult to breakdown and therefore persist in the environment. One such class of chemicals are per- and polyfluoroalkylated substances (PFAS).

PFAS are organic chemicals which mainly consist of carbon chains which have several fluorine atoms attached in place of hydrogen, so that the compounds contain the moiety C_nF_{2n+1} [7]. Since the mid twentieth century, they have been used widely in commercial and industrial applications primarily because of their surfactant properties, ability to repel certain substances, fire resistance, chemical stability, among other useful attributes [8], [9]. Popular uses of PFAS include fire-fighting foams and as protective coating on household items. Various applications of PFAS can lead to several entry points of the substances into the environment.

Over the years, studies have shown that PFAS have the potential to negatively affect human health and the environment [8], [10]. Certain PFAS have been suspected to be linked to cancer, adverse liver and reproduction effects in humans, as well as be toxic to terrestrial and aquatic organisms [8]. In addition, the exposure to PFAS has only increased in the last two to three decades [11]. The same properties that make PFAS such useful compounds also make them difficult to decompose in the environment.

PFAS are typically described as being recalcitrant with a large portion of them shown to be bioaccumulative and resistant to the usual water treatment methods – biotic and abiotic included [12]. The C-F bonds prevalent throughout PFAS are strong, have a high binding energy, leading to the compounds being extremely stable at high temperatures and various environmental conditions [9], [11], [13]. As a result, several treatment methods have been evaluated for their effectiveness in degrading PFAS to remove them from water bodies.

Some treatment methods for PFAS include separation techniques such as sorption and ion exchange technologies [8]. These are commonly used to meet drinking water quality requirements within a short timeframe. However, the drawback of these methods is that the PFAS are only physically removed from the water body and remain intact when the removal media are disposed of, or require further treatment such as incineration [14], and these are less applicable to wastewater treatment due to the presence and higher load of several contaminants. On the other hand, degradation treatment methods would breakdown the PFAS into non-toxic or easily treatable compounds.

Advanced oxidation processes (AOPs) are methods used for treating organic pollutants in water and which rely on the production of very reactive free radicals or other chemical species that act as oxidising agents to attack the contaminants [11], [15]. Some well-known processes include photochemical oxidation, Fenton processes, activated persulphate oxidation, among others. These AOPs have the advantage of being *in-situ* treatment methods, meaning the contaminated water can be treated on site, with the potential to completely mineralise PFAS. However, they are beset with drawbacks such as high energy consumption, harsh conditions (for example, low pH and high temperature) and expensive equipment [9], [11], [16].

Similar to AOPs, advanced reductive processes (ARPs) utilise highly reactive species such as nucleophiles or radicals as the active species to reduce the presence of contaminants, including PFAS [11]. The presence of the C-F bond make PFAS susceptible to reductive attack due to the high electronegativity of fluorine [14]. Despite this, ARPs do not garner as much attention compared to AOPs. This is mainly due to the limited efficiency reported so far, and the fact that ARPs experience similar operability difficulties as the ones mentioned for AOPs [11].

One developing method that shows great potential for PFAS degradation is electrochemical treatment. It is considered a potentially viable treatment option because of its use of mild conditions, lack of waste generation, and some studies have proven its effectiveness for the degradation of certain PFAS compounds [9], [11], [16], [17]. Most studies have conducted their experiments using boron-doped diamond (BDD) anodes and solely focused on the PFAS degradation by electrooxidation, with little emphasis placed on electroreduction. One drawback that could be encountered is the relatively high concentration of PFAS that would need to be present for electrochemical degradation to be effective. This is a potential obstacle to realistically employing electrodegradation for PFAS remediation, however, there is the potential of using preconcentrating techniques such as nanofiltration or electrocoagulation to waste streams before an electrodegradation treatment step.

The literature review also revealed that the focus of most studies was on common PFAS such as perfluorooctanoic acid (PFOA) and perfluorosulphonic acid (PFOS), both of which are considered to be contaminants of emerging concern [18]. On the other hand, certain other PFAS have not had as much research dedicated to them [9]. One of these chemicals is hexafluoropropylene oxide dimer acid (HFPO-DA), otherwise known as GenX, which was developed to be a replacement for PFOA, but was found to be just as toxic and recalcitrant as its predecessor [8].

1.2 Objectives

As explained earlier in the text, electrochemical degradation is an attractive treatment technique for PFAS remediation in water streams. Several studies have already shown the success of electrooxidation for degrading some PFAS, but there is very little research done on the

electrochemical degradation of PFAS by electroreduction. Most of the work done on electrodegradation of PFAS has concentrated on straight chain PFAS such as PFOA and PFOS. However, the use of these long chain PFAS has already been phased out, and given that GenX has been identified as the corresponding replacement, it is important to investigate the applicability of electrochemical reduction and oxidation in degrading GenX.

Consequently, the objective of this thesis work was to investigate the relative contribution of electrooxidation and electroreduction of GenX towards its electrodegradation and assess the impact of treatment on toxicity of the water. This was accomplished by the following steps:

1. Evaluation of the performance of different cathode materials for the degradation of GenX using a divided cell to select the best one for the remainder of the experiments.
2. Assessment of the effect of different current densities on the electrodegradation of GenX in a divided and undivided cell to select the most optimal for the remainder of the experiments.
3. Determination of the contribution of electrooxidation and electroreduction towards the overall degradation of GenX using a divided cell.
4. Study of the electrodegradation of GenX in different matrices.
    a. Investigation of the effect of different anions on the electrooxidation and electroreduction of GenX by using different electrolyte salt compositions in a divided cell.
    b. Investigation into the effect of using different real water matrices on the electrodegradation of GenX in an undivided cell.
5. Investigation of transformation products and toxicity
    a. Monitoring of total carbon of samples during electrodegradation treatment in the undivided cell.
    b. Evaluation of acute toxicity of GenX samples after electrochemical treatment in both types of cells.
    c. Detection of transformation products from electrodegradation experiments in both type of cells.

6. Investigation of electrocoagulation as a potential technique for the preconcentration of GenX: Evaluation of the performance of different electrodes for the electrocoagulation of GenX

1.3 Organisation of Thesis

This thesis is written in the classical monograph-style. It comprises of five chapters in total. The first chapter is the introduction which presents the problem of existence of PFAS in waters and justifies the need for removing them from these waters, it also gives the rationale for the research performed and it outlines the objectives of the research performed.

Chapter 2 presents a comprehensive review of the literature in order to give the relevant background information on the research topic. This includes the fundamentals of electrochemical degradation of organic pollutants, focussing on the different cell setups and electrode materials. A summary of electrochemical treatment for PFAS including relevant conditions is given as well as a summary for electrocoagulation of PFAS.

The body of the thesis (Chapters 3 and 4) consists of work that has been or will be published, and it has been formatted to fit the guidelines of the classical-style thesis. The methodologies for all the experimental work are presented in Chapter 3, which includes the electrochemical degradation experiments, the analysis methods and the electrocoagulation experiments. The experimental results and discussion are presented in Chapter 4. Comprehensive conclusions are presented in Chapter 5 to summarise all of the findings of this thesis work, highlight the original contributions to science, and to make recommendations on the future work.

Chapter 2 Background and Literature Review

2.1 Electrochemical Degradation of Organic Pollutants

Over the years, electrochemical mineralisation has increasingly been looked at as a viable option for waste-water treatment [17]. As alluded to in the introduction, it has been proven to be effective for the complete degradation of organic pollutants and can be operated at moderate conditions compared to some other treatment options, with the potential to be used for *in-situ* treatment [8]. In this section, the general theoretical mechanisms for the electrochemical degradation of organic pollutants are discussed, while the simplified schematics of the processes occurring at the two electrodes in an electrochemical degradation cell are presented in Figure 2.1.

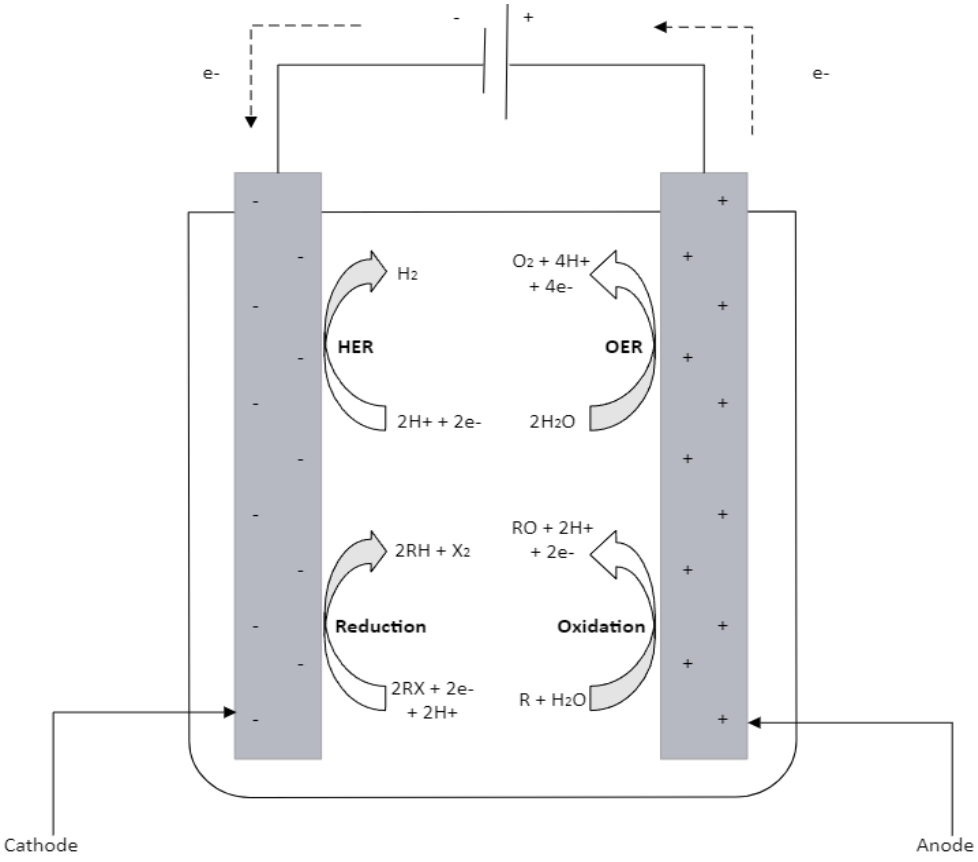

Figure 2.1 Simplified schematic of pollutant electrochemical reactions on the anode and cathode with OER and HER in acidic media

2.1.1 Anodic Reaction

When electrochemical treatment is mentioned, it is usually the anodic oxidation of the pollutant that is being referred to. Thus, it is considered as an AOP. The decomposition of the organic pollutant occurs at the anode either by direct or indirect oxidation. In direct oxidation (as shown in Figure 2.1), the species of interest (e.g. the pollutant molecule(s)) is in contact with the electrode surface where direct electron transfer from the species to the electrode occurs. For indirect oxidation, an intermediate species transfers the electrons between the target chemical and the electrode.

Thermodynamically, it would be preferable for the organic pollutant oxidation reaction to take place at potentials lower than that of the oxygen evolution reaction (OER), which at standard conditions occurs at 1.23 V vs. SHE (standard hydrogen electrode). This would, theoretically, enable formation of a *galvanic cell* characterized by a negative change in Gibbs free energy of the total redox reaction in the cell, where the pollutant would spontaneously be oxidized at the anode and oxygen would be reduced at the cathode, thus producing electricity. Unfortunately, in practice, the kinetics render the organic pollutant reaction extremely slow, shifting its oxidation potential to positive values, beyond the OER [19]. However, with the input of electrical energy, it is possible to degrade organic pollutant chemicals at higher potentials, rendering this system an *electrolytic cell* characterized by a positive change in Gibbs free energy of the total redox reaction in the cell.

In acidic media, the pollutant electrooxidation reaction usually involves oxygen transfer in the form of water to the electrode to form "active oxygen" which is subsequently able to participate in the pollutant oxidation reaction. Comninellis et al. [19], [20] proposed two possible mechanisms by which this is possible: (1) water dissociation and chemical adsorption, or (2) water electrolytic discharge and physical adsorption.

For the former mechanism, the reaction can take place below the thermodynamic potential of oxygen evolution. The reaction equation (presented in the most-simplified form) is as follows:

$$MO_x + H_2O \rightarrow MO_x - OH + H^+ + e^- \qquad (2.1)$$

where MO represents the anode, presumably made of a metal oxide. The oxygen in OH can further interact with oxygen present in the electrode lattice to form a higher-valence metal oxide:

$$MO_x - OH \rightarrow MO_{x+1} + H^+ + e^- \quad (2.2)$$

This "chemisorbed active oxygen" is thought to then oxidize the pollutant molecule, R, to produce selective oxidation products of the organic chemical, RO, yielding back the original state of the electrode, MO_x, with the reduced metal oxidation state:

$$R + MO_{x+1} \rightarrow RO + MO_x \quad (2.3)$$

For this type of oxidation reactions, the pollutant molecule has to get in contact with the electrode surface, which usually involves its adsorption.

In the other mechanism, the water molecule gets oxidised at the MO electrode surface to produce hydroxyl radicals, OH•, which are very powerful oxidants:

$$MO_x + zH_2O \rightarrow MO_x(OH^\bullet)_z + zH^+ + ze^- \quad (2.4)$$

These hydroxyl radicals (i.e. active oxygen) then oxidize the organic molecule, R, which could lead to its complete degradation:

$$R + MO_x(OH^\bullet)_z \rightarrow nCO_2 + zH^+ + ze^- + MO_x \quad (2.5)$$

In both cases above, the OER is a competing, undesirable reaction to the oxidation of organics. In the case of chemisorbed active oxygen, O_2 is evolved following this reaction:

$$MO_{x+1} \rightarrow MO_x + \frac{1}{2}O_2 \quad (2.6)$$

whereas for physisorbed active oxygen, it is:

$$MO_x(OH^\bullet)_z \rightarrow MO_x + \frac{1}{2}zO_2 + zH^+ + ze^- \quad (2.7)$$

For an anode, to control which reaction would take place, whether the decomposition of the organic or the OER, a material with a high enough *oxygen evolution overpotential* needs to be selected.

(The overpotential refers to the extra potential, relative to the thermodynamic/reversible potential, needed to be inputted to drive a certain electrochemical reaction at a certain rate). If the anode has a high oxygen evolution overpotential, the likelihood of the OER occurring at a lower input potential is less compared to the desired oxidation of pollutants. The OER overpotential has been linked to the interaction of the adsorbed OH radicals on the material's surface [19]. The weaker this interaction for a material, the higher the overpotential, and thus better able it is to oxidise the pollutant. Examples of materials with a high OER overpotential are boron-doped diamond (BDD) and certain metal oxides such as tin oxide and lead oxide.

2.1.2 Cathodic Reaction

Although electrochemical oxidation of organic pollutants is the more common degradation technique, their degradation by electroreduction is also a possibility. Whereas the former process has the potential to completely oxidise the organics, the latter process can possibly lead to the transformation of the pollutant into value-added products or to recovery of chemicals, or it can produce a molecule that can further be degraded using other degradation techniques [19]. Electroreduction is a promising technique especially for organohalides (RX) because of the electronegativity of the halogen atoms, as previously alluded to. A possible mechanism for the degradation of a halogenated pollutant, RX, by electroreduction, proposed by Comninellis et al., [19], is as follows (a simplified version is depicted in Figure 2.1):

$$RX + e^- \rightleftarrows RX^{\bullet -} \tag{2.8}$$

$$RX^{\bullet -} \rightarrow R^{\bullet} + X^- \tag{2.9}$$

$$R^{\bullet} + e^- \rightarrow R^- \tag{2.10}$$

The activated organic molecules can potentially react with the solvent or other organic molecules (HA) and continue to propagate the reaction.

$$R^{\bullet} + HA \rightarrow RH + A^{\bullet} \tag{2.11a}$$

$$R^- + RX \rightarrow R - R + X^- \tag{2.11b}$$

$$R^{\bullet} + R^{\bullet} \rightarrow R - R \quad (2.11c)$$

For the cathode, the hydrogen evolution reaction (HER) directly competes with the reduction of the organic chemicals in aqueous solutions. Therefore, similar to the anode, it would be desirable to select an electrode material that gives preference for the latter reaction. Materials such as Ag, Pd, Ni, Pt, Fe and stainless steel are promising cathode materials to promote C-X reduction, while Hg, Pb and Sn are also looked at for their ability to hinder HER [19]. Even though carbon based materials are reported to be inert for halogen cleavage reactions, they show ahigh overpotential for the HER, and because of their robustness and inexpensive nature, they are often used as supports for the cathode materials [19]. However, they also can be considered to be valid cathode materials by themselves because of these properties.

2.1.3 Cell Setup

There have been a few studies performed where the electrochemical oxidation process is combined with the electroreduction process [21]. Scialdone et al., [22], reported that the combined process for tetrachloride ethane abatement was more effective than the oxidative process by itself. Most studies that use the combined oxidation and reduction experiments conduct them in an *undivided* electrochemical cell (the electrodes are not separated by a membrane and the same electrolyte is used in the cell like in Figure 2.1) [19], [21]. While successful results have been reported, there is concern over the transformation products reverting back into their previous forms on the electrodes (e.g. oxidized at the anode and the reduced back at the cathode, or vice-versa) and also over the interference of the products [19]. Although using an undivided cell negates the need to invest in separation membrane, using a divided cell is advantageous because it allows the use of separate electrolytes if necessary, facilitates study on the separate oxidation and reduction processes, prevents interference between the oxidation and reduction products, and allows any value-added products generated to be preserved, among other benefits [19].

2.1.4 Electrode Materials

The current state-of-the-art anode material for the treatment of organic wastewaters is BDD. For BDD electrodes, doping the synthetic diamond with boron atoms increases the conductivity leading to many useful properties for electrochemical oxidation of organics [23]. As previously

mentioned, BDD exhibits good performance for the electrochemical degradation of the PFAS that have been studied, which include perfluorocarboxylic acids (PFCAs) and perfluorosulphonic acids (PFSAs) [19], [24]. This can be attributed to the weak interaction of the physisorbed OH radical with the BDD surface, which leads to a high oxygen evolution overpotential (2.3 V vs SHE)[19]. This means that electrooxidation reactions with organics are preferred and are more likely carried out to complete mineralisation over the OER.

Copper, being a highly abundant and low-cost metal makes it a potential electrode material of interest especially when considering sustainable applications. Being an excellent conductor, copper also has several oxidation states that are available to it, which can possibly lead to it participating in single or double electron transfer reactions [25]. Copper has been speculated to be useful for the reduction of organic halides and has been used in studies for this purpose [26]–[28]. Isse et al. 2012, used copper as a cathode for the electrochemical reductive dehalogenation of polychloromethanes and polychloroethanes in dimethylformamide. They reported that the electrocatalytic activity of Cu for these reactions is good and is enhanced in the presence of a good proton source and that hydrodehalination and dehydrodehalination are possible in the presence of water. A molecular copper electrocatalyst (a Cu-based organic cation, $[CuT2]^+$ was used by Sinha et al. for the defluorination of PFOA in a non-aqueous solvent (acetonitrile) [29]. This led to a degradation of over 93%, with CO_2 and PFAS fragments being the byproducts from the reaction.

2.1.5 Factors that Determine Electrolysis Performance

According to Panizza, 2010 [19], there are several factors that affect the electrodegradation performance. These include the potential and current density, which have been proven to influence which reaction takes place, the degradation rate and efficiency [30], [31]. Other important elements are the current distribution, mass transport considerations, pH and concentration of electrolyte, and the design of the cell which affects the reactant distribution on the electrode as well has reaction rate and efficiency. Finally, a critical consideration for the electrodegradation process is the electrode material. The electrodes used in for the process should be inexpensive, stable and reactive for the desired reactions.

2.2 Electrochemical Degradation of PFAS

As mentioned previously, electrochemical oxidation/reduction is a technique of interest in degrading PFAS, with some studies showing that high percentages of mineralisation can be achieved at moderate conditions with comparably low energy input [32], [33]. Most of these studies were conducted using electrodes of high oxygen overpotential, such as BDD or one of the metal oxides mentioned previously (PbO_2, SnO_2, etc.) [24]. A summary of experiments reported in literature can be found in Table A.1 in the appendix.

Based on the data summarised in Table A.1 in the Appendix, it can be noted that PFOA was the most studied PFAS followed closely by PFOS. Further, 6:2 FTS, PFBA, PFHxA, PFBS, PFHxS and GenX were included in several studies as well, especially in studies that focussed on more than one PFAS. The concentrations of these PFAS ranged from mid µg/L range (~100 µg/L) to mid mg/L range (~100 mg/L). For the anode, after BDD, mixed metal oxide (MMO) and Ti based materials were the most popular material for oxidation, while Ti and stainless steel were the cathode materials most often used. Salts such Na_2SO_4, $NaClO_4$ and NaCl were most often used as the electrolyte in concentrations ranging from around 0.01 – 0.1 M. Real water matrices such as industrial waste streams, ground water, etc., were also used as electrolytes in some studies with comparable percentages of removal depending on the experimental conditions. A variety of current densities were used, however, mid range current densities (between 10 – 50 mA/cm^2) were mostly used, with a few studying current densities below 10 mA/cm^2.

Depending on the parameters used in the studies, varying degrees of removal were reported for the PFAS. The majority of literature that reported lower rates of removal (<50%) of PFAS either used a non-BDD anode, or shorter chain PFAS were used in the experiments, (even when BDD was used as the anode). For example, Trautmann et al., studied the degradation of PFBS, PFHxS and PFOS on BDD in which >90% of PFOS and PFHxS while only 45% of PFBS was removed [24]. The kinetics of the PFAS degradation was mostly reported to be pseudo 1^{st} order, with a few exceptions reporting 0^{th} order reaction for low current densities [34].

The mechanism for PFAS degradation by electrooxidation has been described using PFOA as the model compound [16], [30], [31]. The process is thought to begin with an electron from the carboxyl functional group being directly transferred to the anode (M) to form a PFOA radical:

$$M + C_7F_{15}COO^- \rightarrow M + C_7F_{15}COO^\bullet + e^- \quad (2.12)$$

The functional group then leaves, leaving behind a radical of the main PFOA chain:

$$C_7F_{15}COO^\bullet \rightarrow C_7F_{15}^\bullet + CO_2 \quad (2.13)$$

The PFOA can then react with a free hydroxyl radical to form an alcohol:

$$C_7F_{15}^\bullet + OH^\bullet \rightarrow C_7F_{15}OH \quad (2.14)$$

Since the alcohol form of the PFOA is often unstable, it tends to breakdown further to form a carbonyl:

$$C_7F_{15}OH \rightarrow C_6F_{13}COF + H^+ + F^- \quad (2.15)$$

From there, the carbonyl can further react with water to form another perfluoro carboxylic acid, but this time with a shorter chain than the starting material.

$$C_6F_{13}COF + H_2O \rightarrow C_6F_{13}COO^- + 2H^+ + F^- \quad (2.16)$$

At this point, reaction steps 2.12 – 2.16 can be repeated until the compound is completely degraded.

2.2.1 GenX

The hexafluoropropylene oxide dimer acid (HFPO-DA, Scheme 2.1) and its ammonium salt is often known by its trade name, GenX. It was developed by Chemours as a replacement for the ammonium salt of the toxic PFOA. Unfortunately, studies have proven that GenX exhibits similar toxicity to PFOA, and thus, its discharge into water bodies is of great concern [35], especially since environmental monitoring has shown that there are instances where the chemical has made its way past water treatment and into drinking water [36].

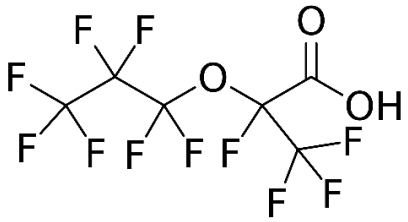

Scheme 2.1 2,3,3,3-Tetrafluoro-2-(heptafluoropropoxy)propanoic acid

Pica et al., [37] studied the effectiveness of electrochemical oxidation of GenX on BDD in conjunction with a pre-treatment by nanofiltration. They proved that significant removal occurred and that the nanofiltration improved the electrochemical performance. Using density functional theory (DFT) calculations, they were able to postulate the GenX degradation reaction mechanism in Scheme 2.2, in which the initial step is due to direct electron transfer:

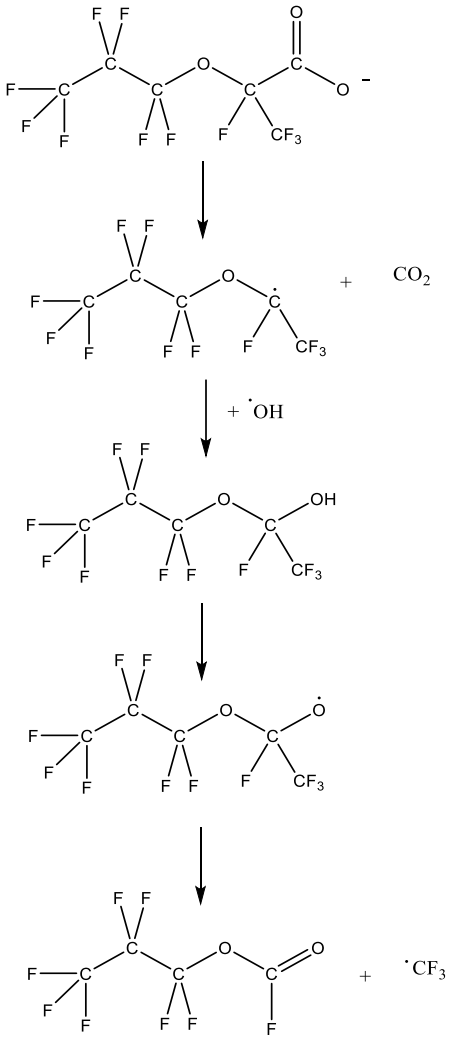

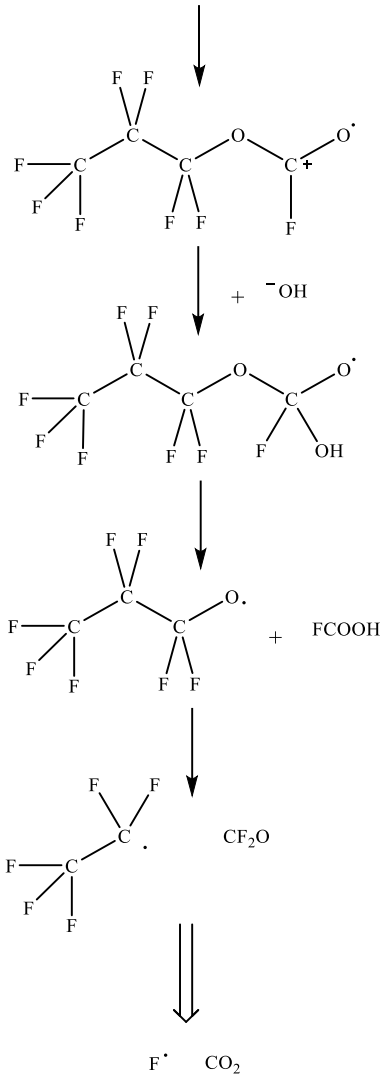

Scheme 2.2 Degradation mechanism of GenX during electrochemical oxidation adapted from Pica et al. [37]

Pica et al. go on to theorise that the ether group remains intact during the initial oxidation of GenX while the α-carbon on the acidic group is where the initial degradation takes place. They also hypothesise that electrochemically activated sulphate aids in the initial degradation of GenX due to their possible participation in forming hydroxyl radicals. This is echoed by Zeidabadi et al. [38], however, they also propose the ether bond as a likely place for initial degradation as seen in Scheme 2.3.

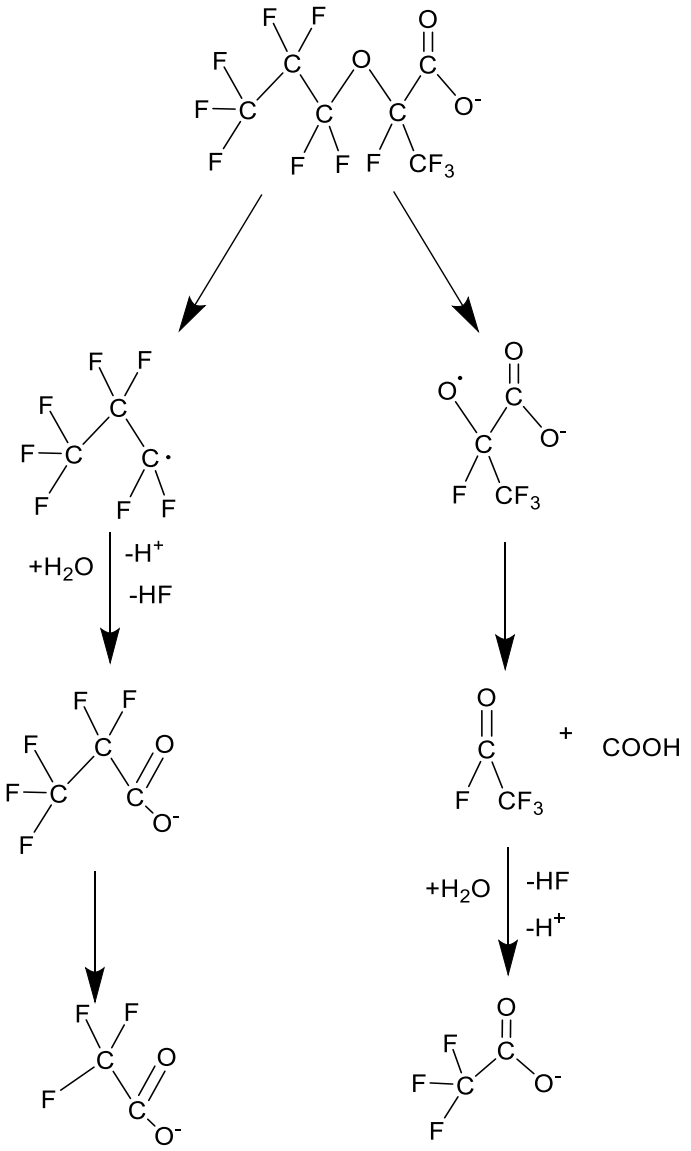

Scheme 2.3 Alternative degradation of GenX during electrochemical oxidation adapted from Zeidabadi et al. [38]

Babu et al. [39], also studied the electrooxidation of GenX on BDD and they concluded direct electron transfer was the rate limiting step. They also stated that sulphate radicals are ineffective for GenX degradation because of stearic hinderance caused by the -CF_3 group which is in contradiction to what Pica et al. and Zeidabadi et al. concluded. Finally, Babu et al. concluded that hydroxyl radicals are essential for the overall mineralisation of GenX.

Conversely, Olvera-Vargas et al. [40], proposed a combined mechanism for the electro-Fenton degradation of GenX which incorporates the cleavage of the ether bond and attack on the carboxylic acid group based on transformation products detected (see Scheme 2.4). This mechanism is more comprehensive as it includes the possibility of more than one reaction pathway at the same time, both leading to the complete mineralisation of GenX.

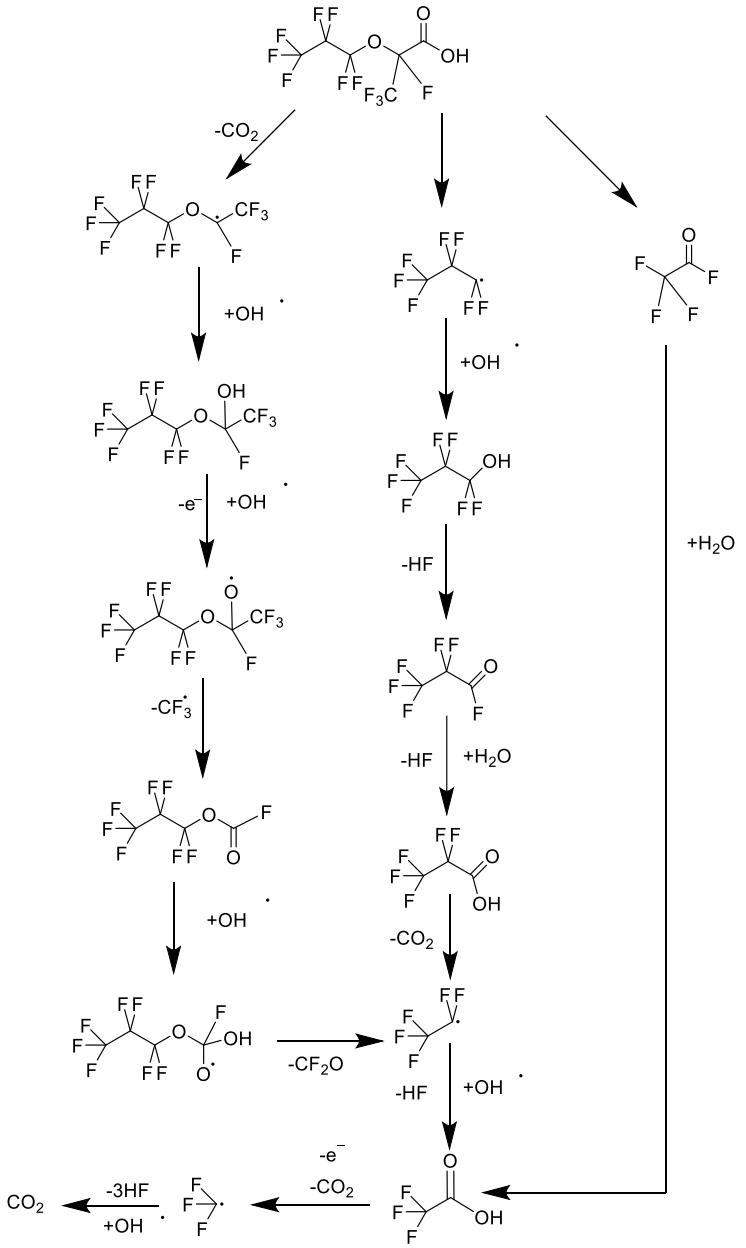

Scheme 2.4 Alternative degradation of GenX during the electro-Fenton process oxidation adapted from Olvera-Vargas et al. [40]

Since GenX is a more recently-developed chemical compared to PFOA and PFOS (the former being introduced in 2009 [41]), and the discovery of its toxicity and contamination of water bodies has occurred only within the last 7 or so years, limited research has been done on the removal of this compound from water [36]. It is the aim of the present project to fill the gap in knowledge by investigating the electrochemical degradation of GenX while developing a general electrochemical degradation treatment method that can be potentially applied to PFAS as a broader class of chemicals and other aqueous contaminants.

2.3 Electrocoagulation

Electrocoagulation is a potential technique used to remove PFAS from water streams and involves using sacrificial electrodes to dissolve into flocs (solid metal-oxide/hydroxide microparticles) which the contaminants adsorb on. Namely, the metal anode is electrochemically dissolved into the solution forming charged metal hydroxides (coagulants) which attract pollutant chemicals by electrophoretic motion and adsorption (see Figure 2.2) [19]. These coagulants and adsorbed pollutants aggregate together to produce bigger flocs which, with the help of simultaneously produced gases from the OER and HER, rise to the surface of the water [42].

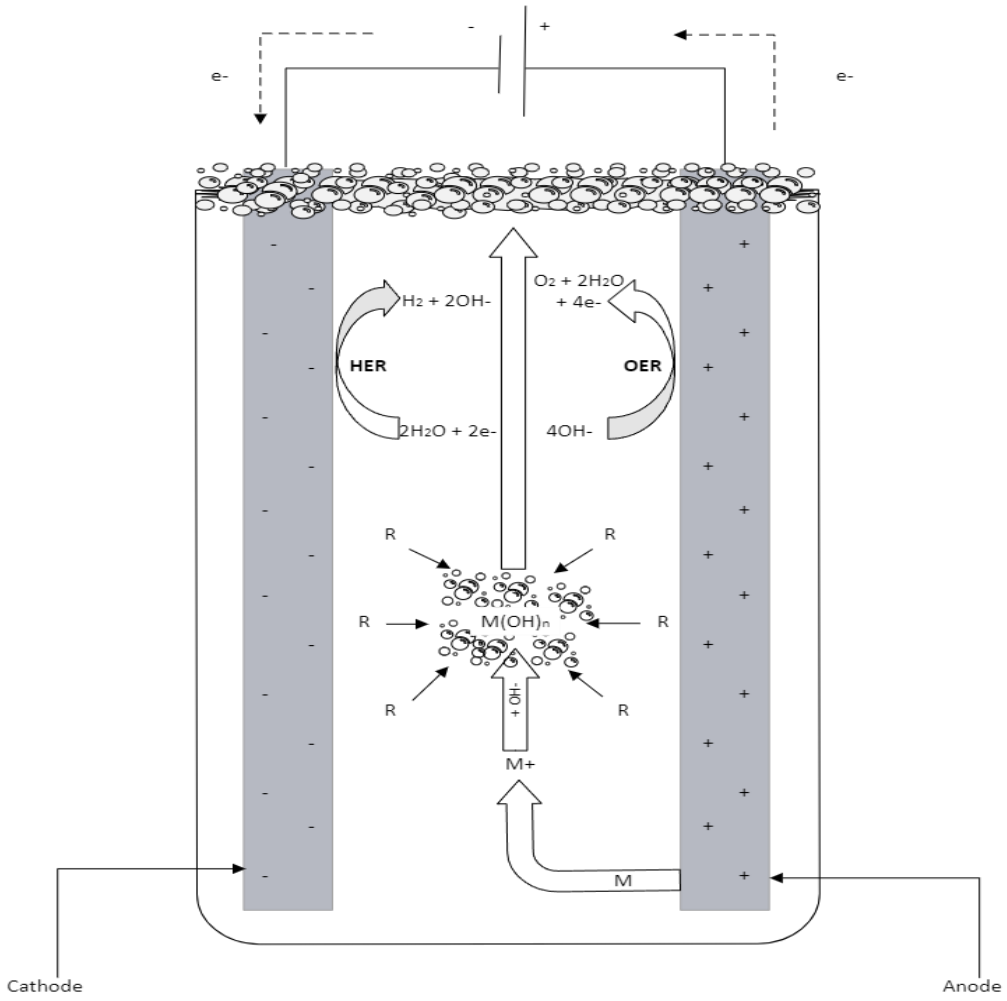

Figure 2.2 Simplified schematic of pollutant electrocoagulation with OER and HER in alkali media

According to Comnellis et al. [19], the electrocoagulation process begins when the metal anode is oxidised to become the metal cation in solution:

$$M_{(s)} \rightarrow M^{n+}_{(aq)} + ne^{-} \tag{2.17}$$

These cations react with hydroxyl ions present in the water to form metal hydroxides which aggregate to each other forming microparticles:

$$M^{n+}_{(aq)} + nOH^{-}_{(aq)} \rightarrow M(OH)_{n\,(s)} \tag{2.18}$$

A parallel anodic reaction is oxygen evolution:

$$4OH^-_{(aq)} \rightarrow O_{2(g)} + 4e^- + 2H_2O \quad (2.19)$$

On the cathode, there is the possibility of dissolved metal ions being reduced and electrodeposited on the cathode:

$$M^{n+}_{(aq)} + ne^- \rightarrow M_{(s)} \quad (2.20)$$

which represents an unwanted side reaction. However, as presented in Figure 2.2, the main cathodic reaction is hydrogen evolution:

$$2H_2O + 2e^- \leftrightarrow H_2 + 2OH^- \quad (2.21)$$

2.3.1 Factors that Determine Electrocoagulation Performance

As with electrodegradation, there are several factors which influence the effectiveness of the electrocoagulation process. One such factor is the electrode material. Most-commonly used anode materials are iron, aluminum, zinc, and magnesium. Metals such as Fe go through complex pathways to form metal hydroxides coagulants due to the multiple oxidation states available to it. Also, Al form hydroxides that are able to disperse throughout the solution well [42]. The rate at which the metal is able to dissolve to form the coagulants is of key importance to the process. Factors such as current density, concentration overpotential and pH of the electrolyte will have an effect on that. The amount of the dissolved anode can be expressed through the Faraday equation:

$$w = \frac{itM_wF}{n} \quad (2.22)$$

where w is the amount of the electrode material that dissolves per unit area (g/m^2), t is the reaction time (s), i is the current density (A/m^2), M_w is the molecular weight (g/mol), F is Faraday's constant (96485 C/mol) and n is the number of electrons that are transferred [19], [42]. Based on this equation, for common metals under the same conditions, the order of amount dissolved into solution would be Zn > Fe > Mg > Al.

Since the current density, i, is a term included in equation 2.22, it is also an important factor in the electrocoagulation process. It is directly proportional to the amount of electrode dissolution. However, lower, current densities have been recommended for electrocoagulation to preserve the longevity of the electrode [19]. Additionally, there is a risk of the current being diverted to

unfavourable reactions such as the OER, or even the electrooxidation of the pollutant when electrocoagulation is desired.

2.3.2 Electrocoagulation of PFAS

Even though it is not a destructive technique like electrodegradation, electrocoagulation is still of interest for its efficiency in removing PFAS and the potential to be used as a preconcentration technique for further treatment by electrochemical degradation [43]. This was done by Shi et al, 2021, who reported success after collecting the flocs from the electrocoagulation of PFOS and dissolving them in sulphuric acid before continuing the treatment with electrooxidation.

Despite the potential of electrocoagulation being a promising step in treating PFAS, the process is not without its drawbacks. A major one includes the passivation of the electrodes and high turnover due to their sacrificial nature [34]. To combat this, alternating current polarity in the cell can prolong the life of the electrodes.

A summary of literature on the electrocoagulation of PFAS can be found in Table A.2 in the appendix. As with electrodegradation, PFOA and PFOS were the subjects of most of the studies. Shorter chain PFAS such as PFBA, PFBS, PFHxA and PFHxS appeared often in the relevant literature as well. For the electrodes, different combinations of Zn, Al and Fe were the most commonly used for the electrocoagulation of PFAS. NaCl of concentrations of 0.01 M and lower was the most prevalent electrolyte; this was followed by electrocoagulation done in natural waters. Concentrations of PFAS below 1 mg/L were most often used for the studies. Higher rates of PFAS removal were reported from the literature for electrocoagulation compared to electrodegradation with most of the studies stated removal percentages of over 99% [44]–[51].

Based on the literature, it can be seen that there is a lack of studies done focussing on GenX. Since it is a shorter chain PFAS, with an ether group as well as a branched CF_3 group, efficiency of removal may differ to the PFCAs reported. To fill in this gap, focus will be placed on using different electrode materials to determine the efficiency of GenX electrocoagulation. This will be done with the purpose of replicating the treatment-train of electrocoagulation and electrodegradation for GenX that was described by Shi et al, [43]. The aim of this treatment train will be to use electrocoagulation as a preconcentration step for GenX at lower concentrations similar to how Pica et al., [37] used nanofiltration to preconcentration GenX for electrooxidation.

Chapter 3 Methodology

3.1 Electrochemical Degradation Experiments

Electrochemical degradation experiments were performed in a divided and undivided two-electrode cell to investigate the removal of GenX by oxidation and reduction. The cell setup is as shown in Figure 3.1 below.

a)

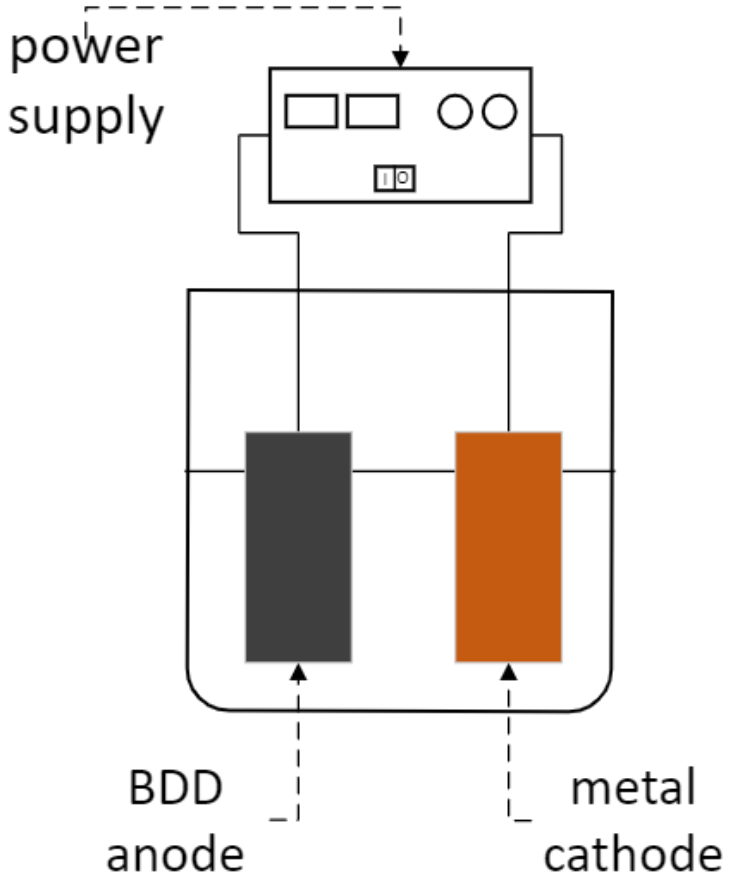

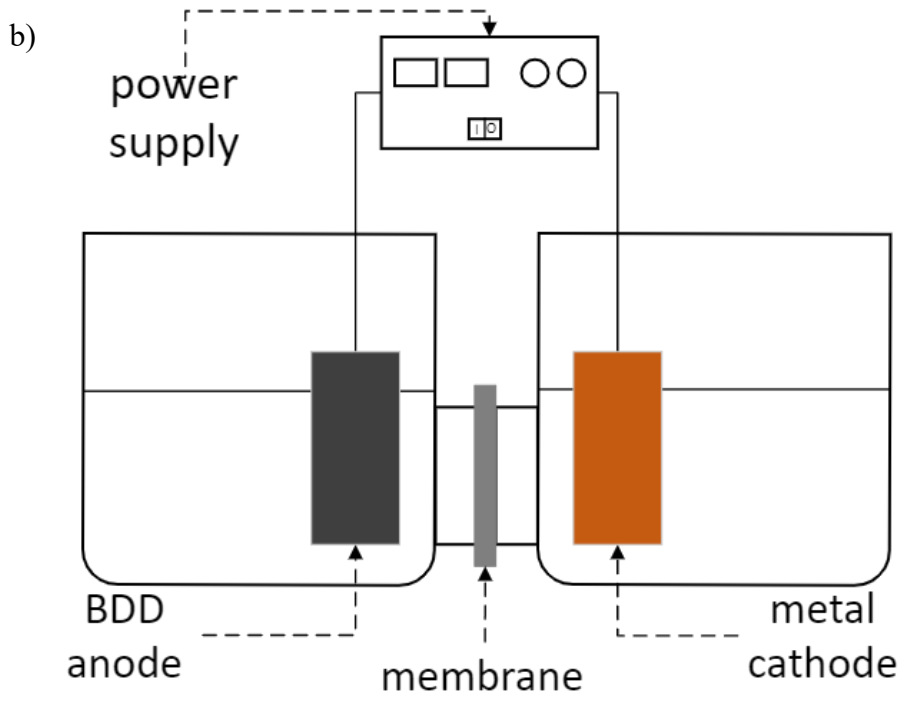

Figure 3.1 Electrochemical cell Setup a) undivided cell b) divided cell

2,3,3,3- tetrafluoro-2-(1,1,2,2,3,3,3-heptafluoropropoxy)propanoic acid (purity ~90%), GenX, was purchased from Toronto Research Chemicals, sodium sulphate (purity 99+%) from Acros Organics, sodium chloride (purity 99+%) from ACS, ≥ 99.9% methanol and ≥ 99.95% acetonitrile were acquired from Fisher Chemical. MilliQ water with a resistivity of 18.2 MΩ ·cm was used to make all solutions.

The working electrolyte used for the degradation experiments was an aqueous solution composed of 5 mg/L GenX + 0.10 M Na_2SO_4 + 0.12 M NaCl, the latter two chemicals serving as the supporting electrolyte. Experiments using only one of the salts as the supporting electrolyte, i.e. only NaCl or only Na_2SO_4, to test the effect of anions on the production of the different active oxidative species present in solution (i.e. active chlorine species and persulphates) were also conducted. Real water matrices were also studied for GenX degradation at the same concentration. Surface water from Lac Saint Pierre (Quebec), wastewater from La Prairie Water Treatment Plant (La Prairie, Quebec) and drinking water from the M. H. Wong building in the University of McGill were filtered then spiked with the same concentration of GenX (5 mg/L) and treated in the undivided cell. The surface water and drinking water was electrochemically degraded at a current

density of 50 mA/cm^2, and the wastewater was degraded at 13.5 mA/cm^2, 20 mA/cm^2 and 50 mA/cm^2.

250 mL of the solution (electrolyte) was placed in a 500 mL-beaker used as the electrochemical cell for the "undivided-cell experiments", while 250 mL of the solution was split evenly between two beakers forming the compartments of a divided cell (H-cell). As a separator in the divided cell, a 2 mm agar membrane containing KNO_3 (see Appendix A for details on its fabrication) was used for experiments performed at lower current densities (≤20 mA/cm^2), and a more temperature-resistant membrane made of Nafion^{TM} 117 was used for experiments at higher current densities, which were employed in some of the "divided-cell experiments". The membranes' resistance was measured using electrochemical impedance spectroscopy (EIS), and the corresponding spectra and the ohmic resistance values can be found in Figure A.1 and Table A.3 in the appendix.

Experiments in the undivided cell were performed at current densities of 13.5, 20 and 50 mA/cm^2. For the divided cell experiments, the current densities used were 13.5 mA/cm^2, 20, 50 and 100 mA/cm^2. The power-supplies were a B&K Precision® 1687B Power Supply and a Wanptek Programmable DC Power Supply (APS1602H model). Commercial boron doped diamond (BDD) was used as the anode for all experiments, except in specific experiments (noted in the text/figures) where it was used as the cathode. In that case, a fabricated $Ni_{40}Co_{60}$-oxide electrode, that was previously developed by the laboratory group [52], was used as the anode. For the cathode, several materials were initially tested as part of a "screening process": commercially-pure titanium, gold, graphite rods, BDD, electroplated tin, 316L stainless steel and copper. The backsides of both anode and cathode were covered with 3M electrical insulating tape in order to enable only the two front-facing opposite sides of the electrodes to be exposed to the solution. Each of the electrodes had 20 cm^2 of surface are exposed to the solution. For the control experiments, no current was applied to evaluate the possible removal of GenX from the working solution by adsorption on the various components of the electrochemical cell. To evaluate the amount of GenX degraded for all degradation experiments, 200 µL of sample was taken at different time points during the degradation experiments and immediately quenched with 200 µL of methanol.

To prepare the samples for the chemical analysis, an additional 400 µL of methanol was added into the samples in two steps, with centrifuging at 4500 G for 10 minutes between each step. The sample

was separated from the precipitated salt in each step by pipetting the supernatant and transferring it into another sample tube. Afterward a 320 µL sample was added into a sample vial with 100 µL acetonitrile and 580 µL water to further dilute the samples, which were then analyzed to measure the concentration of GenX present as described in Section 3.3.1. Using the concentration of GenX in the initial sample point (time zero) as a reference, it was confirmed through calculations that no GenX was lost in the sample preparation.

3.2 Electrochemical Coagulation

The electrochemical coagulation experiments were carried out only in an undivided cell (see Figure 3.1a). The working solution was 1 mg/L GenX to demonstrate that operating at lower concentrations than the what was used for the electrodegradation experiments (5 mg/L) was feasible. This was also the concentration used by Pica et al. for their nanofiltration preconcentrating step [37].

1.016 mm thick zinc, 0.762 mm iron and 0.8128 mm aluminum sheets were purchased from McMaster Carr and cut into 6 cm x 5 cm electrodes. Each metal was used as both the anode and the cathode applying direct current at 10 mA/cm^2, with the electrodes' backside insulated by a 3M tape to expose only 20 cm^2 of the electrode surface area to the electrolyte. 500 µL of sample was taken at different time points. The samples were centrifuged at 4500 G for 10 minutes then filtered through a 0.2 µm polyethersulfone (PES) membrane filter before being centrifuged again. 190 µL of sample and 10 µL methanol were placed in the sample vials to prepare them for analysis. Different syringe filters were tested for their retention of GenX before the PES 0.2 µm filter was selected due to there being only a 13% retention of GenX on the filter. These results can be found in Figure A.2 in the appendix.

To test the viability of electrocoagulation for GenX preconcentration, the flocs from the experiment were collected, centrifuged at 10,000 G for 10 minutes then freeze-dried overnight. 0.2063 g of the dried flocs from the experiment with the Zn electrode were dissolved in 1 mL 4 M sulphuric acid, similar to what was described by Shi et al, 2021 [53] and analyzed for the GenX.

3.3 Analytical Techniques

3.3.1 Monitoring GenX Concentration by Liquid Chromatography Mass Spectrometry

GenX concentration was determined using an Accela 600 HPLC system coupled with a single quadrupole mass spectrometer MSQ Plus (Thermo Scientific). Negative ionization mode was used to perform the detection in heated electro-spray ionization (HESI) for the generation of precursor ions. Optimization of the mass spectrometry parameters for quantitation was done by direct injection at 1 mL/min and a standard solution (5 mg/mL) at 10 µL/min of 1:1 water and methanol mixture, both containing 0.1 vol% acetic acid and 2 mM ammonium acetate. Nitrogen on static mode was used as the gas source while the source capillary voltage was set at 3.0 kV. The temperature for the ion transfer tube was 275°C while no vaporisation was applied during ionisation, and the captured ions were focussed in a beam with -35 V cone voltage. Full scan (150 – 500 m/z) was used to conduct the acquisition with 2 m/z as the range and single ion monitoring was done at 284.98 m/z with a span mode of 2 m/z.

The analytical column assembly (shown in Figure A.9 in the appendix) consisted of an online filter cartridge (2.1 mm ID x 0.2 µm porosity stainless steel filter), an Eclipse Plus C18 RRHD (5 mm x 4.6 mm ID; 5 µm) guard column from Agilent Technologies (Ca, USA) followed by the analytical column Alltima C8 (53 mm x 7 mm ID; 3 µm) from Alltech (KY, USA). The Alltima C18 column was placed on the diverting valve to prevent the interference and precipitation of sulphate and chloride salts in the analytical column between the loading pump and the injector valve. Buffer exchange was done at isocratic conditions and held for 3 minutes at a flow rate of 1 mL/min with 5% methanol in MilliQ water. The valve was switched after 3.1 min and the loading flow was reduced to 0.1 mL/min for 15 minutes before being increased back to a flow of 1 mL/min. Due to the potential PFAS contamination of the tubing and lab environment, an Hypersyl Gold aQ (20 mm x 2.1 mm, 12µ pores size) columns from Thermo Scientific was placed between the pumps and the injection and diverting valve. Additionally, all tubing used on the system was stainless steel. The column temperature was held at 40°C for the entire run. The mobile phase on the analytical column consisted of MilliQ water and HPLC grade methanol, both containing 0.1% acetic acid and 2 mM ammonium acetate at a constant flowrate of 1 mL/min. An initial 5% organic mobile phase was kept constant for 4 minutes followed by a linear increase to 100% over 2 minutes

and held constant for 8 minutes to clean the column. The column was then returned to initial injection conditions at 5% organic solution and equilibrated for 2 minutes making the total analytical running time 16 minutes. Quantitative analysis was performed on the target compound using an eight-point concentration external linear calibration curve with two quality controls (QCs) at low (7.5 µg/L) and medium (150 µg/L) concentrations. Two sets of independently prepared quality control samples were prepared and ran in all batches at 7.5 and 150 ug/L, the acceptance tolerance for these were ±20% and ±15% of their respective concentrations while the analytical criteria required that at least 51% of the QC's comply within their nominal concentration values. Data analysis was done on Xcalibur Quan Browser on Version 4.4 software from Thermo Scientific.

3.3.2 Monitoring Total Organic Carbon

Total organic carbon measurements were conducted using a Shimadzu Total Carbon Analyser (TOC-VCPH) from Mandel. To reduce the salt burden on the instrument, specifically the catalyst bed, experimental samples using just 0.10 M Na_2SO_4 were used for analysis since the GenX electrochemical degradation experiments demonstrated that the rate of degradation does not depend on the salt used to prepare the electrolyte solutions employed. 10 mL of sample was collected at 0, 60 and 120 minutes of degradation. The pH of the samples was adjusted to between 2 – 3 using sulphuric acid. A non-purgeable organic carbon (NPOC) method was selected to measure the carbon in the samples remaining after purging. This method was used because the electrochemical cells were not sealed from the atmosphere and it is not expected that volatile transformation products would form from the degradation of PFAS due to their chemistry (high solubility and low vapour pressures) [8]. The NPOC method was programmed to take 3 injections of 17 µL after a sparging time of one minute.

3.3.3 Monitoring of Transformation Products

The untargeted analysis was performed using a Vanquish UHPLC-RTC system coupled with an Exploris 120 HRMS mass spectrometer from Thermo Scientific (Bremen, Germany). Heated electrospray ionization (HESI) in negative ion mode was optimized by infusing a standard solution (0.5 mg/mL) and a water-methanol mixture at 350 µL/min. The source capillary voltages were set

at 1000 V with activated mild trapping, nitrogen was used as the source and HCD collision gas, with sheath, auxiliary, and sweep gases set at 40, 7, and 0 arbitrary units, respectively. Source temperatures were set at 225ºC for the transfer tube and 250ºC for vaporization, with a lens frequency of 55% for precursor ion beam focusing. Differing from the quantitation analysis, the system used the AcquireX function in order to acquire the greatest number unknown compounds, with full scan data acquisition performed over the range of 70 to 1000 m/z with a full width at half maximum (FWHM) resolution of 120,000 at 200 m/z, after which, a suspect screening analysis was done. Top 4 data-dependent MS2 (dd-MS2) data acquisition was conducted with an FWHM resolution at 30,000 for the generation of product ion spectrum confirmation using dynamic exclusion at 2.5 seconds, targeted mass inclusion and exclusion with apex detection and stepped HCD collision energy at 50 ms injection time to the detector.

5 µL injections of concentrated samples were used for the LC resolution, using the same analytical chromatography parameter as previous: a 2.1 mm ID x 0.2 µm porosity stainless steel filter, a security guard cartridges Polar-RP 4 x 2.0 mm ID PN: AJ0-6075, and the analytical column Synergi 100 mm x 2 mm, 2.5 µm PN: 00D-4371-B0 from Phenomenex (CA, USA). The column temperature was maintained at 40°C throughout the run, and the injection volume was 1 mL. The buffer system included water and 0.1% formic acid (A2) and methanol (B2) 2mM ammonium formate 0.1% formic acid, with a constant flow rate of 0.25 mL/min. The gradient began with 5% organic solvent (B2) for 2 minutes, followed by a linear increase to 30% B2 over 2 minutes, a ramp followed to 55% B2 for 3 minutes. A ramp to 70% B2 over 5 min to then a final ramp to 100% B2 over 1 minute and a hold for 2 minutes. The analytical column assembly was returned to initial conditions over 3 minutes and equilibrated for a total analytical runtime of 17 minutes. Data analysis was performed using Compound Discoverer Version 3.3.2 and FreeStyle software Version 1.8 SP1 from Thermo Scientific (CA, USA).

3.3.4 Acute Toxicity Measurements

Acute toxicity measurements were conducted using a Microtox Analyser Model 500 from SDI. The BioTox WaterTox Standard Kit from Environmental Bio-detection Products Inc., which contained *Aliivibrio Fischeri* and the required reagents, was used for the measurements. The

negative control to assess the viability of the bacteria was the sample diluent provided in the kit while the positive control was 100% methanol.

A trial-and-error approach was employed to determine the best way to eliminate interference of active chlorine species generated from the electrochemical treatment which was shown to create a high background toxicity making the results unreliable. Changing the composition of the background electrolyte to remove the NaCl as well as using different concentrations of quenching agents (fully listed in Table A.4 in the appendix) was investigated in absence of GenX to identify the most suitable sample preparation protocol. Based on these results, 0.10 M Na_2SO_4 was used as the electrolyte to avoid interference of active chlorine species produced in the electrochemical treatment process since chlorine is toxic to the bacteria used and is often used in water treatment to kill microorganisms [54]. The samples from the undivided cell and from the reduction compartment of the divided cell were left unquenched, while the samples from the oxidation compartment of the divided cell were quenched with 2000 mg/L sodium thiosulphate to reduce any effect of formed radical species on the bacteria. The pH of the samples was adjusted to between 6 – 8 before analysis.

3.3.5 Solid Phase Extraction and Analysis of Wastewater

The wastewater used as a matrix in some experiments, was analysed to determine the concentration of native PFAS (concentration present in the wastewater prior to spiking). Considering the low concentrations of PFAS in natural waters, samples were prepared using solid phase extraction (SPE), followed by liquid chromatography analysis. The wastewater was extracted using SPE method with Oasis® HLB cartridges (6 mL, 150 mg) to concentrate PFAS compounds purchased from Waters (Milford, MA, USA). Prior to loading, samples (500 mL) were spiked with a standard solution of labelled surrogates to 320 ng/L concentration to account for recovery during the extraction, possible degradation during storage and matrix effects. The pH was adjusted to 2.5, followed by filtration through 1 μm glass fiber filters (Fisher Scientific, Ottawa, ON, Canada). Samples were then loaded manually on the cartridges at a rate of approximately 5 mL/min. Cartridges were rinsed twice with 3 mL of water pH 2.5 followed by 5% MeOH and dried under vacuum for 10 minutes. PFAS were eluted with three successive 3mL additions of 5% ammonium hydroxide-methanol / hexane / dichloromethane at 10:45:45 (v/v/v) solution with a 5-minute

incubation time between each addition. Finally, eluents were evaporated to dryness and reconstituted in 1mL of methanol before storage at 4ºC.

Analysis of PFAS in the samples extracts from SPE was conducted by liquid chromatography atmospheric pressure heated electrospray ionization tandem mass spectrometry, the system consisting of a Vanquish UHPLC-RTC system coupled with an Exploris 120 HRMS mass spectrometer from Thermo Scientific (Bremen, Germany). Heated electrospray ionization (HESI) in negative ion mode was optimized by infusing a standard solution (0.5 mg/mL) and a water-methanol mixture at 350 µL/min. The source capillary voltages were set at 1000 V with activated mild trapping, nitrogen was used as the source and HCD collision gas, with sheath, auxiliary, and sweep gases set at 40, 7, and 0 arbitrary units, respectively. Source temperatures were set at 225ºC for the transfer tube and 250ºC for vaporization, with a lens frequency of 55% for precursor ion beam focusing. Full scan data acquisition was performed over the range of 70 to 1000 m/z with a full width at half maximum (FWHM) resolution of 60,000 at 200 m/z. Data-dependent MS2 (dd-MS2) was conducted with an FWHM resolution of 15,000 for product ion spectrum confirmation.

UHPLC resolution of diluted samples with concentrations ranging from 10 to 2000 ng/L was conducted using a modified chromatography analysis from the original method. To further mitigate source suppression and prevent matrix effect, the system ran on online SPE mode reconcentrating the PFAS on the extracts. The online SPE was performed on a Hypersil Gold AQ C18 column (20 mm x 2.1 mm ID; 12 µm) from Thermo Scientific (CA, USA), utilizing an isocratic gradient at 1 mL/min for 5 minutes with water and 5% methanol. Following the injection cleanup, a valve switch reverse the flow to elute the reconcentration PFAS from the injection on the SPE-column towards the analytical column to perform the analytical resolution using a setup comprising an inline cartridge with a 2.1 mm ID x 0.2 µm porosity stainless steel filter, a security guard cartridges Polar-RP 4 x 2.0mm ID PN: AJ0-6075, and the analytical column Synergi 100 mm x 2 mm, 2.5 µm PN: 00D-4371-B0 from Phenomenex (CA, USA). The column temperature was maintained at 40°C throughout the run, and the injection volume was 1mL. The buffer system included water and 0.1% formic acid (A2) and methanol (B2) 2mM ammonium formate 0.1% formic acid, with a constant flow rate of 0.25 mL/min. The gradient began with 5% organic solvent (B2) for 2 minutes, followed by a linear increase to 30% B2 over 2 minutes, a ramp followed to 55% B2 for 3 minutes. A ramp to 70% B2 over 5 minutes to then a final ramp to 100% B2 over 1 minute and a hold for 2

minutes. The analytical column assembly was returned to initial conditions over 3 minutes and equilibrated for a total analytical runtime of 17 minutes. Quantitative analysis of the target PFAS compounds (PFBA, PFBS, HFPO-GenX, PFHxA, 6:2 FTS, PFOA, PFHxS, PFOS) was performed using an eight-point linear calibration curve with $R^2 < 0.99$ and 1/x weighting. Data were analyzed using Quan Browser Xcalibur Version 4.4 software from Thermo Scientific (CA, USA).

3.4 Statistical Analysis

GraphPad Prism was used as the software for all statistical analysis. The natural logarithm of the normalised concentration and time data was calculated, then averaged for each experiment. The simple linear regression of that result was done, with the line being forced to go through the origin ($x = 0$, $y = 0$). The residuals from the linear regression were confirmed to scatter evenly around zero to verify the normality of the data and the homogeneity of the variance. From those results, the regression data was entered into a separate table where the mean and standard error of the mean (SEM) were the slope and standard error slope from the regression. The total number of data points from all of the replicates of an experiment, 'N', the mean and the SEM were used in an Ordinary one-way ANOVA Tukey multiple comparisons test to compare selected experimental runs against each other. The alpha used for this test was 0.05. The detailed results from the statistical analyses can be found in Appendix B.

Chapter 4 Results and Discussion

4.1 Preliminary Experiments

Previous literature had reported high rates of degradation (>90%) of several PFAS, including PFOA, in an undivided cell [31], [53], [55]–[57]. Figure 4.1 below displays the results of PFOA degradation in an undivided cell at 22.8 mA/cm^2 in 0.50 M Na_2SO_4 + 0.60 M NaCl. This relatively high concentrations of salts were used to ensure that sufficient ionic conductivity was achieved in the cell in order to minimize potential (voltage) losses and heating of the electrolyte.

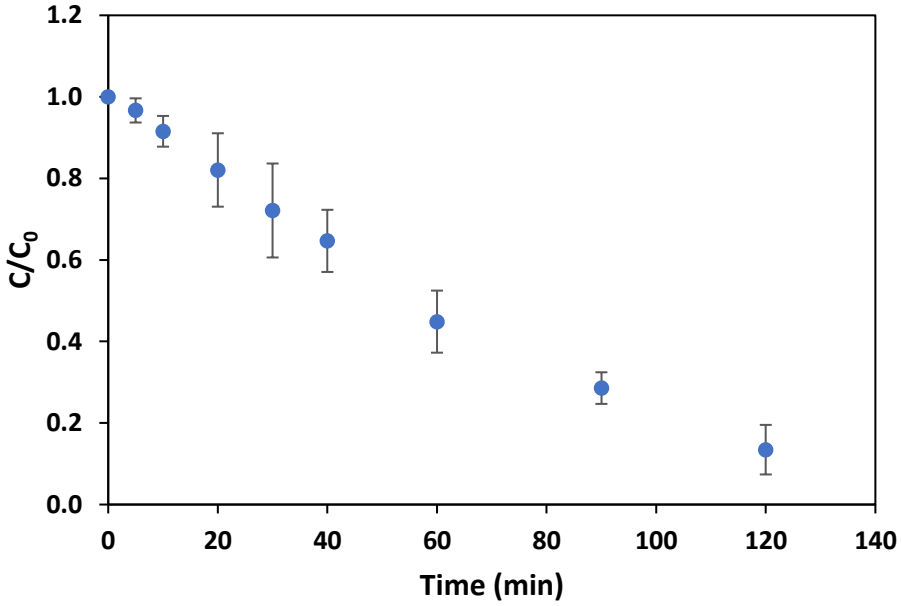

Figure 4.1 Degradation of 100 mg/L PFOA in an undivided cell at 22.8 mA/cm^2; n = 4, error bars = 1 standard deviation; anode = BDD; cathode = 316L stainless steel, 300 rpm.

The preliminary results in Figure 4.1 above indicate that the experimental protocol used provided results comparable with literature. Further references can be found in Table A.1 in Appendix A. After establishing this benchmark, GenX was used for the remainder of the experiments.

As was previously mentioned in Chapter 2, the electrochemical degradation of GenX is possible on a BDD anode, with some sources reporting over 80% degradation [37]–[39].

To verify that significant degradation of GenX could be reproduced, preliminary experiments were conducted using conditions reported in literature and using two different concentrations of electrolyte. Figure 4.2 presents the degradation of GenX up to 4 h in an undivided cell using boron doped diamond (BDD) as the anode and 316L stainless steel as the cathode. In Figure 4.2 0.50 M Na_2SO_4 + 0.60 M NaCl was first used in the initial 2-hour experiment to ensure that sufficient ions were present in solution to conduct the charge, followed by an experiment done for 4 hours in 0.10 M Na_2SO_4 and 0.12 M NaCl. The experiment done at a lower salt concentration showed a faster GenX degradation rate, and this lower salt concentration was then employed in further experiments. In addition, the lower salt concentration reduced the burden that the higher salt concentration would have on the analytical instruments used for the subsequent analysis of GenX concentration.

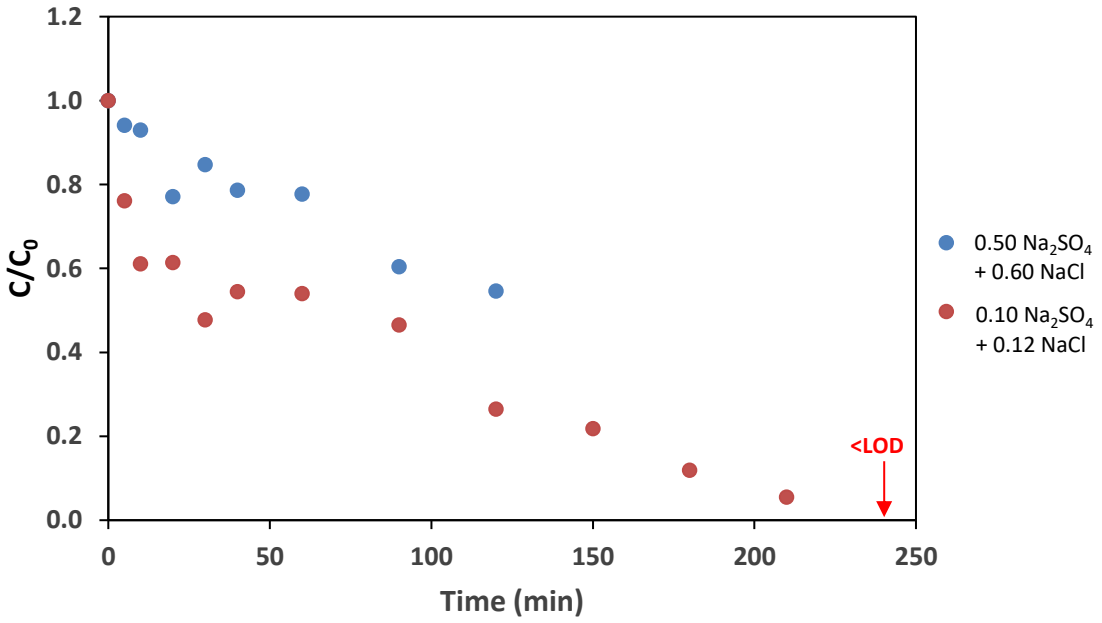

Figure 4.2 Degradation of 5 mg/L GenX in an *undivided* cell at 22.8 mA/cm^2 for 2 h and for 4 h. anode = BDD; cathode = 316L stainless steel, 300 rpm.

Both concentrations of electrolyte tested demonstrated degradation of GenX, with removal of GenX to below detection achieved within the 4-hour period for the less concentrated electrolyte, which provided a faster removal of GenX. This is very apparent when the remaining concentration of GenX after 120 mins is compared for the two experiments. In the 2-hour experiment, 55% of the initial GenX concentration remained which is almost double percentage of GenX that remained

in the 4-h experiment (26%). It could be speculated that this is due to the oxidation of chloride ions to chlorine gas, which is a parallel anodic reaction with GenX oxidation. At a higher chloride concentration in the electrolyte, the contribution of this reaction to the total oxidation reactions is larger, resulting in a smaller proportion of current used for GenX oxidation (see equation 4.1).

$$2Cl^- - 2e^- \rightarrow Cl_2 \quad (4.1)$$

The evolution of chlorine gas, similar to the oxidation evolution reaction in equation 2.6 in Section 2.1.1., is a competing reaction to degradation of GenX. Consequently, in all the subsequent experiments presented further in the thesis, the supporting electrolyte used was 0.10 M Na_2SO_4 + 0.12 M NaCl, if not stated otherwise.

The results in Figure 4.2 can be compared to that of Pica et al. [37], Babu et al. [39] and Zeidabadi et al. [38], [55], [58], who studied in the degradation of GenX on a BDD in slightly different conditions (details can be found in Table A.1). To summarise, Pica et al. investigated the degradation of GenX at an initial concentration of 4.98 mg/L using Na_2SO_4 and NaCl at lower concentrations that what was used in the experiments presented in Figure 4.2 (<0.05 M). Using the most optimised experimental conditions, they reported just below 60% GenX remaining after 2 hours and ~40% of GenX remaining after 4 hours, which are lower removal values than those shown in Figure 4.2 above.

Similarly, Babu et al. reported <30% GenX remaining after degradation of 2 hours and ~ 5% remaining after 4 hours of degradation at 20 mA/cm^2 using a 0.005 M Na_2SO_4. This is more comparable with preliminary results obtained above, however, the initial concentration used was noticeably higher 15 mg/L. Likewise, Zeidabadi et al, studied the degradation of GenX, along with other PFAS at higher concentrations, 20 mg/L [55]. They reported <20% of GenX remained after 2 hours of treatment at 10 mA/cm^2 in 0.1 w/v% Na_2SO_4. Despite, this being is a better result than what was displayed in Figure 4.2, it was decided to keep the experimental parameters at 5 mg/L GenX and 0.10 M Na_2SO_4 + 0.12 M NaCl to avoid using higher concentrations of GenX.

The preliminary results in Figure 4.2 demonstrate that GenX could indeed be degraded electrochemically, as previously reported in literature. This warrants more comprehensive

investigation on its degradation using different electrode materials and a different electrochemical cell type.

4.2 Degradation of GenX on Different Cathode Materials

After proving that GenX degradation using the current conditions result in similar degradation percentages to what was reported in the literature in an undivided cell, the degradation of GenX was studied on different anode and cathode materials in the *divided* cell, the use of which had not been, to the best of the thesis author's knowledge, priorly investigated by others. In Figure 4.3, the results for the oxidation (4.3a) and reduction (4.3b) of GenX are presented for the tested cathode materials. BDD and $Ni_{40}Co_{60}$-oxide were the anodes studied while Au, Ti, Sn, Cu, graphite, BDD and stainless steel were the cathodes studied. These materials were chosen due to combination of several factors: they were either known to be inexpensive, have good conductivity, be stable or be innovative in the context of the current experimental system (in particular the $Ni_{40}Co_{60}$-oxide). It should be noted that the B&K Precision® 1687B Power Supply, available at the time of doing the experiments, was limited to 36.4 V, which meant that due to the higher resistance in the divided cell setup, only lower current densities were possible in the experiments presented in this section. The degradation results in Figure 4.3 are presented along with the adsorption control experiments, which show total adsorption being 7% and 6% for the oxidation and reduction compartments respectively. As with the other results in Figure 4.3, the control experiments were done in duplicate.

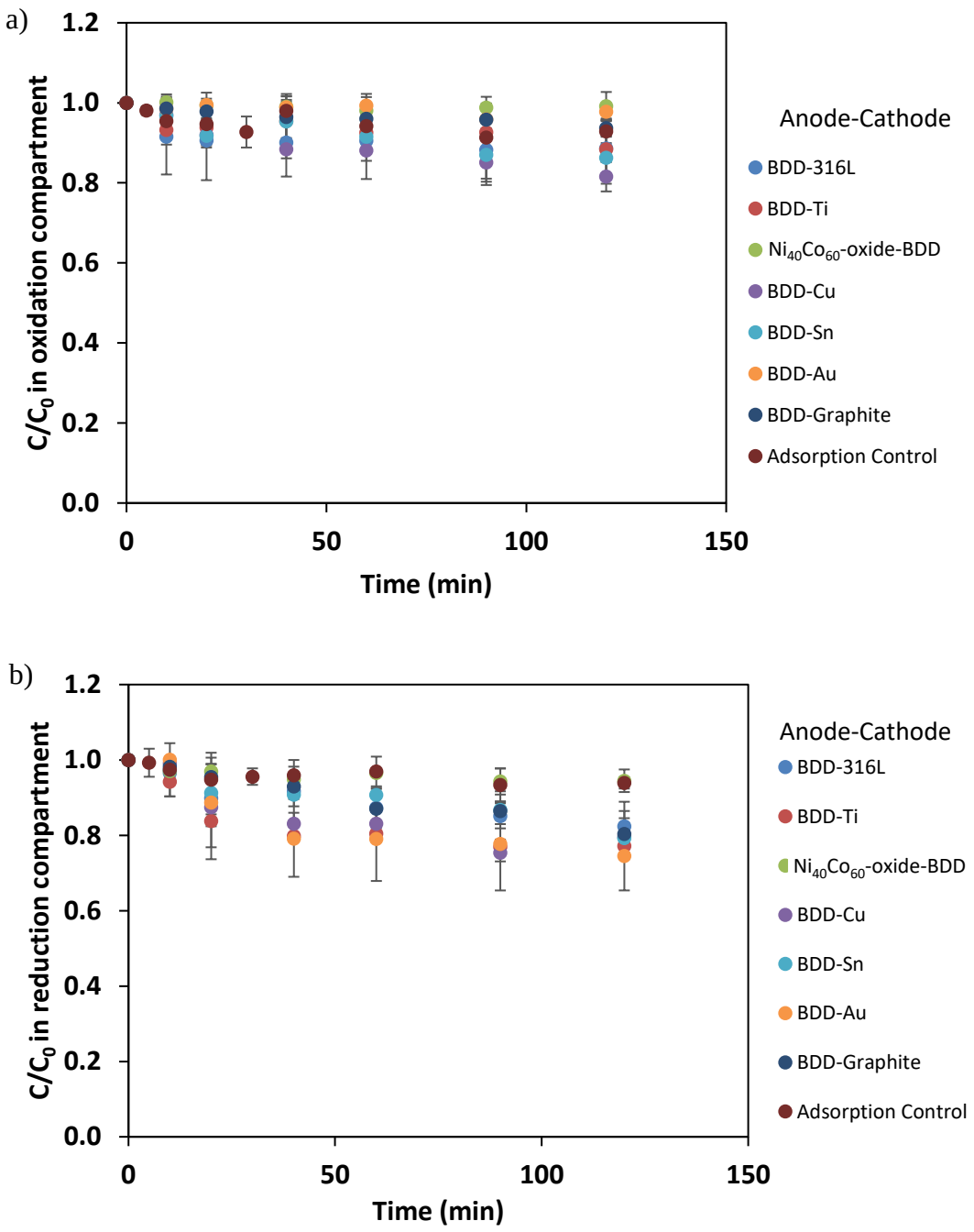

Figure 4.3 Degradation of GenX on different electrode materials in a *divided* cell at 13.5 mA/cm^2 a) oxidation, b) reduction; n = 2, error bars = 1 standard deviation. In all the experiments the anode was BDD except when it was used as the cathode, in which case $Ni_{40}Co_{60}$-oxide was used as the anode. Agar membrane was used to separate the two electrolyte compartments.

The results show that although the current was low (13.5 mA/cm^2) GenX could be degraded by both reduction and oxidation. From the ANOVA tests, it was determined that only the combinations BDD-Cu, BDD-Au and BDD-Ti led to removal by reduction that were statistically different to the adsorption control experiment during which no current was applied. The following experiments were thus limited to this smaller sets of cathode materials.

For the degradation in the oxidation compartment, it appeared that even when the same anode, BDD is used for electrooxidation, there is a slight amount of variation in the degradation (ca. 16%). However, since the current density is fairly low, this effect is not very apparent. Furthermore, the ANOVA tests indicate that there is no significant difference for the degradation in the oxidation compartment between the electrode pairings, except for between BDD-Cu and $Ni_{40}Co_{60}$-oxide-BDD. The differences in the performance of these two anodes are more apparent when the average of the degradation on BDD is compared to that on $Ni_{40}Co_{60}$-oxide. The former anode degrades around 10% of GenX in the oxidation compartment over the different cathode pairings while the latter only degrades ~1% of the GenX when BDD is the cathode.

The use of the *divided* cell enabled the differentiation between the degradation of GenX by oxidation, in the compartment containing the anode, from the degradation by reduction, in the compartment containing the cathode. Figure 4.4 presents a subset of the results presented in Figure 4.3 to focus on the most efficient conditions tested (BDD as the anode and Au, Cu and Ti as the cathode), the data are an average of the values obtained during experiments with Ti, Cu and Au cathodes. The use of BDD indeed leads to the *oxidation* of GenX, which is in accordance with literature [37], [39]. The small degree of GenX degradation (around 10% within the time interval of the experiment) can be explained by the low current density used (13.5 mA/cm^2); as already stated, this was limited to the power supply that was available at the time.

Figure 4.4b shows the performance of a titanium, gold and copper cathode in degrading GenX by *reduction*, while used in combination with BDD in the (separate) anodic compartment. The respective percentages of degradation on the Cu, Ti and Au cathodes, after 2 hours, are 12.8%, 11.7% and 17.7%. There was no statistical significance between these results according to the ANOVA test performed. The p-values obtained between all the cathodes were all >0.99 for an alpha of 0.05 (see Table B.2).

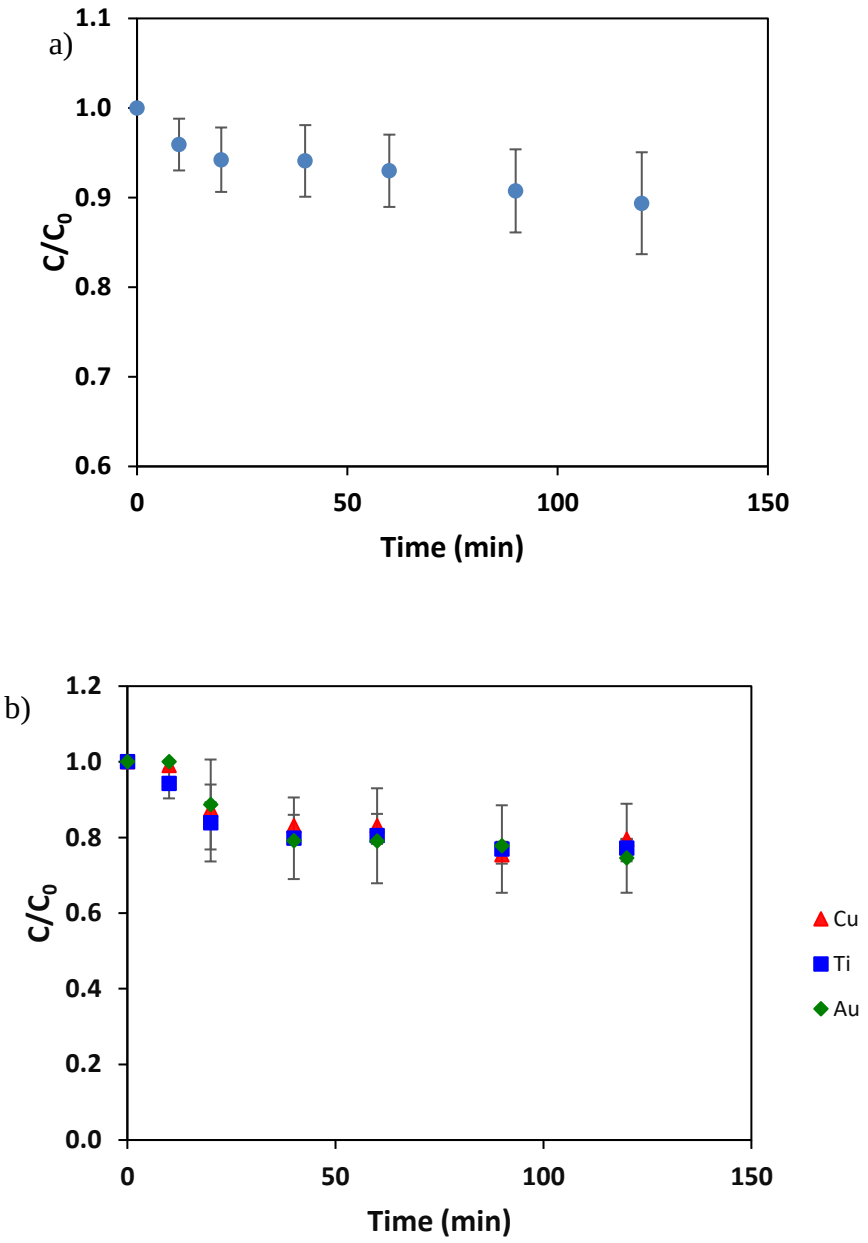

Figure 4.4 Degradation of GenX by a) electrooxidation on a BDD anode, and b) electroreduction on Ti, Cu and Au cathodes in the *divided* cell at a current density of 13.5 mA/cm^2. a) n = 6, b) n = 2; error bars = 1 standard deviation, agar membrane was used

To eliminate the maximum current-density limitation experienced with the *divided* cell, further experiments on GenX degradation using the same power supply were conducted in the *undivided* cell using the optimal combinations obtained in the *divided* cell, i.e. BDD as the anode and Au, Cu

and Ti as the cathode. In Figure 4.4 it can be seen that the degree of removal of GenX at a higher current density is significantly higher than that one at the lower current density (Figure 4.3 and Figure **4.4**). The most efficient cathode material was found to be copper (ca. 76% GenX removed after 120 minutes) compared to gold and titanium which did not statistically differ according to the ANOVA test (ca. 63 and 61%, respectively). The GenX degradation kinetics was found to follow the pseudo-1st-order kinetics, yielding the apparent rate constants of: $k_{Cu} = 10.8\times10^{-3}$ min^{-1} ($R^2 = 0.971$), $k_{Au} = 7.90\times10^{-3}$ min^{-1} ($R^2 = 0.983$), and $k_{Ti} = 7.88\times10^{-3}$ min^{-1} ($R^2 = 0.981$).

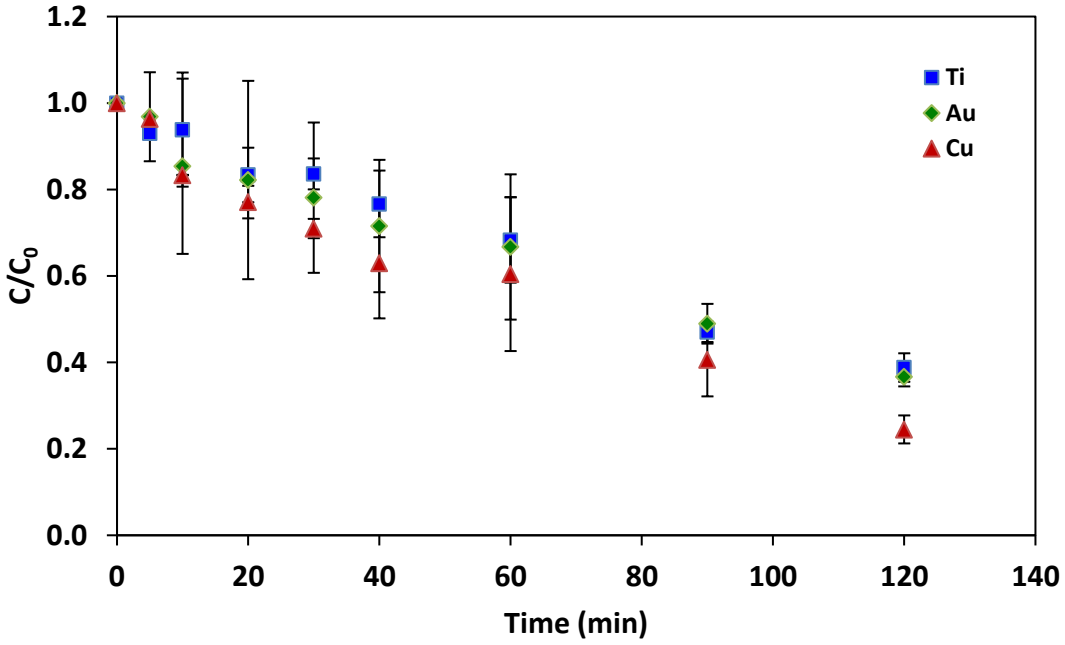

Figure 4.5 GenX degradation in the *undivided* cell using different cathode materials with BDD as the anode at 50 mA/cm^2. n =3, error bars = 1 standard deviation.

Taking into account the results in Figure 4.4 and Figure 4.5, with the former evidencing a higher degree of GenX degradation when Cu was used as the cathode, it was decided to use copper as the cathode material in all subsequent experiments, while BDD was used as the anode material.

4.3 Degradation of GenX at Different Current Densities

Albeit done in two different types of the electrochemical cell, the results in Figure 4.4 and Figure 4.5 showed that the current density has a profound effect on the rate of GenX degradation. Hence it was of interest to study the effect of current density on the rate of GenX degradation in more detail. Given that at the time of performing these experiments the power supply used was limited to enabling only lower current densities in the *divided* cell (due to the high resistance between the two electrolyte compartments), the rate of degradation of GenX at different current densities was studied in the *undivided* cell, employing the BDD anode and Cu cathode. As expected, the higher the current density used, the higher the degradation rate of GenX was recorded (see Figure 4.6). This is in accordance with the modified Faraday law:

$$\nu = \frac{I}{nF} \tag{4.2}$$

which, in the form presented, shows the direct relationship between the amount of redox species reacted in a unit time, i.e. the reaction rate, v (mol/s) and current I (A), where n stands for the number of electrons transferred, and F for the Faraday constant (96485 C/mol). The results from the statistical tests show that there is a significant difference between the degradation occurring at 13.5 mA/cm^2 and 50 mA/cm^2, and at 20 mA/cm^2 and 50 mA/cm^2. However, the degradation at 13.5 mA/cm^2 and that at 20 mA/cm^2 do not show a significant difference ($p = 0.97$), likely due to the large variation in the degradation results obtained at 20 mA/cm^2, leading to a larger standard deviation.

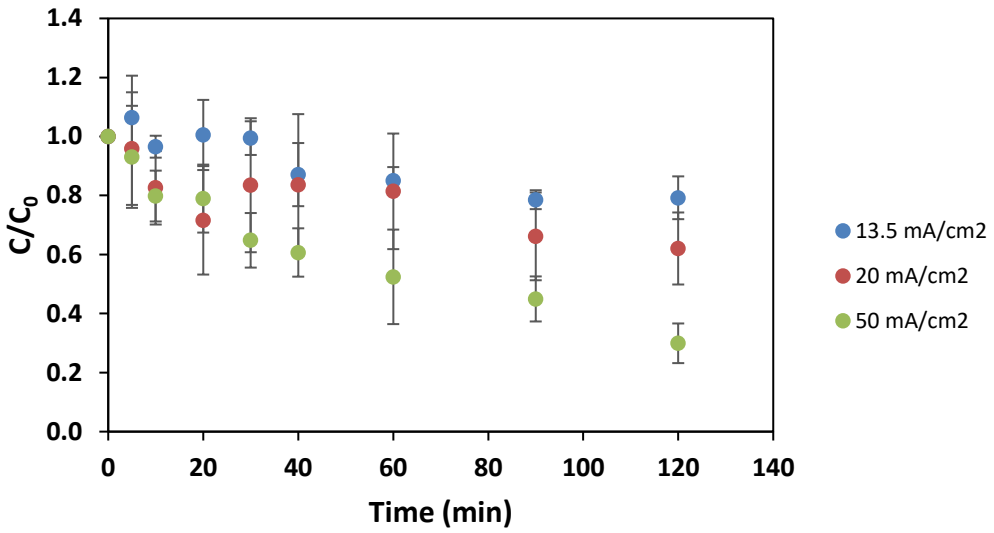

Figure 4.6 Degradation of GenX at different current densities in an undivided cell, n = 3, error bars = 1 standard deviation

The rate of degradation of GenX at different current densities exhibits pseudo-first order kinetics, yielding the following rate constant: at 50 mA/cm^2 $k_{50} = 10.8\times10^{-3}$ min^{-1}, at 20 mA/cm^2 and 13.5 mA/cm^2 the constants are $k_{20} = 3.9\times10^{-3}$ min^{-1} and $k_{13.5} = 2.2\times10^{-3}$ min^{-1}, respectively. This dependence was found to be linear ($R^2 = 0.9996$), as shown in Figure 4.7, indicating that the efficiency of the GenX degradation process, i.e. how much of the current is used toward degrading GenX, remains constant *within the investigated current range*. Namely, it is common to expect a decrease in current efficiency in electrochemical degradation processes based on oxidation/reduction of a pollutant due to the increase in kinetics of the parallel oxygen/chlorine oxidation and hydrogen reduction reactions, respectively. If this was the case, a deviation from the linear behaviour with an increase in current density towards the logarithmic-like dependence would have been noticed in Figure 4.7 [59].

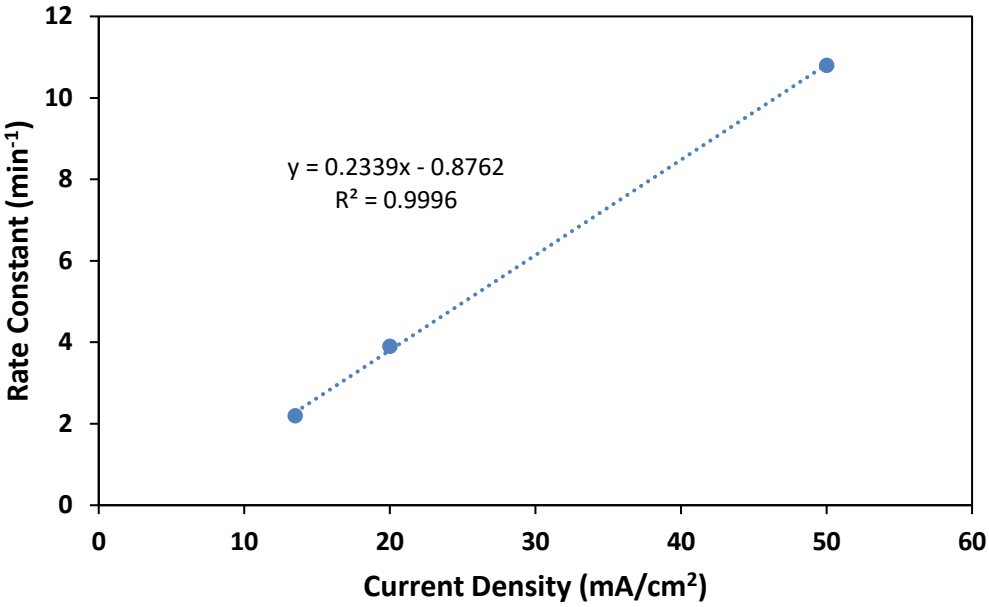

Figure 4.7 Rate constants of GenX degradation vs current density in an undivided cell, anode = BDD, cathode = Cu

Following the acquisition of a high-current/high-voltage power supply, it was possible to also investigate the electrochemical degradation of GenX at higher current densities in the *divided* cell., allowing the independent study of reduction and oxidation of GenX at higher current densities. Consequently, these experiments were done in the current range from 13.5 mA/cm^2 to 100 mA/cm^2 and the corresponding results are presented in Figure 4.8.

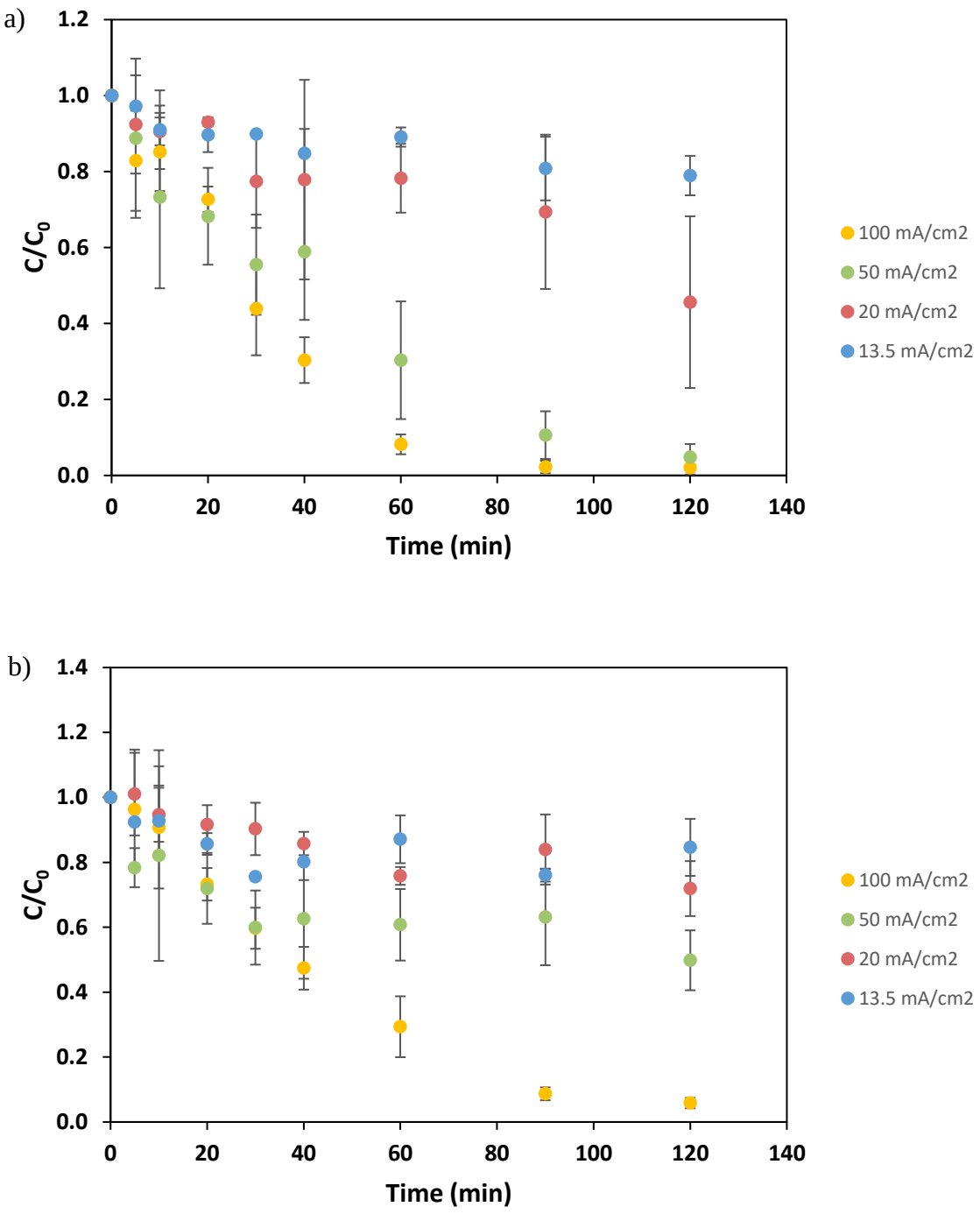

Figure 4.8 Degradation of GenX at different current densities in a *divided* cell by a) oxidation and b) by reduction. n = 3, error bars = 1 standard deviation, anode = BDD, cathode = Cu. At 13.5 and 20 mA/cm^2 the agar membrane was used, at 50 and 100 mA/cm^2 the Nafion 117^{TM} membrane was used

Similar to the undivided cell, the degradation rate increased with increasing current density, and it was observed that the trend applies to both oxidation and reduction. Although near complete GenX removal has been reported in the literature (e.g. up to 97% reported by Babu et al.[39]), this was in terms of the overall process, i.e. the sum of oxidation and reduction. The literature did not distinguish between the two, and referred the degradation process as electrooxidation only. The results in Figure 4.8b demonstrate that its almost complete removal by reduction is also possible on the Cu electrode, under the experimental conditions employed.

The GenX reduction/oxidation curves in Figure 4.8 exhibited a pseudo-1st order kinetics (see Figures A.6 in the appendix); however, the corresponding rate constants were not calculated due to the wide temperature variation during the reaction at higher current densities (ca. 20^{o}C difference from the beginning to the end of the experiment) caused by the high ion-transport resistance in the divided cell between the two electrodes. In addition, the high temperature in the cell resulted in the agar membrane melting at current densities of 50 mA/cm^2 and higher. As a result, the membrane was switched at the higher current densities from the agar membrane to the Nafion^{TM} 117 membrane. Nafion^{TM} 117 was chosen because of its high thermal stability (up to 190℃) and excellent performance as a proton exchange membrane [60]. Despite Nafion^{TM} 117 being fabricated with a polytetrafluoroethylene backbone (PTFE), it was assumed that there would be little interference due its stability and the comparatively high GenX concentration used in the experiments (5 mg/L).

The charge efficiency of the two GenX redox reactions (oxidation and reduction) at the different current densities was investigated by plotting the dependence of GenX removed as a function of charge passed through the electrochemical cell. In Figure 4.9, the efficiency of the reaction appears to remain the same for both the GenX oxidation and reduction within the current density range investigated. Taking this into account, it could be concluded that it is preferable degrading GenX at higher current density since the degradation rate is faster, while no additional charge losses due to the occurrence of parallel reactions are invoked, which is of practical importance. Nevertheless, due to the temperature increase at high current density and the danger of membrane degradation, 50 mA/cm^2 was chosen as the optimal current density in the experiments to follow.

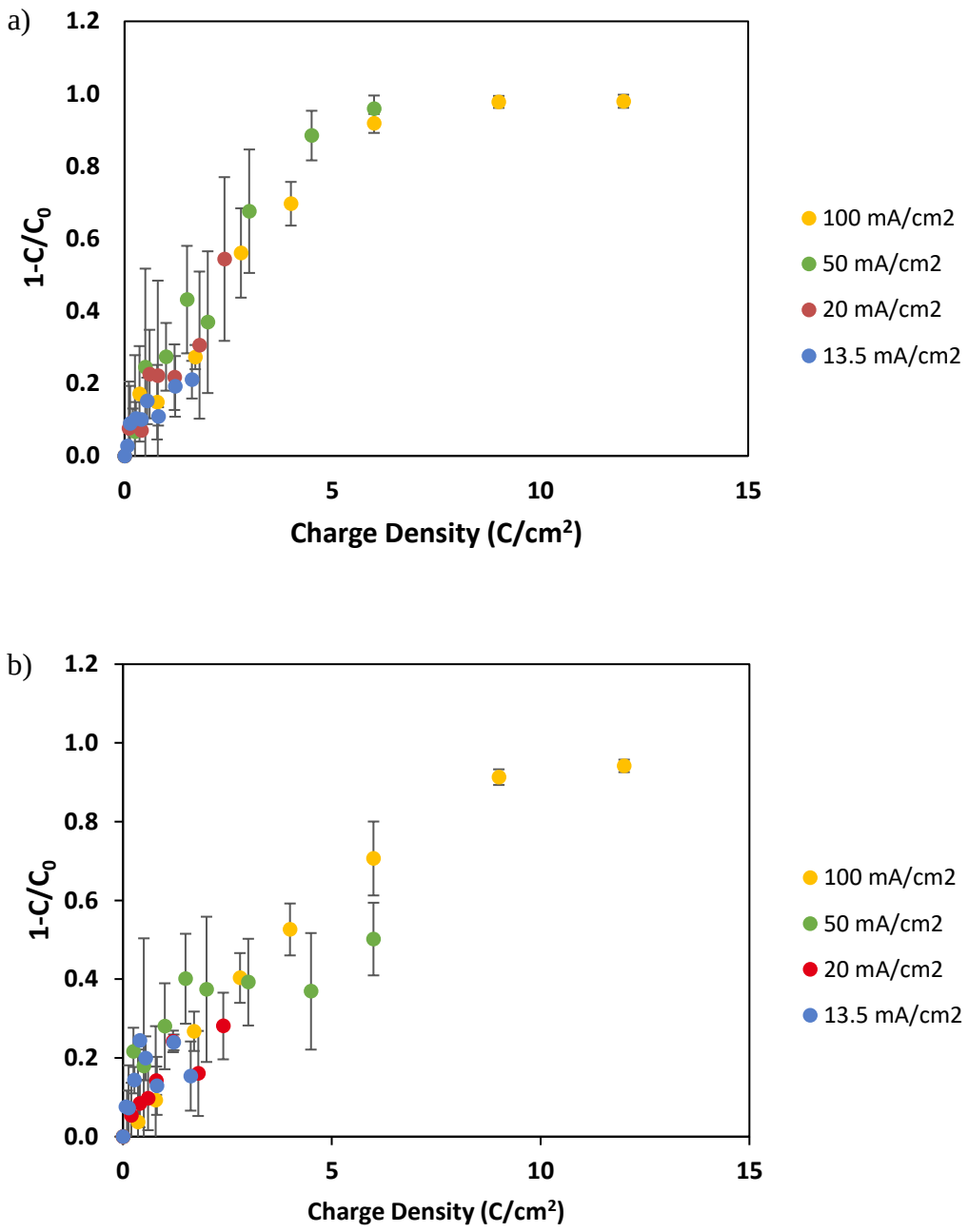

Figure 4.9 Dependence of the relative amount of GenX degraded at different current densities on the amount of charge passed through the electrochemical divided cell for GenX a) oxidation and b) reduction. n= 3, error bars = 1 standard deviation, anode = BDD, cathode = Cu. At 13.5 and 20 mA/cm^2 the agar membrane was used, at 50 and 100 mA/cm^2 the Nafion 117^{TM} membrane was used

4.4 Comparison of Performance in Undivided and Divided Cell

Seeing that there is literature evidence for the electrochemical degradation of GenX in the undivided cell [37]–[39], typically reported as just the electrooxidation of GenX, and none specifically on the electroreduction of GenX, it is of interest to investigate how much the latter reaction contributes to the overall GenX electrodegradation. In order to do this, we first had to confirm that the overall removal of GenX was similar in both types of setups. To confirm this, the same experiment was performed in the undivided and divided cell and results were compared to determine the total number of moles degraded by each method. These results can be seen in Figure 4.10, where the number of moles degraded in the oxidation and reduction compartments of the divided cell are summed and compared to the number of moles degraded in the undivided cell (note that the total electrolyte volume in both types of cells was the same, 250 mL, allowing for the comparison to be made).

a)

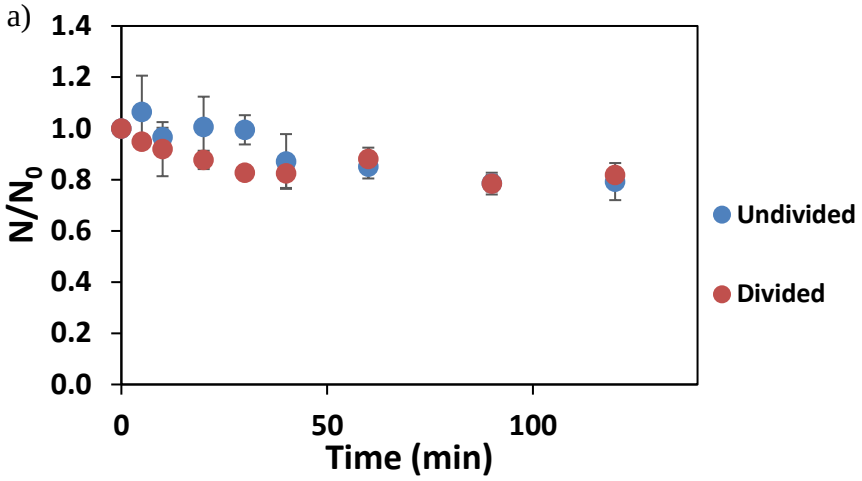
1.4
1.2
1.0
0.8
0.6
0.4
0.2
0.0
N/N0
0
50
100
Time (min)
Undivided
Divided

b)

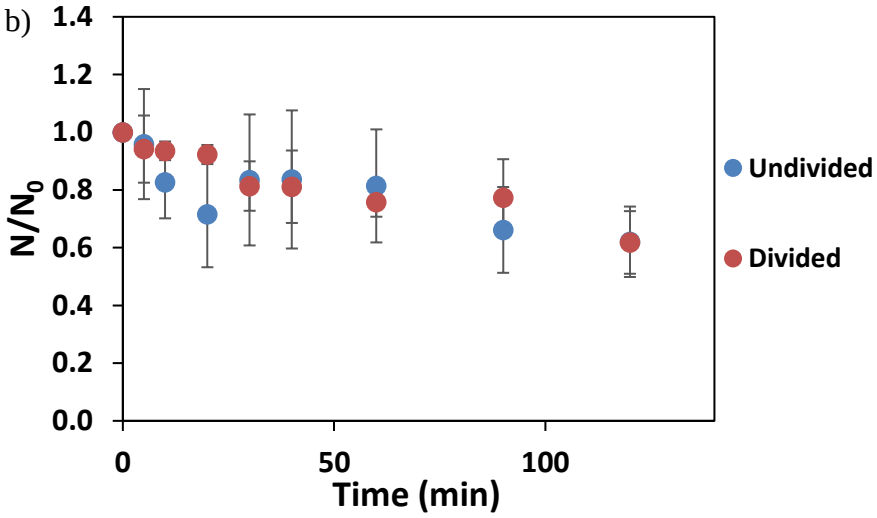
1.4
1.2
1.0
0.8
0.6
0.4
0.2
0.0
N/N0
0
50
100
Time (min)
Undivided
Divided

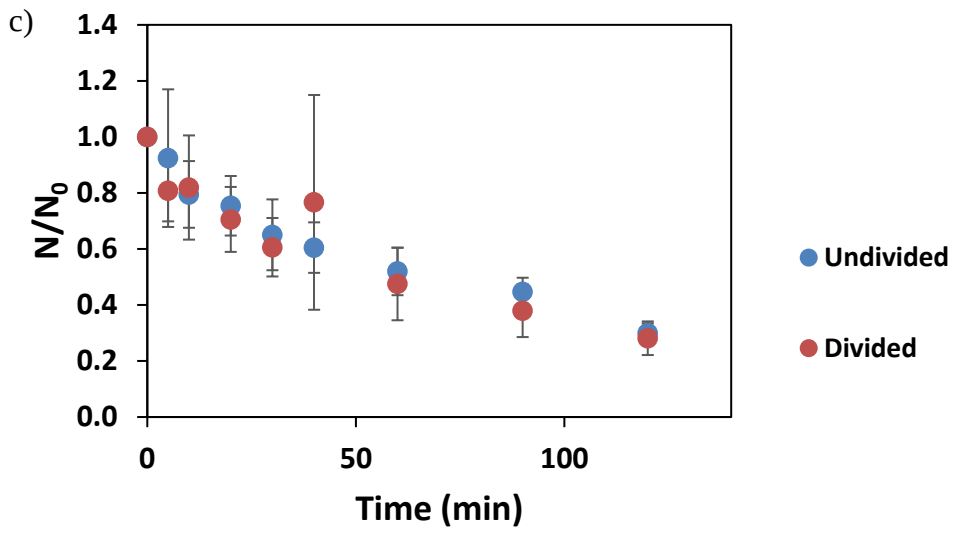

Figure 4.10 Number of moles of GenX degraded in an undivided and divided cell at a) 13.5 mA/cm^2, b) 20 mA/cm^2, and c) 50 mA/cm^2, n = 3, error bars = 1 standard deviation, anode = BDD, cathode = Cu, agar membrane at 13.5 and 20 mA/cm^2, Nafion 117^{TM} at 50 mA/cm^2

According to the results from the ANOVA tests, the number of moles degraded by the undivided and the combined compartments of the divided cell show no statistical difference for all three current densities tested. This means that the overall degradation is the same, independent of the cell type chosen, suggesting that the findings on the separate reduction and oxidation reactions in the divided cells could potentially be applicable to the undivided cell, at least in terms of the contribution of GenX oxidation and reduction to the overall GenX degradation. Additional results with Ti and Au as the cathode done at 13.5 mA/cm^2 are consistent with these results, as can be seen in Figure A.3 in the appendix.

As seen in Figure 4.10, the overall degradation of GenX in both the divided and undivided cell at lower current densities was an average 19.5% at 13.5 mA/cm^2 and 38% at 20 mA/cm^2 with an initial GenX concentration of 5 mg/L. This is much lower to what was found in literature where, 84.9% degradation at 10 mA/cm^2 and 97% degradation at 20 mA/cm^2 were reported by Zeidabadi et al. and Babu et al. respectively. However, these studies used higher initial concentrations of GenX (20 mg/L and 15 mg/L) than what was used in the experiments shown in Figure 4.10 (5 mg/L GenX). On the other hand, when the results were compared to a study at a similar GenX

concentration and current density (4.98 mg/L GenX at 50 mA/cm^2) by Pica et al. [37], the results displayed in Figure 4.10 were better, 71% compared to ca. 60% GenX degradation they reported.

As previously mentioned, when the literature reports electrochemical GenX degradation it refers to the overall degradation process as the GenX "electrooxidation" in an undivided cell [37]–[39]. However, the results above demonstrated that GenX can be degraded by both reduction and oxidation, and the results also indicate that both are occurring in the undivided cell. Referring to the above-presented results in Figure 4.9 and Figure 4.10, the relative contribution of the reduction and oxidation reactions to the overall GenX degradation was determined and the results are presented in Figure 4.11 at different current densities.

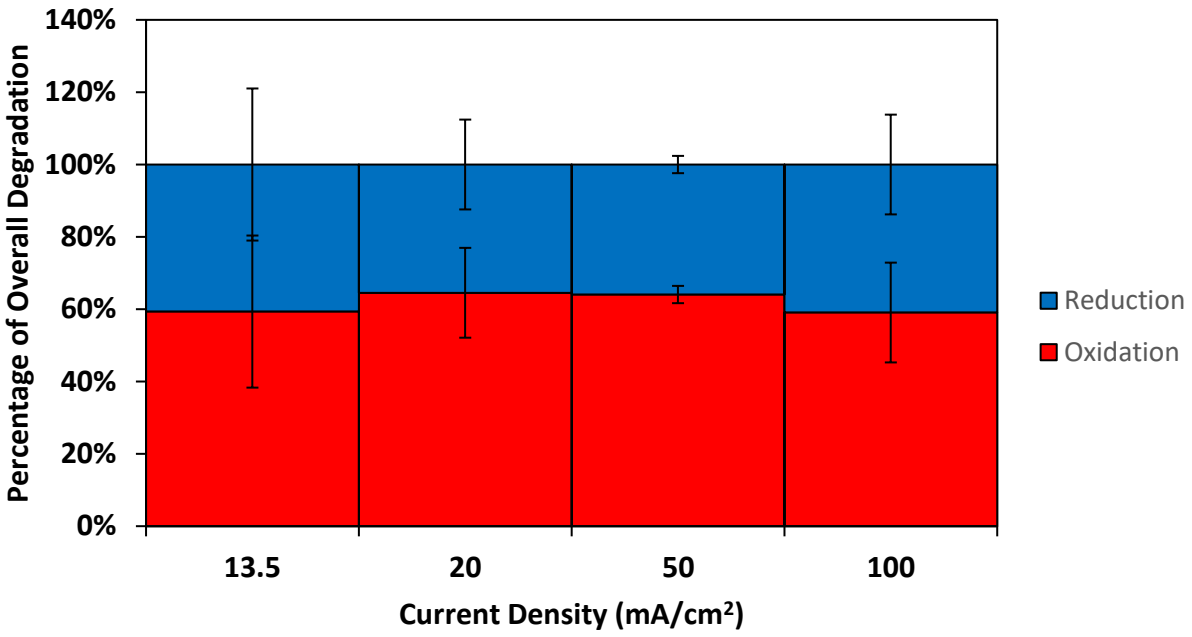

Figure 4.11 Contribution of electrooxidation and electroreduction towards the overall degradation of GenX at different current densities. n = 3, error bars = 1 standard deviation, anode = BDD, cathode = Cu

The overall trend from Figure 4.11 suggests that over the current density range shown, the average contribution of electrooxidation to the overall reaction is 62 ± 3% compared to the 38 ± 3% from electroreduction. This result highlights the significance of electroreduction to the overall reaction

demonstrating that it contributes greatly to the overall degradation of GenX. The higher contribution of electrooxidation to the overall degradation can be attributed to the excellent performance of the BDD anode (its stability and high overpotential for the OER) which is currently a state-of-the-art anode used in electrochemical waste-water-treatment reactors. It should be noted that these results are specific to electrodegradation of GenX using *copper* as the cathode. The contribution of electrooxidation and electroreduction to the overall degradation was also studied at 13.5 mA/cm^2 using Au and Ti as the cathodes with BDD as the anode as seen in Figure 4.12 below.

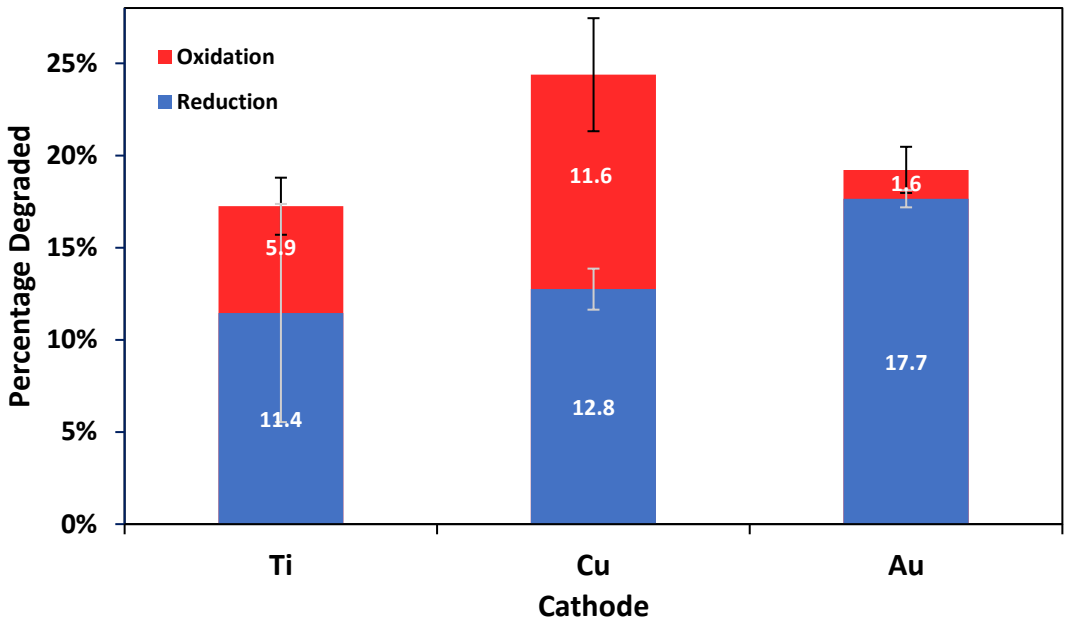

Figure 4.12 Relative contribution of GenX degradation by electroreduction (Ti, Cu or Au) and electrooxidation (BDD) after two hours of treatment. The degradation current density was 13.5 mA/cm^2.

Even though the total degree of degradation with each cathode material employed is similar and within 10% of each other, the relative contribution of GenX degraded by electroreduction differs between the cathode materials. For copper, the relative amount of GenX degraded by electroreduction is around 52%, whereas titanium yielded a higher degree of GenX degradation by reduction (ca. 66%). On the other hand, the largest relative contribution of electroreduction to the

total amount of GenX degraded was recorded when gold was used as the cathode, ca. 92%. The variability of the contribution to the removal by reduction, while the overall removal remained fairly consistent (which holds true at 50 mA/cm^2, as seen in Figure 4.5), suggests that the oxidation of GenX on the BDD electrode was influenced by the cathode material used. This result was not expected given that the experiments were performed in the divided cell with separate cell compartments using the same BDD anode for all the cathode material tested.

In order to investigate the origin of this behaviour, electrode potential in each compartment was measured with respect to the saturated-calomel-reference-electrode for the different cathodes using BDD as the anode, with the aim of testing the hypothesis that the absolute electrode potential played a role in producing the differences in Figure 4.12. It can be seen in Figure 4.13, that the potential for the cathodes does not vary between the electrodes studied, while there is a slight variation in the anode potential when BDD is paired with different cathodes. An ANOVA test, however, proved that this variation was insignificant with a p-values > 0.99 for the comparisons of BDD potentials measured with the different cathode pairings. Hence, under the experimental conditions, the absolute potential of the electrodes was found not to be responsible for the differences in relative contribution of reduction/oxidation at different cathodes that is seen in Figure 4.12.

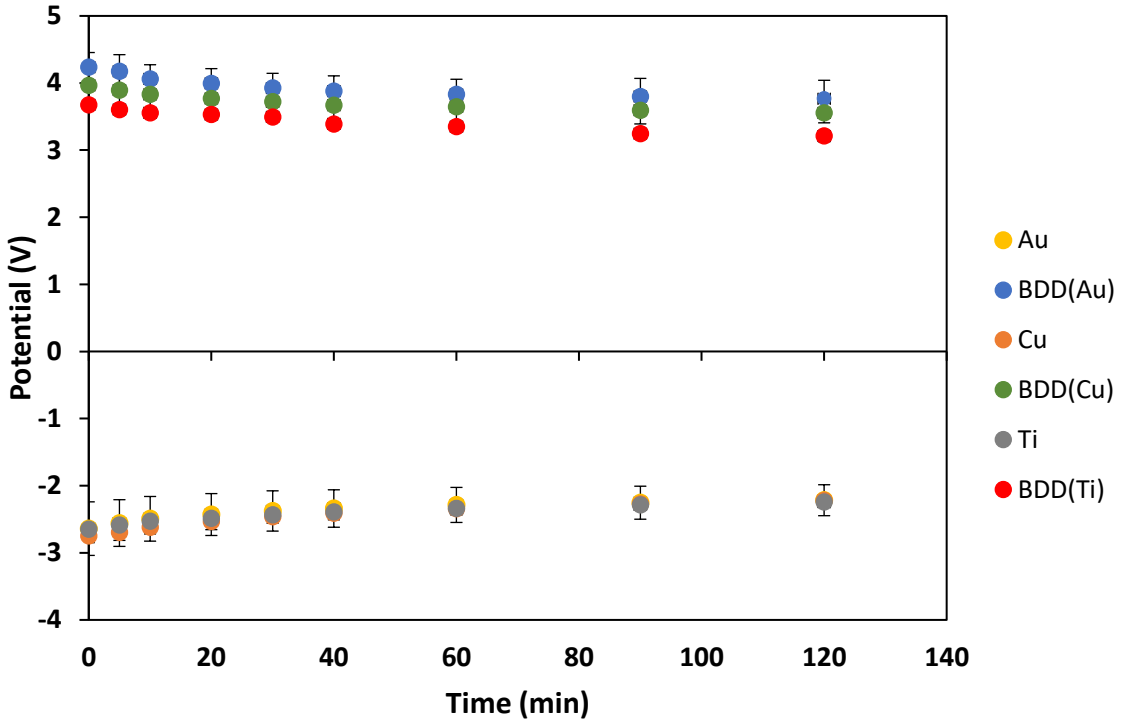

Figure 4.13 Potential of different electrodes during the degradation of GenX in the divided cell at 13.5 mA/cm^2. BDD() in the legend denotes the BDD anode and the cathode it was paired with shown within the parentheses.

4.5 Influence of Different Matrices on GenX Degradation

4.5.1 Influence of Electrolyte Composition

As stated in the background section of the thesis (Section 2.1), organic pollutant molecules can be oxidized either directly at the electrode surface or by strong oxidizing agents formed at the anode surface, such as hydroxyl radicals, persulphates and/or active chlorine species. In the current system, hydroxyl radicals are always formed at the BDD electrode surface since the electrolyte is aqueous. Further, since sulfate and chloride anions are also present in the electrolyte, the remaining two oxidative species (persulphates and active chlorine species) could also be formed and be responsible for oxidative GenX degradation. Hence, in order to investigate the potential influence of different anions and the corresponding radicals on the GenX degradation rate, degradation

experiments were also performed in the divided cell using only Na_2SO_4 and only NaCl at 0.22 M to match total concentration of the anions in all three electrolytes. The corresponding results are presented in Figure 4.14. It is not to expected to see any influence of the anions on the rate of GenX degradation by reduction. This is also evidenced by the results shown in Figure 4.14b. However, the results that represent the GenX degradation by oxidation (Figure 4.14a) indicate a slight influence of the electrolyte composition on the rate of GenX degradation. However, this difference is between the degradation experiments when the electrolyte containing both anions and the degradation when the electrolyte containing a single anion type were performed, *not* between the degradation using Na_2SO_4 and that using NaCl. This implies that the electrochemical oxidation and reduction are most likely driven by direct electron transfer between the electrode surface and GenX, as reported by literature for electrodegradation [61], [62]. Thus, contribution of persulphate ions or active chlorine species in GenX oxidation can possibly be considered to be less significant under the experimental conditions employed, based on these results. However, $OH^{\bullet}$ radicals remain as possible contributors to the GenX oxidation.

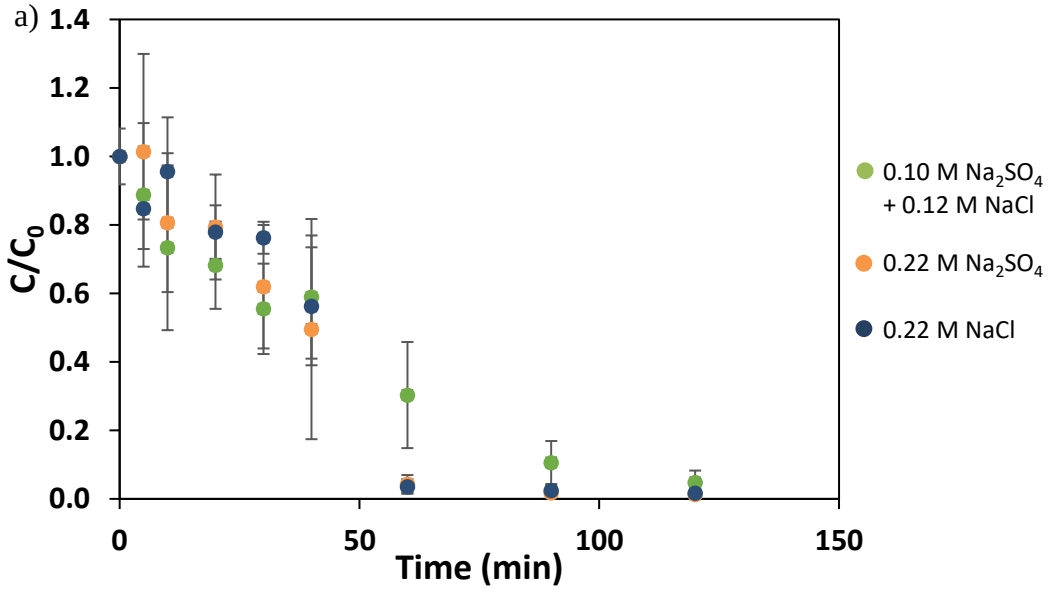

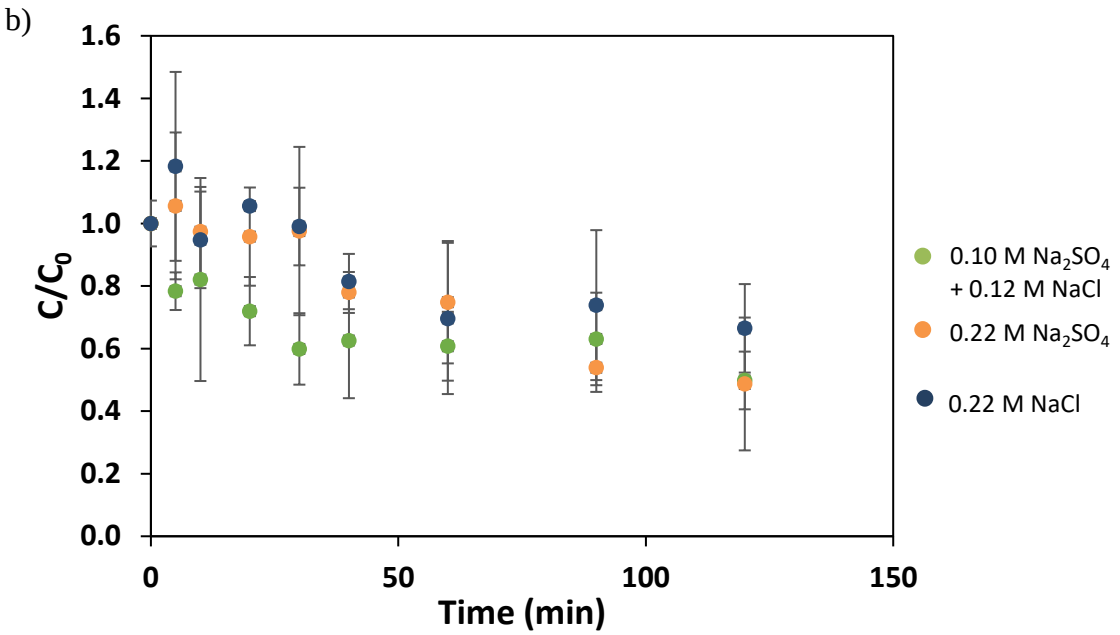

Figure 4.14 Degradation of GenX in different electrolytes in a *divided* cell at 50 mA/cm^2: a) oxidation, b) reduction. n = 3, error bars = 1 standard deviation, anode = BDD, cathode = Cu

Additionally, the influence of concentration of only Na_2SO_4 and only NaCl was also tested, Figure 4.15. When less than half of the salt is present (0.10 M Na_2SO_4 in Figure 4.15a), the shape of the degradation curve in the anodic compartment changes than when both salts are used or when a higher concentration of Na_2SO_4 is used. The ANOVA tests revealed that there was no significant difference in the degradation of GenX in 0.10 M Na_2SO_4 compared to 0.10 M Na_2SO_4 + 0.12 M NaCl. However, there was a significant difference between 0.10 M Na_2SO_4 and 0.22 M Na_2SO_4.

Similarly, there is a difference in the shape of the degradation curve in Figure 4.15b when only 0.12 M NaCl is used. When the degradation of GenX in 0.10 M Na_2SO_4 was compared to the degradation in 0.12 M NaCl, a significant different between the two was found.

Conversely, in the cathodic compartment, it was difficult to see changes in the degradation of GenX in different salt compositions in Figure 4.15c and d. This is confirmed by the lack of significant difference found for GenX degradation in all salt compositions tested in the cathodic compartment. Furthermore, despite the all the changes in the electrolyte composition, the GenX degradation can still be described, to a certain degree, by pseudo-first order kinetic (see Figure A.5 in the appendix, and note the large data scattering).

a)

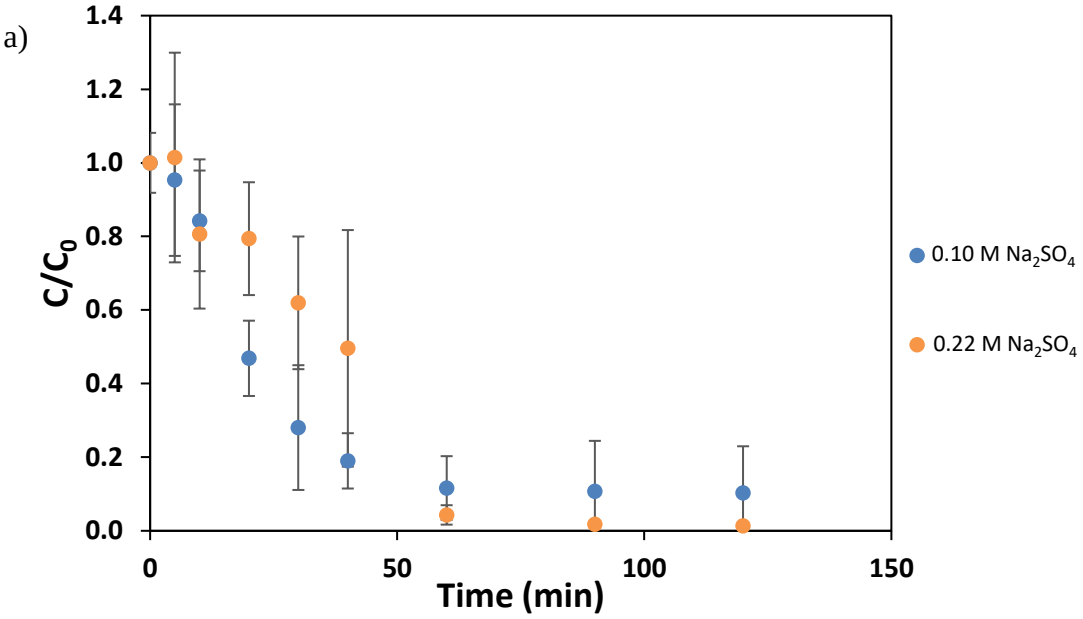
1.4
1.2
1.0
0.8
0.6
0.4
0.2
0.0
C/C0
0
50
100
150
Time (min)
0.10 M Na2SO4
0.22 M Na2SO4

b)

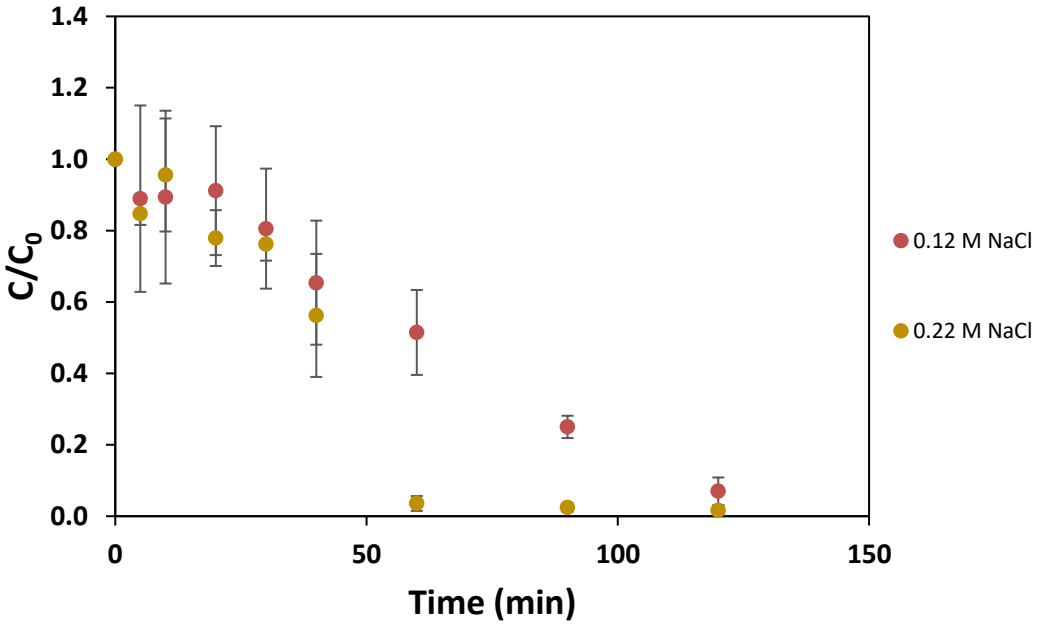
1.4
1.2
1.0
0.8
0.6
0.4
0.2
0.0
C/C0
0
50
100
150
Time (min)
0.12 M NaCl
0.22 M NaCl

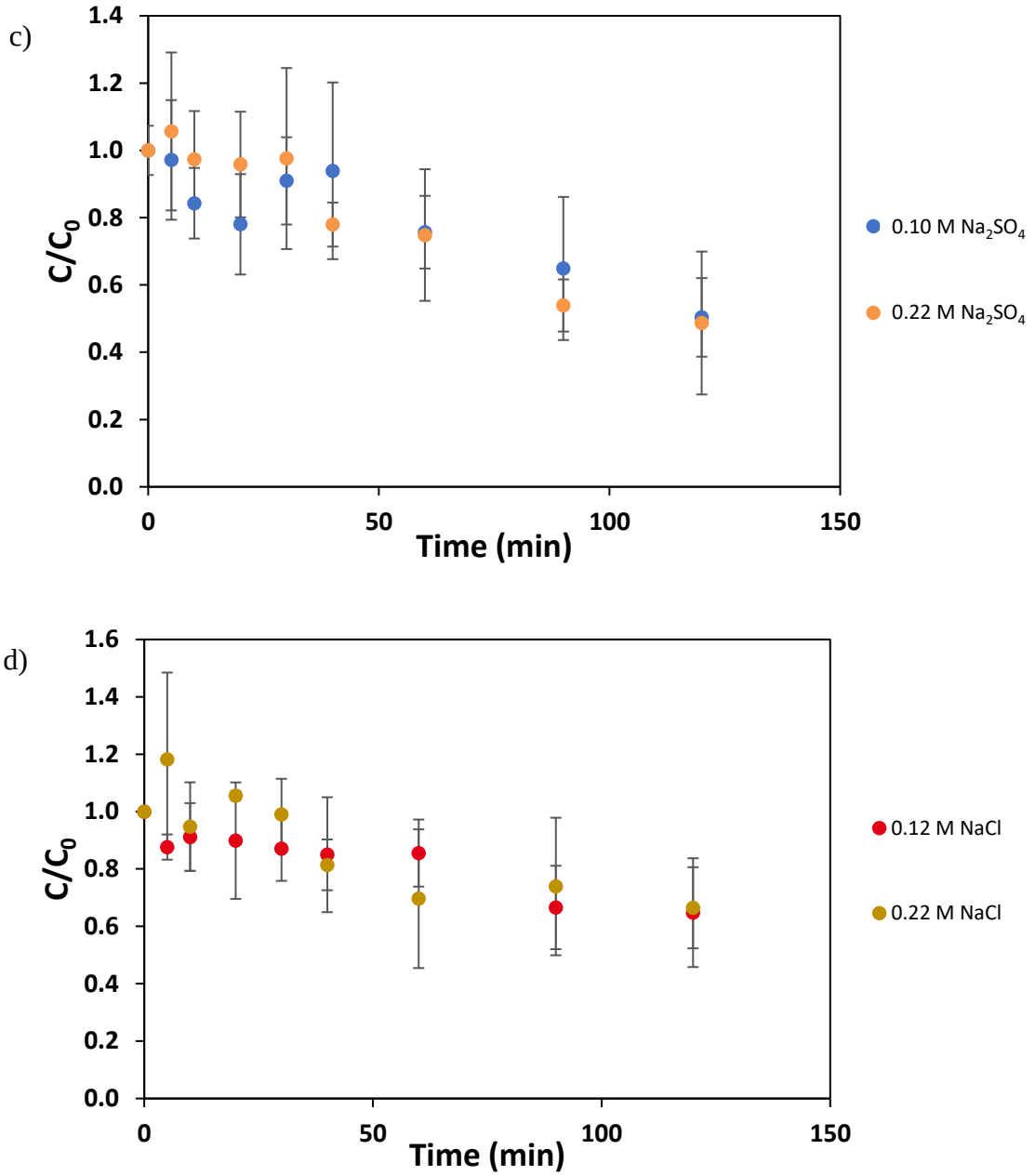

Figure 4.15 Degradation of GenX in different electrolytes in a *divided* cell at 50 mA/cm^2: comparing different concentrations of a) Na_2SO_4 for oxidation, b) NaCl for oxidation, c) Na_2SO_4 for reduction and d) NaCl for reduction. n = 3, error bars = 1 standard deviation, anode = BDD, cathode = Cu

In literature, Pica et al., previously studied the effects of using lower concentration of Na_2SO_4, while keeping the same ion conductivity, on the GenX degradation and reported lower rates of removal [37]. They concluded that sulphate oxidative species are an important part of the GenX

degradation, which is echoed by Zeidabadi et al [38]. Pica et al., however, did not test the effect of a different NaCl concentration on the reaction. On the other hand, Babu et al. concluded that increasing the concentration of sulphate ions present *decreases* the degradation of GenX [39]. They attributed this result to the decreased cell voltage due to increasing ion conductivity. They also cited the formation of persulphate ions, through sulphate radicals, as a competing reaction for the oxidation of GenX and intermediates on the anode:

$$SO_4^{2-} \rightarrow SO_4^{\cdot -} + e^- \quad (4.3)$$

$$2SO_4^{\cdot -} \rightarrow S_2O_8^{2-} \quad (4.4)$$

Similarly, when Babu et al. studied the effect of increasing the concentration of chloride ions in the solution, they reported a corresponding *decrease* in the degradation of GenX. They cited similar reasons to what was earlier proffered in Section 4.1 and equation 4.1, with chlorine gas production being a competing reaction and taking up active sites on the anode. They also suggested that Cl^- quenches the $OH^{\bullet}$:

$$Cl^- \rightarrow Cl_{ads}^{\cdot} + e^- \quad (4.5)$$

$$Cl^{\cdot} + OH^{\cdot} \rightarrow ClO^- + H^+ \quad (4.6)$$

From what was reported in literature and what is observed in Figure 4.15, it can be concluded that there is an optimal balance between the concentration of sulphates present in solution and the ionic conductivity to optimise the removal of GenX. Higher concentrations (0.22 M) of Na_4SO_4 and NaCl have similar degradation performance, implying that once there is sufficient ion conductivity, the oxidative species derived from these anions do not greatly affect degradation. However, at lower concentrations, 0.10 M Na_2SO_4 and 0.12 M NaCl individually, the degradation in the former is better, which may suggest that at lower salt concentrations, the effect of sulphate oxidative species is more apparent when only SO_4^{2-} ions are present. As mentioned earlier, since there was no significant difference between the experiments using 0.10 M Na_2SO_4 and 0.10 M Na_2SO_4 + 0.12 M NaCl, it was determined that removing 0.12 M NaCl from the electrolyte is not going have a significant effect on the overall degradation. This is useful for later experiments where NaCl had to be eliminated from the system for certain analyses, due to the interference of active chlorine species or out of a desire to reduce the salts passing through certain analysis equipment. Additionally, removing chloride ions would eliminate the possibility of the formation of chlorate

and perchlorate which could present an additional problem in wastewater treatment applications due to their toxicity.

4.5.2 GenX Degradation in Real Water Matrices

Since the electrodegradation of GenX was established in different experimental conditions using a controlled electrolyte, it was of interest to investigate if uncontrolled (real water) matrices had any effect on the degradation of GenX. Table 4.1 shows that the wastewater collected had the following concentrations of PFAS that was determined using solid phase extraction before UHPLC. Since the concentration of GenX was very low, more GenX was added into the wastewater to compare to the previous experiments done.

Table 4.1 Concentration of different PFAS in wastewater samples collected

Tested PFAS chemical	**PFBA**	**PFHxA**	**HFPO-DA GenX**	**PFBS**	**6:2 FTS**	**PFOA**	**PFHxS**	**PFOS**
Concentration (ppt)	20.57	3.77	0.27	1.69	11.78	7.39	2.65	1.29
Reported limit	N/A	<LOQ	<LOD	<LOQ	N/A	N/A	<LOQ	<LOQ

First, wastewater spiked with GenX at the same working concentration used throughout this research (5 mg/L) was tested at different current densities without any additional salts added. Figure 4.16 displays these results at different current densities in an undivided cell (the divided cell was not used for these experiments because of the high ionic resistance due to the very low concentration of inorganic salts dissolved in the wastewater matrix).

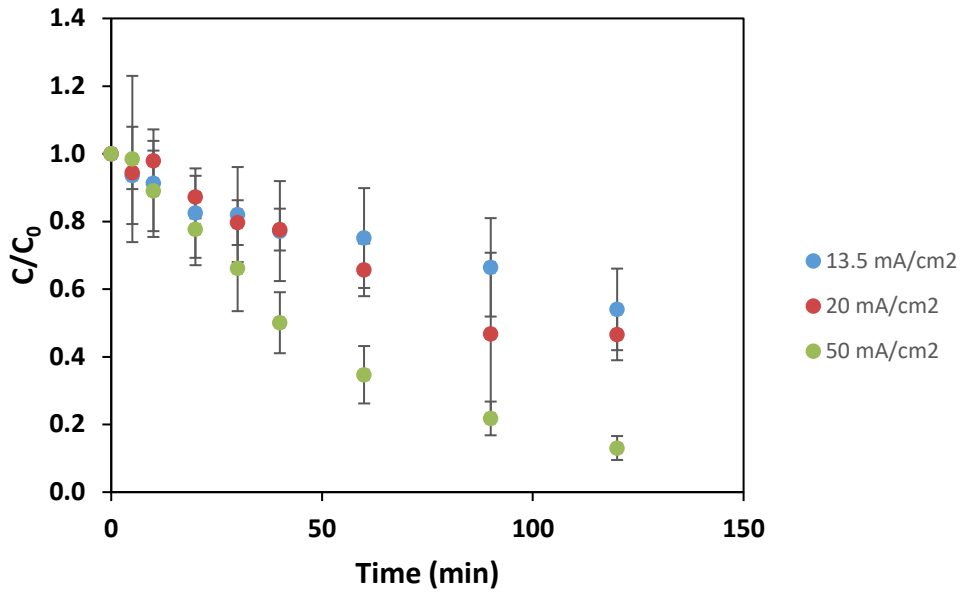

Figure 4.16 Degradation of GenX in wastewater in an undivided cell at different current densities. n = 3, error bars = 1 standard deviation, anode = BDD, cathode = Cu

The results in Figure 4.16 mirror those in Figure 4.6 where the higher current densities lead to higher degradation of GenX. For better comparison, the two experiments are displayed in Figure 4.17at each current density where the difference in the degradation of GenX in the wastewater and the laboratory electrolyte (deionised water with 0.10 M Na_2SO_4 + 0.12 M NaCl).

a)

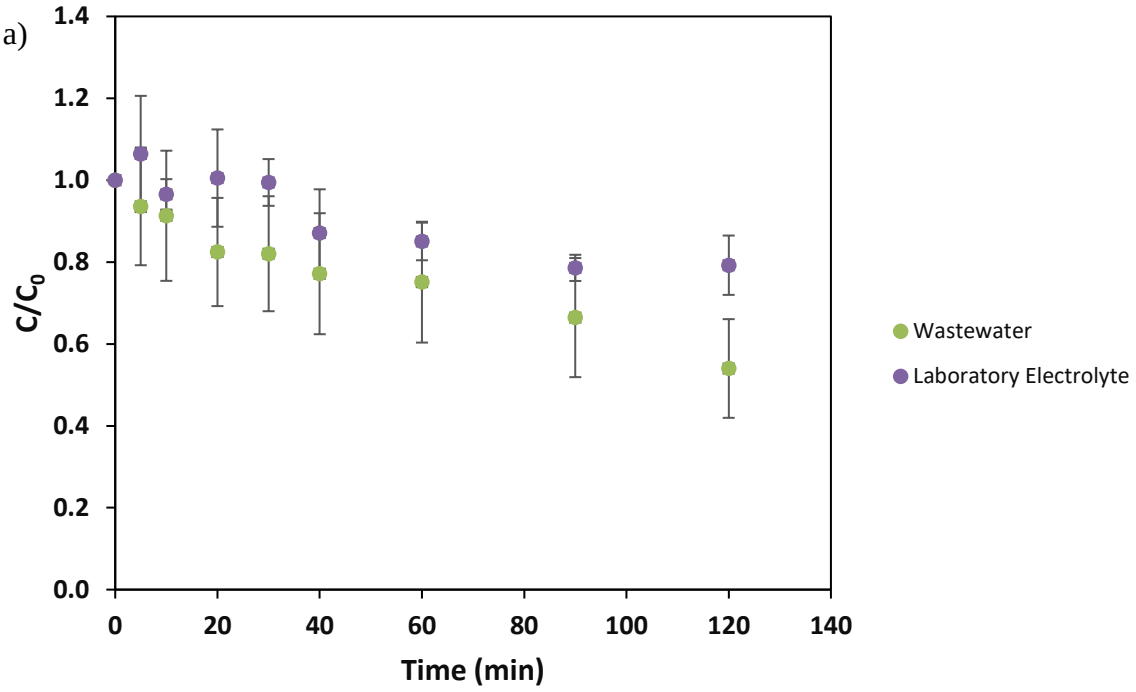
1.4
1.2
1.0
0.8
0.6
0.4
0.2
0.0
C/C0
0
20
40
60
80
100
120
140
Time (min)
Wastewater
Laboratory Electrolyte

b)

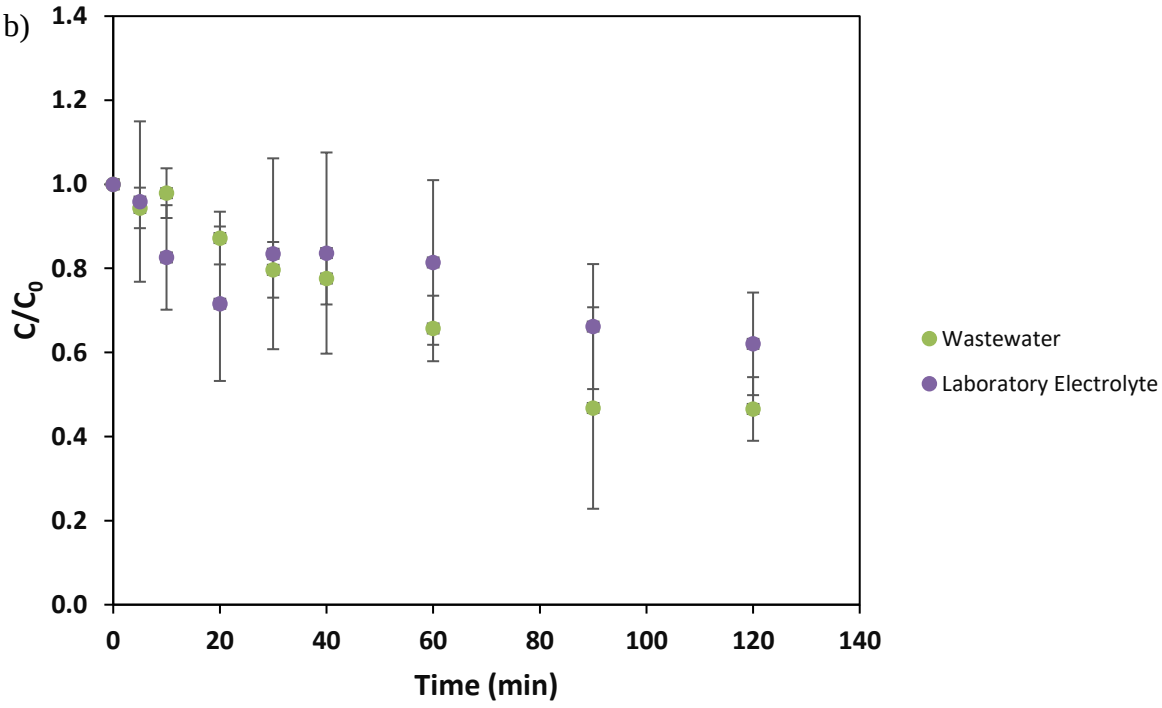
1.4
1.2
1.0
0.8
0.6
0.4
0.2
0.0
C/C0
0
20
40
60
80
100
120
140
Time (min)
Wastewater
Laboratory Electrolyte

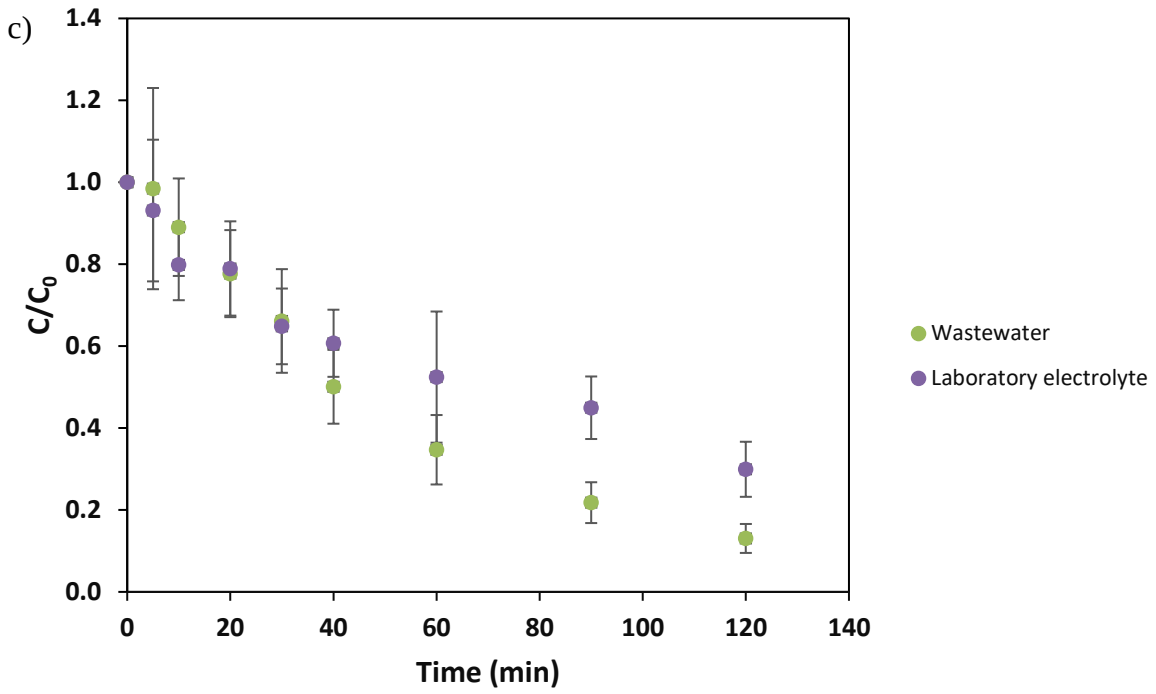

Figure 4.17 Degradation of GenX in wastewater compared to matrix prepared in laboratory electrolyte performed at different current densities: a) 13.5 mA/cm^2, b) 20 mA/cm^2, and c) 50 mA/cm^2. n = 3, error bars = 1 standard deviation, anode = BDD, cathode = Cu

Similar to the experiments in the electrolyte, the degradation of GenX exhibits pseudo-1st-order kinetics; however, the large variation in temperature over the experiment course due to the high ionic resistance of the liquid phase meant that the rate constant could not be determined. Results presented in Figure 4.17also indicate that the overall degradation of GenX after 2 hours is higher in wastewater than in the laboratory electrolyte for all current densities. However, ANOVA tests only show statistical significance between the wastewater and the laboratory electrolyte at 20 mA/cm^2 and not for 13.5 mA/cm^2 and 50 mA/cm^2. A possible explanation is that there might be species present in the wastewater which contribute to the enhanced degradation of GenX, or that lower concentrations of chloride ions reduce the competing reaction of chlorine active species formation or chlorine gas evolution (see equations 4.1, 4.5 and 4.6) on the anode. In literature, Uwayezu et al. [56], reported lower degradation percentages of PFOA in industrial wastewater than in the laboratory electrolyte, which contrasts the results in Figure 4.17 above. They attribute the difference (70% degradation in industrial wastewater compared to 99.5% in laboratory electrolyte), to the presence of shorter chain PFAS present in the industrial wastewater which also

undergo electrochemical degradation. However, Duinslaeger et al. [63], studied the degradation of PFOA and PFOS both in 10 mM phosphate buffer and landfill leachate. Their results are more in line with those shown in Figure 4.17, reporting an improved degradation both PFAS in the landfill leachate (95% PFOA, 75% PFOS) compared to the phosphate buffer (77% PFOA, 57% PFOS).

On the other hand, when drinking water and surface water are compared with the wastewater and laboratory electrolyte at 50 mA/cm^2, the degradation of GenX is better in those matrices than in wastewater as can be seen in Figure 4.18 (note that these two matrices were also used "as is", without addition of any inorganic salts to improve their ionic conductivity).

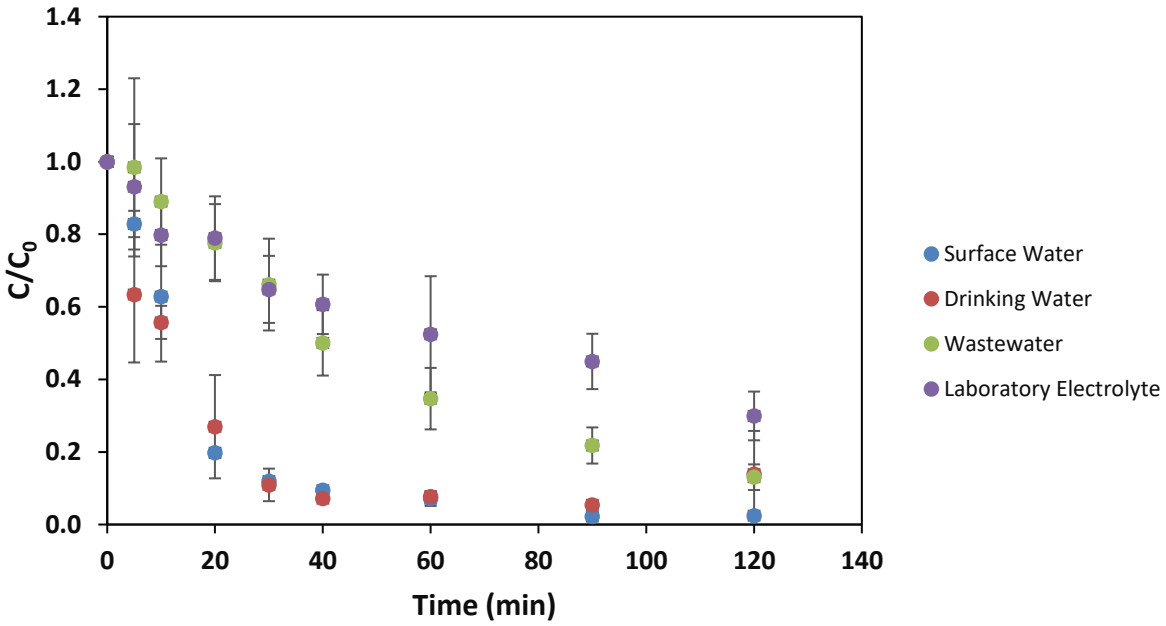

Figure 4.18 Degradation of GenX in different water matrices at 50 mA/cm^2, n = 3, error bars = 1 standard deviation, anode = BDD, cathode = Cu

The degradation of GenX may be better in drinking water and surface water than the electrolyte due to similar reasons for the better performance in wastewater. However, since wastewater is more likely to contain more organic pollutants than the surface water and drinking water, more of the electrical current may be diverted to degrading these other contaminants which, in turn, decreases the proportion of input current used to degrade GenX. The lack of these additional contaminants in surface water and drinking water can be the reason why the degradation of GenX

is higher in those matrices. The results from theses experiments are promising seeing that not only is the electrochemical degradation of GenX possible in real water matrices, but it is also better compared to the electrolyte made in the laboratory.

4.6 Nature and Toxicity of Transformation Products

The results presented so far demonstrate that GenX can be electrochemically removed from the water. However, the degree of GenX oxidation (partial vs. complete) and the nature of transformation products should also be known. To obtain such information, total organic carbon was monitored as an indicator of mineralisation, acute toxicity was assessed and a suspect screening analysis was done to assess the presence of transformation products previously reported in literature by Pica et al.[37], Zeidabadi et al. [38], Xu et al. [64] and Verma et al. [65]..

4.6.1 Total Organic Carbon Measurements

Measuring the total organic carbon was done in order to determine the amount of mineralisation of GenX that was degraded. The non-purgeable organic carbon (NPOC) method was chosen to eliminate any interference with the measurement from volatile carbon species. The results from the TOC measurement are shown in Figure 4.19 and are compared to the amount of GenX left in the reactor at the same time points.

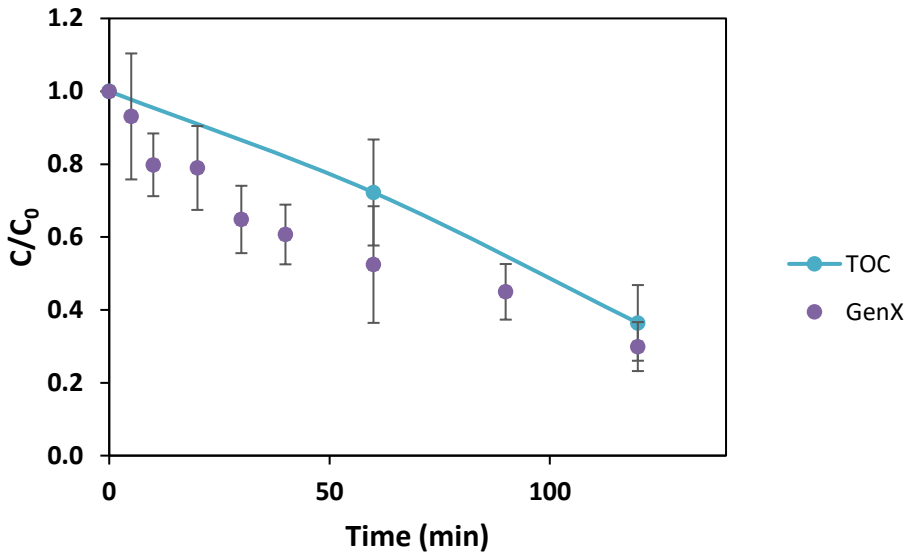

Figure 4.19 TOC measurements compared to GenX degradation at 50 mA/cm^2. n = 3, error bars = 1 standard deviation, anode = BDD, cathode = Cu

From Figure 4.19, it can be speculated that most of the GenX degraded is nearly completely mineralised since there is not a significant difference between the amount of GenX degraded and the remaining total organic carbon in the sample according to the ANOVA tests. Any significant amount of unmineralised GenX was most likely in the form of volatile carbon since they would be purged in the NPOC method. In order to gain more insight into the potential mineralisation of GenX, further analysis is needed.

4.6.2 Microtox Bioassay

To assess the viability of electrochemical treatment of GenX, testing the acute toxicity of the reaction products is of interest. It is reported that GenX, and several other PFAS, are chronically toxic [66], [67]. To measure the acute toxicity, 12,310 mg/L of GenX was added to the electrolyte most often used for the electrodegradation experiments (0.10 M N_2SO_4 + 0.12 M NaCl) and the resulting EC50 value was 2338 mg/L after 15 minutes of exposure to the bacteria. As a preliminary assessment of a potential change in the acute toxicity of GenX after treatment, Microtox BioAssay was used on the samples collected after treatment from the undivided cell and from both compartments in the divided cell. These results are summarised in Table 4.2 below:

Table 4.2 Summary of Microtox BioAssay results on background electrolyte (no GenX present) after 2 hours treatment at 50 mA/cm^2 with 15 minutes bacteria exposure, anode = BDD, cathode = Cu

Background matrix	Cell type	EC 50	Quenching
0.10 M Na_2SO_4 + 0.12 M NaCl	Undivided	0.064%*	Unquenched
0.10 M Na_2SO_4 + 0.12 M NaCl	Divided – oxidation	0.10%	Unquenched
0.10 M Na_2SO_4 + 0.12 M NaCl	Divided – reduction	Not toxic**	Unquenched
0.10 M Na_2SO_4	Undivided	Not toxic	Unquenched
0.10 M Na_2SO_4	Divided – oxidation	0.0062%	Unquenched
0.10 M Na_2SO_4	Divided – reduction	Not toxic	Unquenched
0.10 M Na_2SO_4	Divided – oxidation	0.098%	100 mg/L $Na_2S_2O_3$
0.10 M Na_2SO_4	Divided – oxidation	0.33%	500 mg/L $Na_2S_2O_3$
0.10 M Na_2SO_4	Divided – oxidation	0.39%	1000 mg/L $Na_2S_2O_3$
0.10 M Na_2SO_4	Divided – oxidation	Not toxic	2000 mg/L $Na_2S_2O_3$

* The EC50 values with a percentage represent the % of the initial concentration of the sample before dilutions since the exact concentration of the treated sample is unknown

** The program could not provide an EC50 value because there was not a significant enough difference with the positive control, thus the 'Not toxic' designation

Once a way was found to eliminate the toxicity stemming from the treated background electrolyte, the toxicity of GenX after 2 hours of degradation at 50 mA/cm^2 was measured and can be found in Table 4.3.

Table 4.3 Summary of Microtox BioAssay results on GenX degradation samples after 2 hours treatment at 50 mA/cm^2 with 15 minutes bacteria exposure, anode = BDD, cathode = Cu,

Background Matrix	Cell Type	EC50	Quenching
0.10 M Na_2SO_4	Undivided	Not toxic*	Unquenched
0.10 M Na_2SO_4	Divided – oxidation	23%	2000 mg/L $Na_2S_2O_3$
0.10 M Na_2SO_4	Divided – reduction	Not toxic	Unquenched

* The program could not provide an EC50 value because there was not a significant enough difference with the positive control, thus the 'Not toxic' designation

From Table 4.2 it can be seen that even in the absence of GenX, there is some toxicity from the background electrolyte containing chlorides after electrochemical treatment (see equations 4.5 and 4.6). This posed an issue as it would be difficult to distinguish any toxicity that could be from the treated GenX from that coming from the electrolyte. The exception was the reduction compartment

in the divided cell that displayed no background toxicity, since no active chlorine species, hydroxyl and persulphate radicals formed by reduction of the electrolyte species.

In order to combat this, the chloride ions were removed from the electrolyte, leaving just the sodium sulphate. This improved the background toxicity in the undivided cell but not the oxidation compartment of the divided cell in which hydroxyl and persulphate radicals are formed. Several attempts at quenching were done in order to avoid this background toxicity. Sodium thiosulphate at 100 mg/L was first attempted according to recommendations of the Microtox manual [68]. The concentration of thiosulphate was increased until the background toxicity was eliminated, which resulted in a sodium thiosulphate concentration of 2000 mg/L.

After the issue with the background toxicity was addressed, the treated GenX samples were tested for their acute toxicity. For the experiments conducted in the undivided cell and the reduction compartment of the divided cell, no toxicity was measured. However, for the oxidation compartment in the divided cell, the EC50 after 15 minutes of exposure of the bacteria to the solution was recorded at 23% of the initial concentration after treatment. The exact source of this toxicity is unclear, but it is most likely stemming from one of the transformation products of GenX, seeing that untreated GenX is not acutely toxic and the background toxicity of the solution was controlled beforehand. Further optimisation and analysis would be of interest to determine the exact source of the toxicity and to eliminate it.

So far, Microtox measurements on GenX alone have not been found in literature, but measurements were done by Lashuk et al. on a PFAS mixture which included GenX before photocatalytic ozonation, which yielded an initial EC20 of 2.02 mg/L [69]. After the treatment, the toxicity measurements were not detectable. This result highlights the importance of optimisation to ensure that any potential acute toxicity is eliminated after the treatment.

4.6.7 Transformation Products

In order to streamline the search for potential transformation products, a suspect screening search was done in the AcquireX program on certain “expected compounds” based on proposed mechanisms for GenX electrodegradation (shown in Chapter 2) and previous transformation products confirmed in literature [37], [38]. These can be found in Table 4.4 below.

Table 4.4 Expected transformation products for the electrodegradation of GenX from mechanisms previously proposed in literature [37]–[40]

Name	Chemical Formula	Chemical Structure
Pentafluoroethane	C_2F_5H	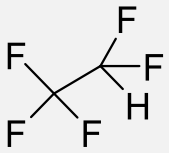
Perfluoroethanol	C_2F_5OH	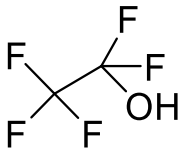
Trifluoroacetic acid	$C_2F_3O_2H$	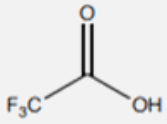
Flupropanate	$C_3F_4O_2H_2$	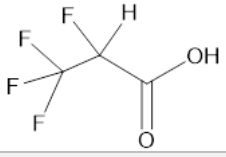
Perfluoropropionic acid	$C_3F_5O_2H$	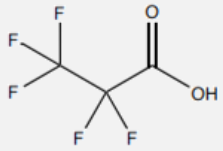
Heptafluoropropane	C_3F_7H	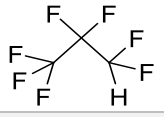
Perfluoropropanol	C_3F_7OH	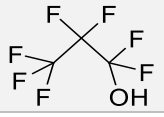
Heptafluorobutyric acid	$C_4F_7O_2H$	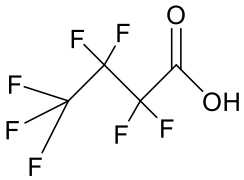
Heptafluoropropyl 1,2,2,2-tetrafluoroethyl ether	$C_5F_{11}OH$	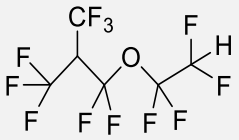
GenX (Parent compound)	**$C_6F_{11}O_3H$**	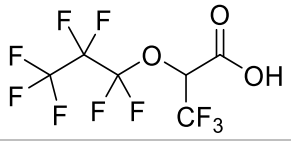

From the proposed compounds listed in Table 4.4, the nature of two of them were confirmed in earlier studies: trifluoroacetic acid which was reported by Zeidabadi et al. [38] and Olvera-Vargas et al. [40] and perfluoropripionic acid which was reported by Zeidabadi et al., Olvera-Vargas et al. and Babu et al. [39]. No literature on the electrochemical degradation of GenX confirming the other products in Table 4.4 has been found to date.

Figure 4.20 shows the plots of the different transformation products, the timepoints at which they were found, and the electrochemical conditions they were found in, which was obtained from the UHPLC results. From these results, there were several compounds that appeared in all the conditions tested (i.e. in the undivided cell and in the oxidation and reduction compartments of the divided cell), at all time points. These include perfluoroethanol (C_2F_5OH), trifluoroacetic acid ($C_2F_3O_2H$), heptafluoropropane (C_3F_7H), perfluoroethanol (C_3F_7OH), heptafluoropropyl 1,2,2,2-tetrafluoroethyl ether ($C_5F_{11}OH$) and GenX, the parent compound.

The presence of these compounds would typically lend credence to the oxidative mechanisms proposed by both Pica et al. [37] (Scheme 4.1) and Zeidabadi et al. [38] (Scheme 4.2), and the latter mechanism containing more of the shorter chain fragments such as trifluoroacetic acid, while the mechanism published by Pica et al. containing the longer chain heptafluoropropyl 1,2,2,2-tetrafluoroethyl ether as an intermediate. Since the mechanism proposed by Olvera-Vargas et al. [40] for the electro-Fenton process (Scheme 4.3) contains the possibility of both pathways with the same intermediates and complete mineralisation, it is also of interest to compare with the observed transformation products.

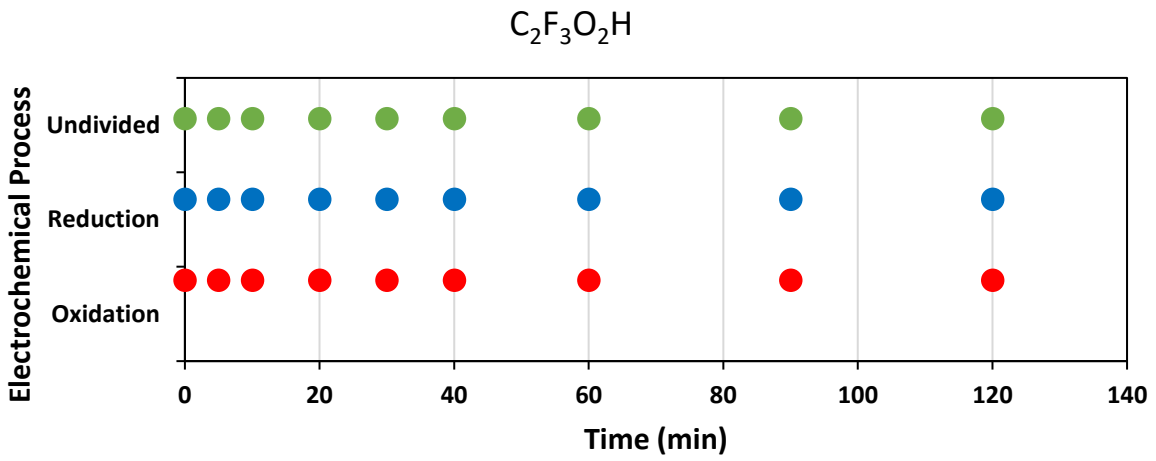
$C_2F_3O_2H$
Electrochemical Process
Undivided
Reduction
Oxidation
0
20
40
60
80
100
120
140
Time (min)

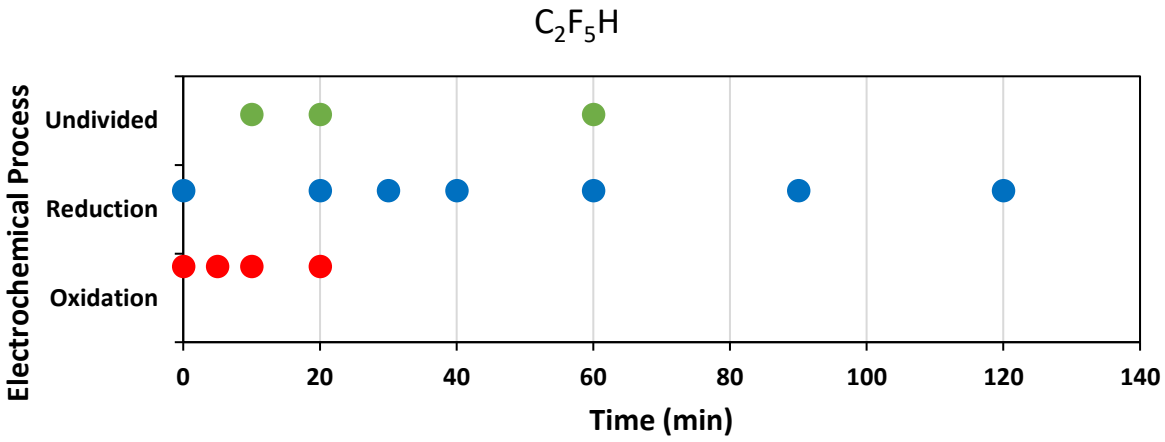
C_2F_5H
Electrochemical Process
Undivided
Reduction
Oxidation
0
20
40
60
80
100
120
140
Time (min)

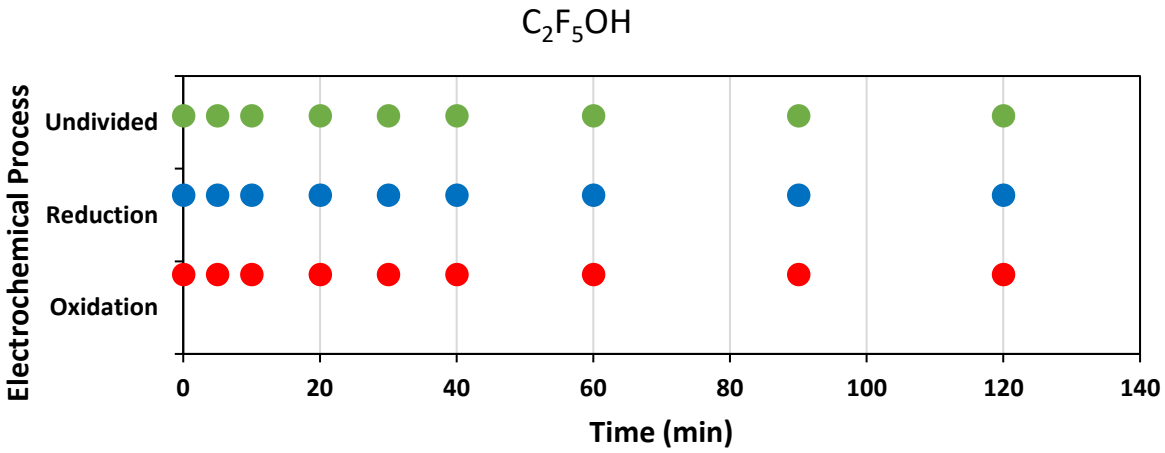
C_2F_5OH
Electrochemical Process
Undivided
Reduction
Oxidation
0
20
40
60
80
100
120
140
Time (min)

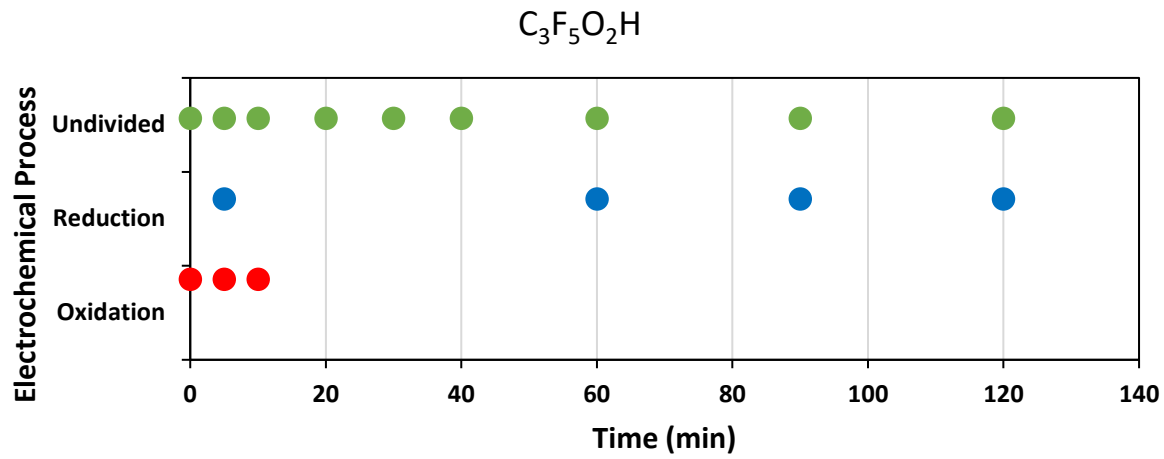
$C_3F_5O_2H$
Electrochemical Process
Undivided
Reduction
Oxidation
0
20
40
60
80
100
120
140
Time (min)

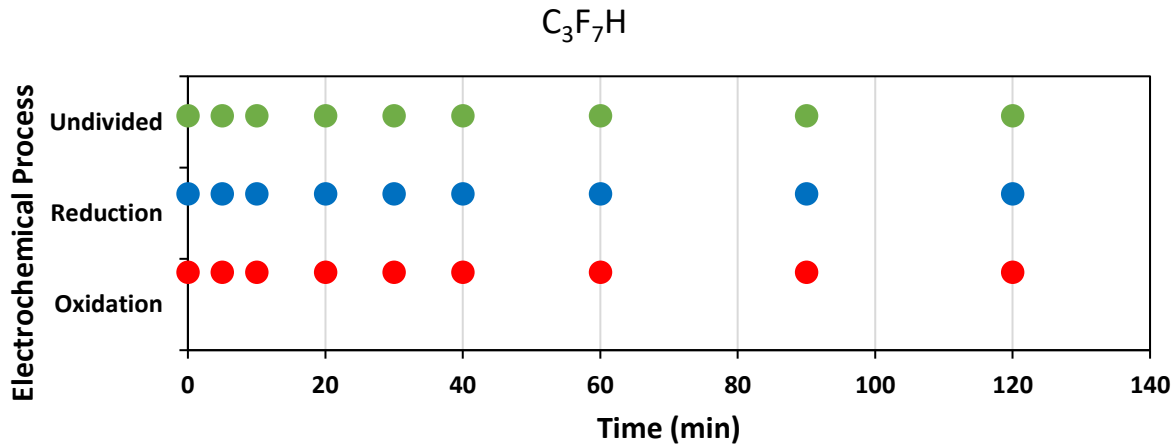
C_3F_7H
Electrochemical Process
Undivided
Reduction
Oxidation
0
20
40
60
80
100
120
140
Time (min)

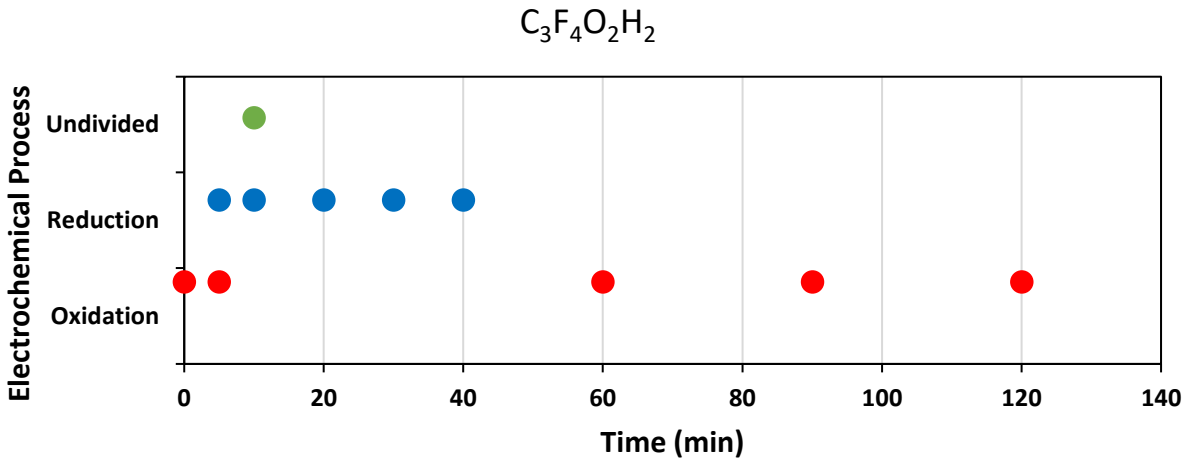
$C_3F_4O_2H_2$
Electrochemical Process
Undivided
Reduction
Oxidation
0
20
40
60
80
100
120
140
Time (min)

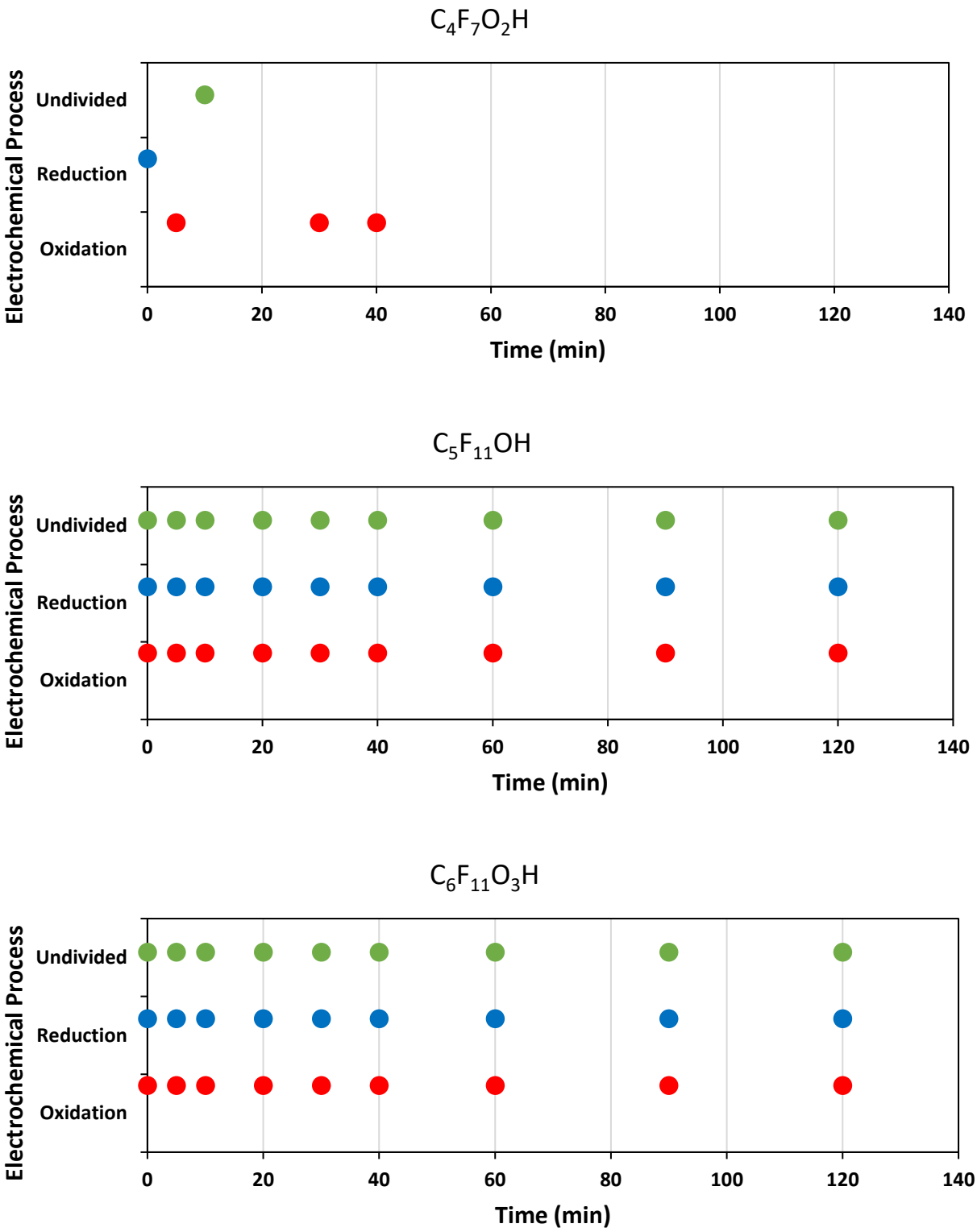

Figure 4.20 Plots of observed GenX transformation products from UHPLC over time in the undivided cell and oxidation and reduction compartment of the divided cell

The transformation products that were found by suspect screening, were highlighted in the different mechanisms found in literature in Schemes 4.1 – 4.3 below to better visual the possible reaction mechanism pathways.

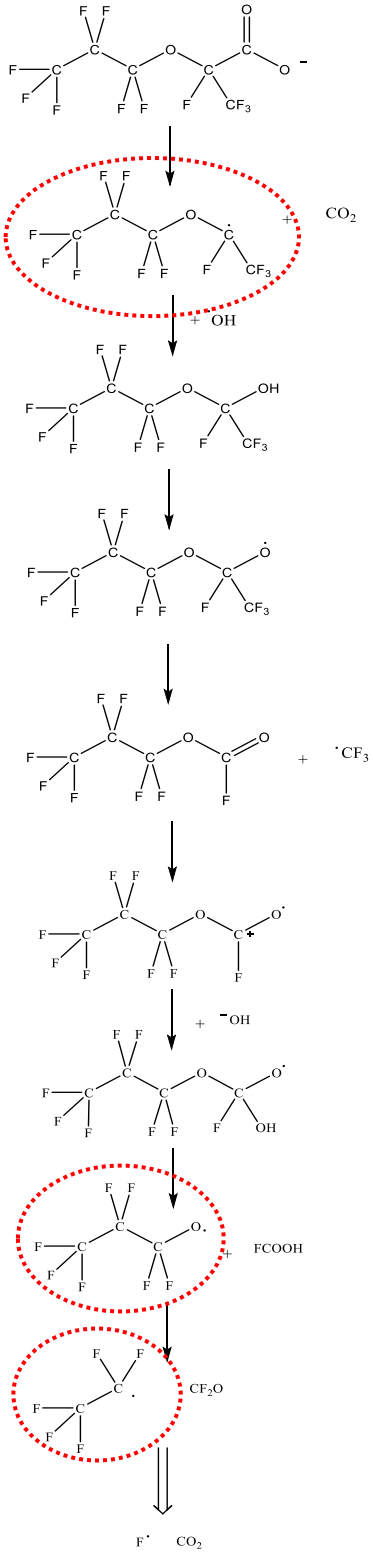

Scheme 4.1 Degradation mechanism of GenX during electrochemical oxidation adapted from Pica et al. [37] with transformation products found in results highlighted

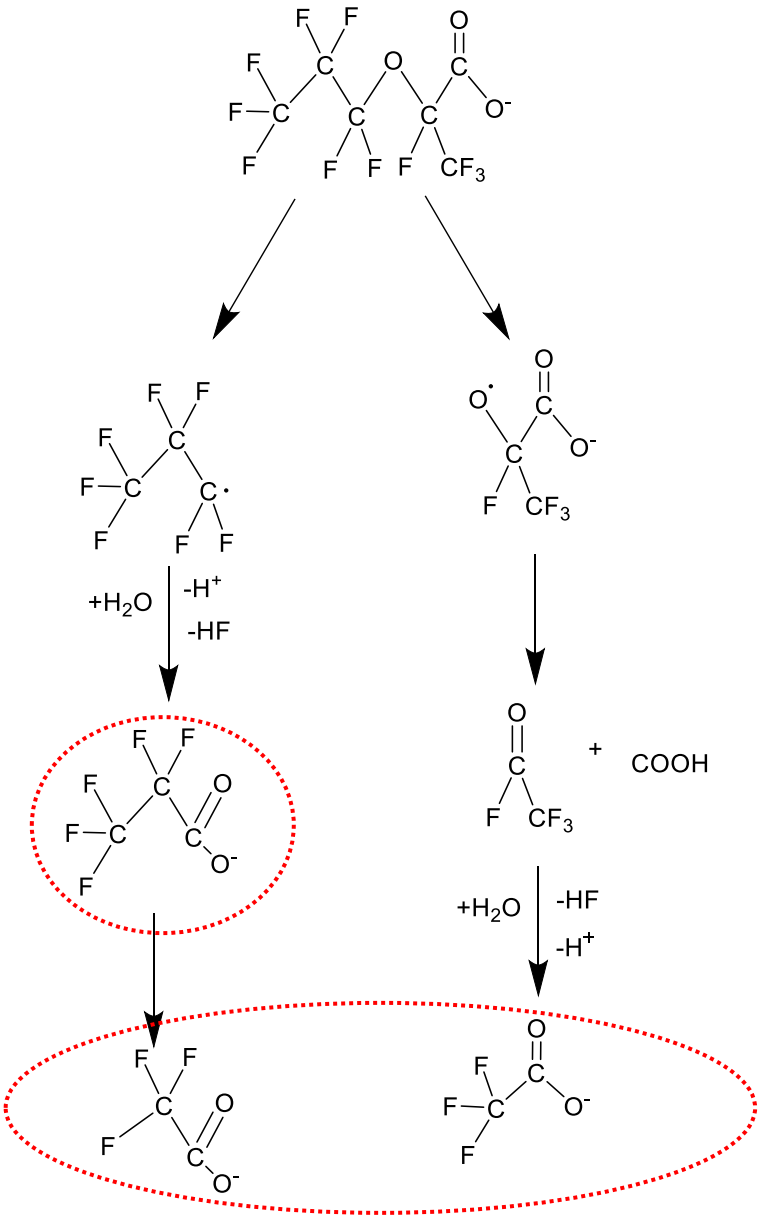

Scheme 4.2 Alternative degradation of GenX during electrochemical oxidation adapted from Zeidabadi et al. [38] with transformation products found in results highlighted

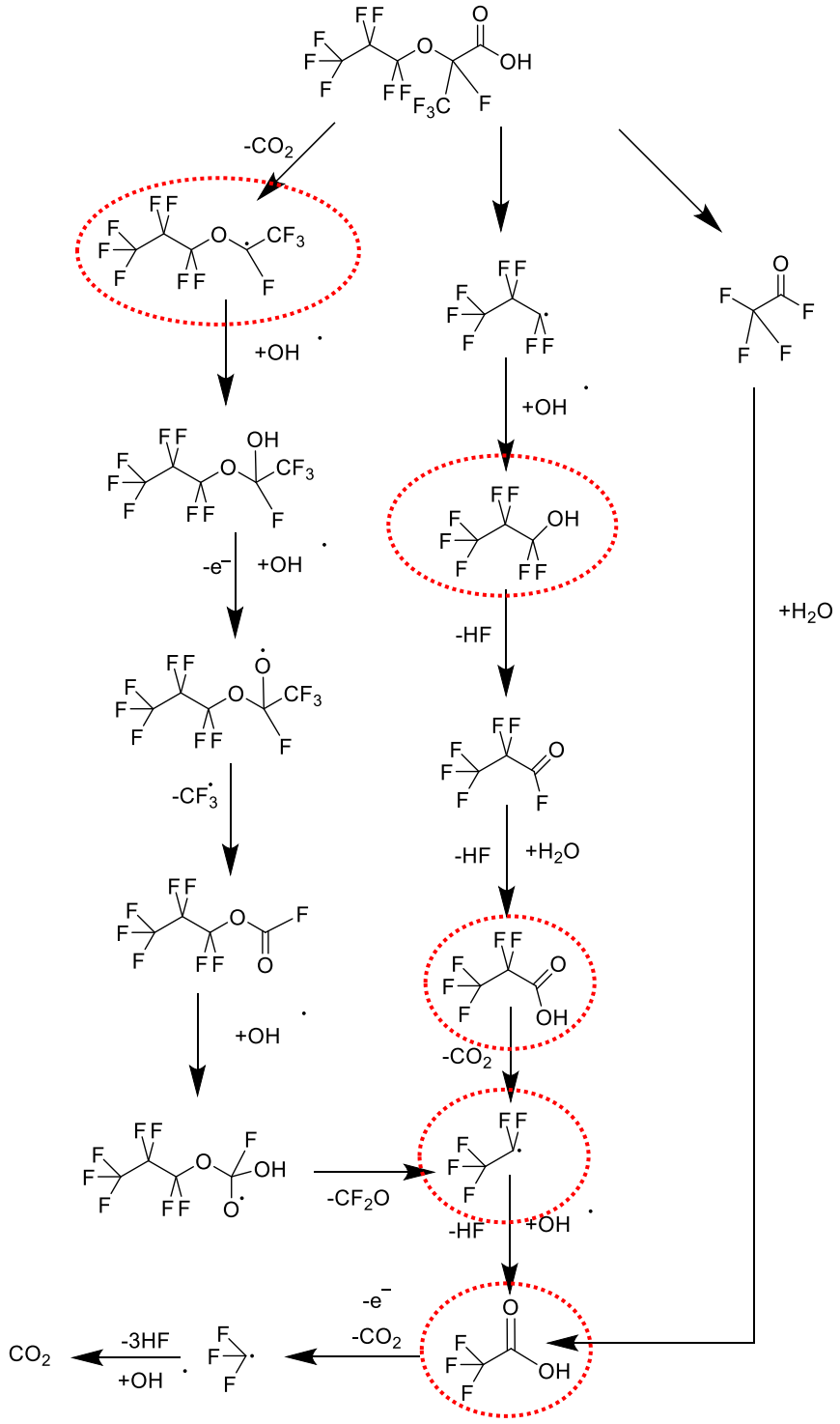

Scheme 4.3 Alternative degradation of GenX during the electro-Fenton process adapted from Olvera-Vargas et al. [40] with transformation products found in results highlighted

Despite detecting several of the transformation products proposed by the different mechanisms above, there are several more transformation products shown in Schemes 4.1 – 4.3 that were not detected, most likely due to their instability.

It can also be noted in Figure 4.20 that, with the exception of heptafluorobutyric acid at 10 minutes, none of the compounds were unique to the undivided cell. The transformation products detected were mostly found in both the undivided and divided cell (although there is a difference in which products are predominant in the separate divided cell compartments). This suggests that both the electrooxidation and reduction processes contribute to the breakage of the GenX molecule to yield some of the same byproducts proposed by literature to be found in the undivided cell. This is further supported by the results in Section 4.4 where it was shown that at the different current densities, the total number of moles degraded in the undivided cell were the same as the total number of moles degraded in the divided cell.

Other compounds of interest include pentafluoroethane and perfluoropropionic acid which are found predominately in the reduction compartment and oxidation compartment in the divided cell respectively. This implies that they could be predominately formed by electroreduction and electrooxidation respectively. Both compounds are assumed to be found from the fragmentation of GenX around the ether bond based on their structure. Also noteworthy, is flupropanate, which appears to be found predominately in both compartments at different time points. This structure, like the former two, is mostly likely formed from similar fragmentation of the ether bond.

From the transformation products formed and the cell compartment they were located in, it can be assumed that the mechanism proposed by Olvera-Vargas et al. [40] in Scheme 4.3 is the most reflective of the mechanism of overall GenX degradation occurring. The similar products found in both the oxidation compartment and reduction compartment of the divided cell implies that both processes contribute to the overall mechanism. Therefore, it is imperative that electroreduction be taken into account when considering the degradation of GenX in an undivided cell instead of just labelling the process as ‘electrooxidation’ as what is commonly observed in literature.

4.7 Electrocoagulation of GenX

The electrocoagulation of GenX was carried out in order to evaluate its potential as a preconcentration technique to precede electrochemical degradation, which requires concentration of contaminants higher than what is observed in the natural waters [38]

The results of testing three different electrodes (Al, Zn and Fe) at 10 mA/cm^2 for a concentration of 1 mg/L GenX (the same as Pica et al. used for nanofiltration) are shown in Figure 4.18 below. Zn was demonstrated to be the most efficient in removing GenX from the solution compared to Al and Fe. This was verified by the ANOVA test despite the large variations in the results for one metal which determined that electrocoagulation using Zn was significantly different from Fe and Al ($p_{Al\text{-}Zn} = 0.0005$, $p_{Fe\text{-}Zn} < 0.0001$).

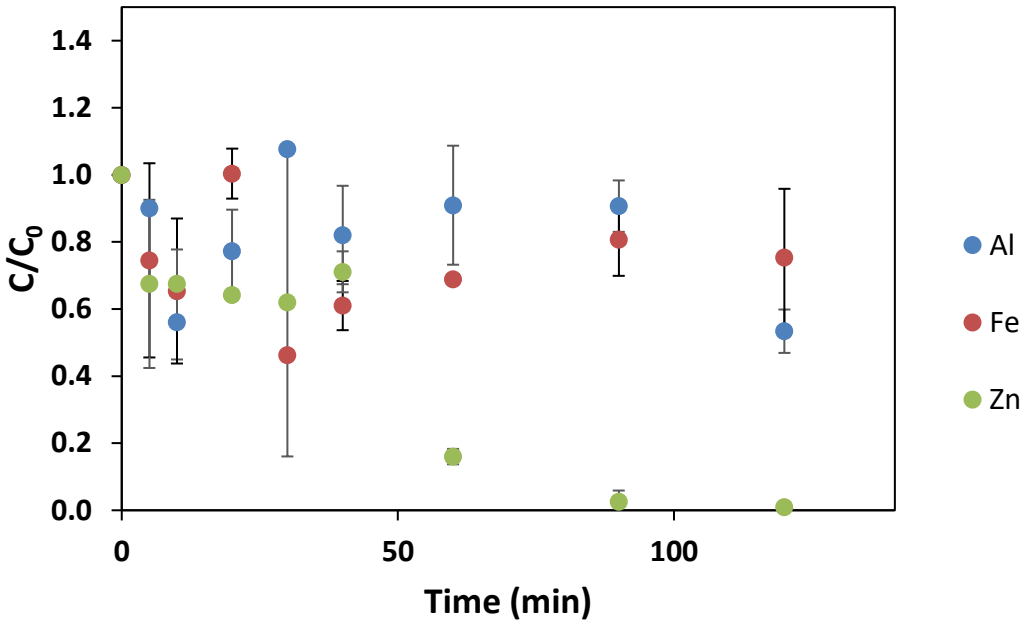

Figure 4.21 Electrochemical coagulation of GenX (initial concentration 1 mg/L) on different electrodes at 10 mA/cm^2 in 2 g/L NaCl an undivided cell, n = 2, error bars = 1 standard deviation

The removal of GenX on Zn demonstrated pseudo-first order kinetics with an apparent rate constant of 39.4×10^{-3} min^{-1}. This is much higher than the rate constant for the different current densities found for the degradation of GenX in an undivided cell in Section 4.3 (10.8×10^{-3} min^{-1}). On the other hand, the apparent removal process order for the removal of GenX on Fe and Al

was not able to be determined (see Figure A.8 in the appendix). When the rate integrated equations for 0^{th}, 1^{st} and 2^{nd} order removal were plotted, none of them showed a strong correlation ($R^2 < 0.5$) for the removal of GenX with time for Al and Fe electrodes

The mass of the metal hydroxide flocs collected was 0.837 g, 2.01 g and 1.04 g for the Zn, Fe and Al electrodes, respectively, with an approximate 10% mass loss in the freeze drier. The mass of Zn flocs collected does not respect the dissolution order for the different metals proposed in Section 2.3.1 (Zn>Fe>Al), being the metal with the lowest mass of flocs collected. Comparing these mass values with the results in Figure 4.21, one can conclude that Zn was the most efficient anode in terms of the current (faradayic) efficiency. Namely, although the mass of Zn solid phase collected was the lowest, the GenX removal efficiency was, at the same time, the highest, which is contra intuitive (a larger solid mass, in the first approximation, implies more GenX can also be adsorbed on it). A possible explanation for this could be that the specific area of the Zn-formed flocks was significantly higher than that one of the other two elements, thus enabling a larger degree of adsorption (removal) of GenX. However, further analysis (imaging of the flocs, BET analysis) is needed to verify this assumption.

An attempt to concentrate the GenX removed from the flocs was made by dissolving 0.2063 g of Zn flocs (ca. 25% of what was collected) in 1 mL sulphuric acid, the adding MilliQ water for a total volume of 12.5 mL (5% of the initial volume used for electrocoagulation). The actual concentration of this solution was measured to be 1.49 mg/L. Despite the mass loss in the floc collection, a higher concentration than the 1 mg/L in the initial electrocoagulation working solution was achieved.

In literature, the electrocoagulation of 40 μM (19.8 mg/L) HFPO-TA was studied by Xu et al. [51] using a Zn anode at 20 mA/cm^2. They reported 99% removal after 3 hours, which is similar to the 99% removal in Figure 4.21 after 2 hours for GenX. Likewise, other research conducted using Zn as the anode reported high (>85%) removal of various long and short-chain PFAS in synthetic electrolyte [44], [45], [48], [50], [53], [70] at varying initial concentrations (ca. 0.05 – 500 mg/L). Two studies reported moderate removal percentages (55% - 80%) in natural ground water for PFBS and PFOA [44], [70]. However, under the same conditions in the synthetic electrolyte, the removal reported was above the 85% mentioned.

Although no studies using electrocoagulation for GenX were found to date, the literature on electrocoagulation for other PFAS indicate that the results obtained on Zn shown Figure 4.21 are promising, despite the lack of optimisation. The results obtained from dissolving the flocs in a smaller volume also indicate that the there is a potential for preconcentrating GenX using electrocoagulation, similar to what was described by Shi et al. [53] for several PFAS and Pica et al. [37] using nanofiltration for GenX.

Chapter 5 Conclusions

5.1 Summary of Findings

In order to address the pressing concerns about the persistence of PFAS in the environment, this thesis work aimed to investigate the electrochemical degradation of GenX, particularly how oxidation and reduction play in the overall degradation. In doing so, a significant gap in the study of GenX electrochemical degradation and studying how electrochemical reduction plays a role in this process was filled. From the results presented in the body of this thesis work, it can be seen how the objectives set out in Section 1.2 of Chapter 1 were met. The electrochemical degradation of GenX was firstly established to occur as previously reported by literature using a boron doped diamond (BDD) anode in an undivided cell. Following this, experiments were then conducted in a divided cell which allowed the oxidation reaction to be decoupled and studied separately to the reduction reaction. By screening through several cathode materials at a low current density, it was determined that copper provided the best performance towards the electrochemical degradation of GenX. Gold and titanium also had better cathodic performances compared to the other cathodes studied but were outperformed by copper at higher current densities.

By studying the degradation of GenX at different current densities, the expected behaviour of faster degradation occurring at higher current density was upheld, following Faraday's law. This is the case for experiments conducted in the undivided cell and in the divided cell. All the experiments exhibited pseudo-first order kinetics for the degradation of GenX, in keeping with what was previously reported for GenX specifically and the electrochemical degradation of PFAS in general (see Table A.1 for literature comparisons). Additionally, by analysing the degradation as a function of charge passed through the cell, it was shown that the Faradaic (current) efficiency for the degradation process does not change over the current density range studied, indicating no charge losses were incurred with the increase in current density.

The direct comparison between the degradation of GenX in the undivided cell and the divided cell demonstrated that among the current densities studied there was no significant difference between the degradation occurring in the undivided cell and in the two compartments of the divided cell. This result implied that the combined electrooxidation and electroreduction both contribute to the

overall degradation that occurred in both cells, which has not been reported in the literature so far. Furthermore, the fraction of GenX degraded by electrochemical reduction in the overall degradation process was found to diminish with an increase in current density.

Furthermore, the effects different matrices on the degradation of GenX were studied in the divided cell. First, it was determined that there was little influence of the anions present in the electrolyte on the electroreduction of GenX. For electrooxidation, when only 0.12 M NaCl was used as the electrolyte, the degradation rate was reduced, whereas there was no significant difference between using 0.10 M Na_2SO_4 and 0.10 M Na_2SO_4 + 0.12 M NaCl. However, when using only 0.22 M Na_2SO_4 and only 0.22 M NaCl were used, the degradation of GenX was better than when 0.10 M Na_2SO_4 + 0.12 M NaCl was used. Additionally, there was not a significant difference between the degradation using 0.22 M Na_2SO_4 to the degradation using 0.22 M NaCl. Thus, it is unlikely that active chlorine species formed in the oxidation compartment participate in the GenX electrooxidation reaction. On the other hand, in the undivided cell the degradation of GenX was markedly improved using real water matrices, with the degradation improving following this trend: laboratory electrolyte < wastewater < drinking water and surface water. This implies that dissolved species that maybe present in real water matrices that may enhance the degradation of GenX.

Investigating the transformation products of the degradation of GenX yielded several interesting results. By measuring the total organic carbon, it was shown that most of the degraded GenX is most likely completely transformed to non-carbon-containing species dissolved in the electrolyte, as the resulting TOC measurement corresponded closely to the proportion of remaining GenX that would be present in the system in the undivided cell. By measuring the acute toxicity at the end of the degradation experiments, it was noted that, with the exception of the oxidation compartment of the divided cell, there was no acute toxicity measured. Even though extensive measures were taken to eliminate the effect of toxicity from the treatment of the background matrix, efforts to eliminate any toxicity in the oxidation compartment need to be taken in order to better assess the potential toxicity of transformations products.

From the identification of the transformation products using suspect screening, where the “expected compounds” were taken from what was proposed in literature, several useful results were obtained. The presence of compounds previously reported in literature [38], [39] were

confirmed (trifluoroacetic acid and perfluoropropionic acid) as were as additional compounds listed in Table 4.4. It was noted that compounds found suggested that the mechanism for the *overall* GenX degradation mostly likely occurs through both the fracturing of the ether bond and by attacking the carboxylic acid group. This is supported by a mechanism previously reported in literature by Olvera-Vargas et al. [40] that proposed both pathways as possibilities.

Finally, electrocoagulation of GenX was briefly investigated as a potential preconcentration technique, with the objective of taking influent streams with lower concentrations of PFAS than what was used in this study ($\ll$ 5 mg/L) and producing a more concentrated stream of PFAS. This more concentrated stream would then be treated by electrochemical degradation. From initial experiments, it was shown that GenX can be removed from solution *via* electrocoagulation on different electrodes using direct current. The removal of GenX on Zn was significantly better than the removal on Al and Fe electrodes, the former also demonstrated a better faradayic efficiency, with less metal oxide mass removing more GenX. Finally, by dissolving the recovered flocs into a smaller volume, a more concentrated solution of GenX was obtained, supporting the hypothesis that electrocoagulation might be a viable approach to preconcentrate Genx prior to treatment by electrochemical degradation.

5.2 Original Contributions to Knowledge

As part of this Ph.D. thesis, the following original contributions to knowledge were made:

- The successful decoupling of the electrooxidation reaction from the electroreduction reaction of GenX and quantifying the amount that electrochemical reduction contributes to the overall degradation.
- Demonstrating the effect of using different cathodes for the electrochemical reduction of GenX.
- Identifying the transformation products of GenX produced by both the electrochemical oxidation and reduction, confirming the presence of degradation products reported in literature (trifluoroacetic acid and perfluoropropionic acid) in addition to those not reported in literature: pentafluoroethane, perfluoroethanol, flupropanate, heptafluoropropane,

perfluoropropanol, heptafluorobutyric acid and heptafluoropropyl 1,2,2,2-tetrafluoroethyl ether.

- Evaluating the electrochemical coagulation of GenX on different electrodes.

5.3 Suggestions for further work

Having studied the electrochemical oxidation and reduction of GenX, there remain other areas that can be explored to further provide insight into this research topic. Being that the focus was placed on solely GenX due to it being a more recently introduced PFAS, the effect of electrochemically degrading a mixture of PFAS at the same time is still unknown in terms of the contribution of electroreduction and electrooxidation. There are studies conducted that used a variety of PFAS at the same time (see Table A.1), however, none of them separated the electroreduction from the electrooxidation to study the parallel processes. It can be assumed that other PFAS would display similar results based on what was already studied in an undivided cell in literature (Table A.1) and in the preliminary results in this study with PFOA (Figure 4.1), however, this needs to be proven experimentally in a divided cell.

As previously mentioned in Chapter 2, BDD is an anode that it very effective for the electrochemical degradation of organic pollutants, including PFAS. However, it is an expensive anode so it is desirable to develop alternatives that are comparable in performance but more inexpensive. Previous studies have explored this option as reported in Table A.1 in Appendix A to varying degrees of success. On the other hand, since this is the first study into investigating the contribution of electroreduction towards the degradation of GenX, it would be of interest to research to study cathode development to optimise this reaction as well. The limited study mainly involved solid metal cathodes, however, developing a cathode material to optimise the electrochemical reduction would be a further advancement in this area of study.

Studying the contribution of the electroreduction of GenX towards its overall degradation was a major objective fulfilled in this study. However, an unexpected result was the differing contributions of reduction and oxidation produced by different cathodes while the same anode BDD was used. Measuring the half cell potentials for the different cathode pairings did not reveal a sufficient explanation for this result (see Figure 4.13). Therefore, exploring the differing

contributions of electrochemical oxidation and reduction to overall degradation using Au, Cu and Ti cathodes (and potentially other electrode materials) is recommended.

When investigating the effect of different current densities on the degradation of GenX, two different membranes were used in the divided cell. As mentioned previously, the agar membrane melted at 50 mA/cm^2 and a Nafion 117^{TM} membrane was used instead. Unfortunately, Nafion 117^{TM} is fabricated having a polytetrafluoroethylene (PTFE) backbone which is not ideal when analysing transformation products. However, since the concentration of GenX used in the degradation experiments is relatively high (5 mg/L) and that GenX does not contain any sulphonic acid groups it is likely that any interference resulting from using this membrane is minimal. Additionally, Nafion 117^{TM} is stable for the operating conditions used [60] and the results in the undivided cell and divided cell show no significant difference in the moles of GenX degraded at 50 mA/cm^2. To completely eliminate the possibility of interference, a non-PFSA membrane is being used for future studies in the divided cell by other members of the laboratory.

In this work, the total organic carbon removal was monitored during the degradation of GenX using the NPOC method as measure of the mineralisation of GenX; however, assessing the extent of defluorination using techniques such as Combustion Ion Chromatography (CIC) would be beneficial. This was not able to be pursued for this work due to incompatibilities of the instrument with the high-salt-concentration electrolyte and lower initial concentrations of GenX (5 mg/L) which limited the extent of dilution possible. Additionally, the identification of certain transformation products for the electrodegradation of GenX was done using suspect screening; however, transformation products could have been potentially overlooked by narrowing the search. It is recommended to identify and *quantify* other possible transformation products to better elucidate the mechanism of GenX electrodegradation by both oxidation and reduction as well as monitoring the rate of defluorination.

Using electrochemical coagulation as a preconcentration technique was a concept that was explored in a simplified manner, but its potential was demonstrated in this work. Further exploration into this possibility can lead to the optimisation of this technique, namely using lower GenX concentrations, different anode-cathode pairings, different current regimes (AC vs DC) and

different pH conditions to name just a few. Studying the effect a mix of PFAS (including GenX) at different electrocoagulation conditions is underway in by another Master's student.

Finally, combining the electrochemical degradation with other AOPs and ARPs would be of interest to further improve the degradation of PFAS. The successful removal of PFAS can be potentially improved further by combing other techniques such as photochemical electrodegradation or ozonation. The latter technique combined with electrodegradation is being currently studied by another Master's student.

References

[1] UN-Water, “Coping with water scarcity: Challenge of the twenty-first century,” 2007. [Online]. Available: http://ci.nii.ac.jp/naid/40005232449/

[2] USGS, “How Much Water is There on Earth?” https://www.usgs.gov/special-topic/water-science-school/science/how-much-water-there-earth?qt-science_center_objects=0#qt-science_center_objects (accessed Nov. 03, 2020).

[3] USGS, “Ice, Snow, and Glaciers and the Water Cycle.” https://www.usgs.gov/special-topic/water-science-school/science/ice-snow-and-glaciers-and-water-cycle?qt-science_center_objects=0#qt-science_center_objects (accessed Nov. 30, 2020).

[4] The Conscious Challenge, “Water & Natural Resources,” 2019. https://www.theconsciouschallenge.org/ecologicalfootprintbibleoverview/water-natural-resources (accessed Nov. 03, 2020).

[5] J. Savedge, “Water Pollution: Causes, Effects, and Solutions,” *ThoughtCo.*, 2019.

[6] The Conscious Challenge, “Water & Pollution,” 2019. https://www.theconsciouschallenge.org/ecologicalfootprintbibleoverview/water-pollution (accessed Nov. 03, 2020).

[7] R. C. Buck *et al.*, “Perfluoroalkyl and polyfluoroalkyl substances in the environment: Terminology, classification, and origins,” *Integr. Environ. Assess. Manag.*, vol. 7, no. 4, pp. 513–541, 2011, doi: 10.1002/ieam.258.

[8] The Interstate Technology & Regulatory Council, “Per- and Polyfluoroalkyl Substances (PFAS),” 2020.

[9] J. Niu, Y. Li, E. Shang, Z. Xu, and J. Liu, “Electrochemical oxidation of perfluorinated compounds in water,” *Chemosphere*, vol. 146, pp. 526–538, 2016, doi: 10.1016/j.chemosphere.2015.11.115.

[10] European Environment Information and Observation Network (Eionet), “Emerging chemical risks in Europe - ‘PFAS,’” *European Environment Agency*, 2019. https://www.eea.europa.eu/themes/human/chemicals/emerging-chemical-risks-in-europe (accessed Nov. 04, 2020).

[11] M. Boshir *et al.*, “Advanced treatment technologies efficacies and mechanism of per- and poly-fluoroalkyl substances removal from water,” *Process Saf. Environ. Prot.*, vol. 136, pp. 1–14, 2020, doi: 10.1016/j.psep.2020.01.005.

[12] C. E. Schaefer *et al.*, “Electrochemical Transformations of Perfluoroalkyl Acid (PFAA) Precursors and PFAAs in Groundwater Impacted with Aqueous Film Forming Foams,” *Environ. Sci. Technol.*, 2018, doi: 10.1021/acs.est.8b02726.

[13] P. M. Dombrowski, S. D. Chiang, and F. Barajas-rodriguez, “Technology review and evaluation of different chemical oxidation conditions on treatability of PFAS,” pp. 135–150, 2018, doi: 10.1002/rem.21555.

[14] J. Horst *et al.*, “Advances in Remediation Solutions Water Treatment Technologies for

PFAS : The Next Generation," no. 2, 2018, doi: 10.1111/gwmr.12281.

[15] S. Song *et al.*, "Electrochemical degradation of azo dye C . I . Reactive Red 195 by anodic oxidation on Ti / SnO 2 – Sb / PbO 2 electrodes," vol. 55, pp. 3606–3613, 2010, doi: 10.1016/j.electacta.2010.01.101.

[16] T. Ochiai *et al.*, "Efficient electrochemical decomposition of perfluorocarboxylic acids by the use of a boron-doped diamond electrode," 2010, doi: 10.1016/j.diamond.2010.12.008.

[17] J. Radjenovic and D. L. Sedlak, "Challenges and Opportunities for Electrochemical Processes as Next- Generation Technologies for the Treatment of Contaminated Water," 2015, doi: 10.1021/acs.est.5b02414.

[18] US EPA, "Emerging Contaminants and Federal Facility Contaminants of Concern," 2019. https://www.epa.gov/fedfac/emerging-contaminants-and-federal-facility-contaminants-concern (accessed Nov. 04, 2020).

[19] C. Comninellis and G. Chen, *Electrochemistry for the Environment*. Springer, 2010.

[20] C. Comninellis, "Electrocatalysis in the electrochemical conversion/combustion of organic pollutants for waste water treatment," *Electrochim. Acta*, vol. 39, no. 11–12, pp. 1857–1862, 1994, doi: 10.1016/0013-4686(94)85175-1.

[21] E. Mousset and K. Doudrick, "A Review of Electrochemical Reduction Processes to Treat Oxidized Contaminants in Water," *Curr. Opin. Electrochem.*, 2020, doi: 10.1016/j.coelec.2020.07.008.

[22] O. Scialdone, A. Galia, C. Guarisco, and S. La Mantia, "Abatement of 1,1,2,2-tetrachloroethane in water by reduction at silver cathode and oxidation at boron doped diamond anode in micro reactors," *Chem. Eng. J.*, vol. 189–190, pp. 229–236, 2012, doi: 10.1016/j.cej.2012.02.062.

[23] M. Panizza, E. Brillas, and C. Comninellis, "Application of Boron-Doped Diamond Electrodes for Wastewater Treatment," *J. Environ. Eng. Manag.*, vol. 18, no. 3, pp. 139–153, 2008, [Online]. Available: http://ser.cienve.org.tw/download/18-3/jeeam18-3_139-153.pdf

[24] A. M. Trautmann, H. Schell, K. R. Schmidt, K. M. Mangold, and A. Tiehm, "Electrochemical degradation of perfluoroalkyl and polyfluoroalkyl substances (PFASs) in groundwater," *Water Sci. Technol.*, vol. 71, no. 10, pp. 1569–1575, 2015, doi: 10.2166/wst.2015.143.

[25] M. B. Gawande *et al.*, "Cu and Cu-Based Nanoparticles: Synthesis and Applications in Catalysis," *Chem. Rev.*, vol. 116, no. 6, pp. 3722–3811, 2016, doi: 10.1021/acs.chemrev.5b00482.

[26] C. Bellomunno *et al.*, "Building up an electrocatalytic activity scale of cathode materials for organic halide reductions," *Electrochim. Acta*, vol. 50, no. 11, pp. 2331–2341, 2005, doi: 10.1016/j.electacta.2004.10.047.

[27] A. A. Isse, B. Huang, C. Durante, and A. Gennaro, "Electrocatalytic dechlorination of volatile organic compounds at a copper cathode. Part I: Polychloromethanes," *Appl. Catal.*

B Environ., vol. 126, pp. 347–354, 2012, doi: 10.1016/j.apcatb.2012.07.004.

[28] C. Durante, B. Huang, A. A. Isse, and A. Gennaro, "Electrocatalytic dechlorination of volatile organic compounds at copper cathode. Part II: Polychloroethanes," *Appl. Catal. B Environ.*, vol. 126, pp. 355–362, 2012, doi: 10.1016/j.apcatb.2012.07.003.

[29] S. Sinha, A. Chaturvedi, R. K. Gautam, and J. "Jimmy" Jiang, "Molecular Cu Electrocatalyst Escalates Ambient Perfluorooctanoic Acid Degradation," *J. Am. Chem. Soc.*, vol. 145, no. 50, pp. 27390–27396, 2023, doi: 10.1021/jacs.3c08352.

[30] Q. Zhuo, S. Deng, B. Yang, J. Huang, and G. Yu, "Efficient electrochemical oxidation of perfluorooctanoate using a Ti/SnO2-Sb-Bi anode," *Environ. Sci. Technol.*, vol. 45, no. 7, pp. 2973–2979, 2011, doi: 10.1021/es1024542.

[31] Q. Zhuo *et al.*, "Degradation of perfluorinated compounds on a boron-doped diamond electrode," *Electrochim. Acta*, vol. 77, pp. 17–22, 2012, doi: 10.1016/j.electacta.2012.04.145.

[32] H. Lin *et al.*, "Highly Efficient and Mild Electrochemical Mineralization of Long- Chain Per fl uorocarboxylic Acids (C9 − C10) by Ti/SnO 2 − Sb − Ce, Ti/ SnO 2 − Sb/Ce − PbO 2 , and Ti/BDD Electrodes," 2013.

[33] J. Niu, H. Lin, J. Xu, H. Wu, and Y. Li, "Electrochemical mineralization of perfluorocarboxylic acids (PFCAs) by Ce-doped modified porous nanocrystalline PbO2 film electrode," *Environ. Sci. Technol.*, vol. 46, no. 18, pp. 10191–10198, 2012, doi: 10.1021/es302148z.

[34] A. Yanagida, E. Webb, C. E. Harris, M. Christenson, and S. Comfort, "Using Electrochemical Oxidation to Remove PFAS in Simulated Investigation-Derived Waste (IDW): Laboratory and Pilot-Scale Experiments," *Water (Switzerland)*, vol. 14, no. 17, Sep. 2022, doi: 10.3390/w14172708.

[35] Z. R. Hopkins, M. Sun, J. C. DeWitt, and D. R. U. Knappe, "Recently Detected Drinking Water Contaminants: GenX and Other Per- and Polyfluoroalkyl Ether Acids," *J. Am. Water Works Assoc.*, vol. 110, no. 7, pp. 13–28, 2018, doi: 10.1002/awwa.1073.

[36] A. Ahearn, "A Regrettable Substitute: The Story of GenX," *Podcasts: The Researcher's Perspective*, no. 1. 2019. doi: 10.1289/ehp5134.

[37] N. E. Pica *et al.*, "Electrochemical Oxidation of Hexafluoropropylene Oxide Dimer Acid (GenX): Mechanistic Insights and Efficient Treatment Train with Nanofiltration," *Environ. Sci. Technol.*, vol. 53, no. 21, pp. 12602–12609, 2019, doi: 10.1021/acs.est.9b03171.

[38] F. Asadi Zeidabadi, E. Banayan Esfahani, R. Moreira, S. T. McBeath, J. Foster, and M. Mohseni, "Structural dependence of PFAS oxidation in a boron doped diamond-electrochemical system," *Environ. Res.*, vol. 246, Apr. 2024, doi: 10.1016/j.envres.2024.118103.

[39] D. Suresh Babu, J. M. C. Mol, and J. G. Buijnsters, "Experimental insights into anodic oxidation of hexafluoropropylene oxide dimer acid (GenX) on boron-doped diamond anodes," *Chemosphere*, vol. 288, no. P1, p. 132417, 2022, doi:

10.1016/j.chemosphere.2021.132417.

[40] H. Olvera-Vargas, Z. Wang, J. Xu, and O. Lefebvre, “Synergistic degradation of GenX (hexafluoropropylene oxide dimer acid) by pairing graphene-coated Ni-foam and boron doped diamond electrodes,” *Chem. Eng. J.*, vol. 430, p. 132686, Feb. 2022, doi: 10.1016/J.CEJ.2021.132686.

[41] C. Hogue, “The hunt is on for GenX chemicals in people,” *Chem. Eng. News*, vol. 97, no. 14, Apr. 2019, [Online]. Available: https://cen.acs.org/environment/persistent-pollutants/hunt-GenX-chemicals-people/97/i14

[42] P. Gautam, S. Kumar, and S. Lokhandwala, “Advanced oxidation processes for treatment of leachate from hazardous waste landfill: A critical review,” *Journal of Cleaner Production*, vol. 237. Elsevier Ltd, Nov. 10, 2019. doi: 10.1016/j.jclepro.2019.117639.

[43] H. Shi *et al.*, “An electrocoagulation and electrooxidation treatment train to remove and degrade per- and polyfluoroalkyl substances in aqueous solution,” *Sci. Total Environ.*, vol. 788, p. 147723, Sep. 2021, doi: 10.1016/J.SCITOTENV.2021.147723.

[44] J. Bao, W. J. Yu, Y. Liu, X. Wang, Z. Q. Liu, and Y. F. Duan, “Removal of perfluoroalkanesulfonic acids (PFSAs) from synthetic and natural groundwater by electrocoagulation,” *Chemosphere*, vol. 248, p. 125951, 2020, doi: 10.1016/j.chemosphere.2020.125951.

[45] T. Mu, M. Park, and K. Y. Kim, “Energy-efficient removal of PFOA and PFOS in water using electrocoagulation with an air-cathode,” *Chemosphere*, vol. 281, no. March, p. 130956, 2021, doi: 10.1016/j.chemosphere.2021.130956.

[46] M. K. Kim, T. Kim, T. K. Kim, S. W. Joo, and K. D. Zoh, “Degradation mechanism of perfluorooctanoic acid (PFOA) during electrocoagulation using Fe electrode,” *Sep. Purif. Technol.*, vol. 247, no. April, p. 116911, 2020, doi: 10.1016/j.seppur.2020.116911.

[47] Y. Liu *et al.*, “Removal of perfluorooctanoic acid in simulated and natural waters with different electrode materials by electrocoagulation,” *Chemosphere*, vol. 201, pp. 303–309, 2018, doi: 10.1016/j.chemosphere.2018.02.129.

[48] H. Lin, Y. Wang, J. Niu, Z. Yue, and Q. Huang, “Efficient Sorption and Removal of Perfluoroalkyl Acids (PFAAs) from Aqueous Solution by Metal Hydroxides Generated in Situ by Electrocoagulation,” *Environ. Sci. Technol.*, vol. 49, no. 17, pp. 10562–10569, 2015, doi: 10.1021/acs.est.5b02092.

[49] Y. Liu *et al.*, “Periodically reversing electrocoagulation technique for efficient removal of short-chain perfluoroalkyl substances from contaminated groundwater around a fluorochemical facility,” *Chemosphere*, vol. 334, no. May, p. 138953, 2023, doi: 10.1016/j.chemosphere.2023.138953.

[50] Y. Liu *et al.*, “Simultaneous removal of multiple PFAS from contaminated groundwater around a fluorochemical facility by the periodically reversing electrocoagulation technique,” *Chemosphere*, vol. 307, no. P2, p. 135874, 2022, doi: 10.1016/j.chemosphere.2022.135874.

[51] A. Xu *et al.*, “The key role of hydrophobic forces during the electrocoagulation of

perfluorooctanoic acid substitute (HFPO-TA) revealed by the interfacial thermodynamics," *Sep. Purif. Technol.*, vol. 343, no. January, p. 127127, 2024, doi: 10.1016/j.seppur.2024.127127.

[52] E. O. Nwanebu, X. Liu, E. Pajootan, V. Yargeau, and S. Omanovic, "Electrochemical degradation of methylene blue using a ni-co-oxide anode," *Catalysts*, vol. 11, no. 7, 2021, doi: 10.3390/catal11070793.

[53] H. Shi *et al.*, "An electrocoagulation and electrooxidation treatment train to remove and degrade per- and polyfluoroalkyl substances in aqueous solution," *Sci. Total Environ.*, vol. 788, p. 147723, 2021, doi: 10.1016/j.scitotenv.2021.147723.

[54] Microbics Corporation, "Microtox ® Acute Toxicity Basic Test Procedures," 1995.

[55] F. Asadi Zeidabadi, E. Banayan Esfahani, S. T. McBeath, K. L. Dubrawski, and M. Mohseni, "Electrochemical degradation of PFOA and its common alternatives: Assessment of key parameters, roles of active species, and transformation pathway," *Chemosphere*, vol. 315, Feb. 2023, doi: 10.1016/j.chemosphere.2023.137743.

[56] J. N. Uwayezu *et al.*, "Electrochemical degradation of per- and poly-fluoroalkyl substances using boron-doped diamond electrodes," *J. Environ. Manage.*, vol. 290, Jul. 2021, doi: 10.1016/j.jenvman.2021.112573.

[57] S. Liang, R. David, P. Jr, H. Lin, S. D. Chiang, and Q. J. Huang, "Electrochemical oxidation of PFOA and PFOS in concentrated waste streams," pp. 127–134, 2018, doi: 10.1002/rem.21554.

[58] F. A. Zeidabadi, E. B. Esfahani, S. T. McBeath, and M. Mohseni, "Managing PFAS exhausted Ion-exchange resins through effective regeneration/electrochemical process," *Water Res.*, vol. 255, May 2024, doi: 10.1016/j.watres.2024.121529.

[59] P. M. V Raja and A. R. Barron, "PHYSICAL METHODS IN CHEMISTRY AND NANO SCIENCE." [Online]. Available: https://libretexts.org

[60] S. Ahmad, T. Nawaz, A. Ali, M. F. Orhan, A. Samreen, and A. M. Kannan, "An overview of proton exchange membranes for fuel cells: Materials and manufacturing," *Int. J. Hydrogen Energy*, vol. 47, no. 44, pp. 19086–19131, 2022, doi: 10.1016/j.ijhydene.2022.04.099.

[61] K. Sivagami *et al.*, "Electrochemical-based approaches for the treatment of forever chemicals: Removal of perfluoroalkyl and polyfluoroalkyl substances (PFAS) from wastewater," *Sci. Total Environ.*, vol. 861, no. 160440, 2023, doi: 10.1016/j.scitotenv.2022.160440.

[62] C. E. Schaefer *et al.*, "Electrochemical treatment of perfluorooctanoic acid and perfluorooctane sulfonate : Insights into mechanisms and application to groundwater treatment," *Chem. Eng. J.*, vol. 317, pp. 424–432, 2017, doi: 10.1016/j.cej.2017.02.107.

[63] N. Duinslaeger, A. Doni, and J. Radjenovic, "Impact of supporting electrolyte on electrochemical performance of borophene-functionalized graphene sponge anode and degradation of per- and polyfluoroalkyl substances (PFAS)," *Water Res.*, vol. 242, Aug. 2023, doi: 10.1016/j.watres.2023.120232.

[64] B. Xu *et al.*, “PFAS and their substitutes in groundwater: Occurrence, transformation and remediation,” *J. Hazard. Mater.*, vol. 412, p. 125159, 2021, doi: 10.1016/j.jhazmat.2021.125159.

[65] S. Verma, R. S. Varma, and M. N. Nadagouda, “Remediation and mineralization processes for per- and polyfluoroalkyl substances (PFAS) in water: A review,” *Science of the Total Environment*, vol. 794. Elsevier B.V., Nov. 10, 2021. doi: 10.1016/j.scitotenv.2021.148987.

[66] “Human Health Toxicity Values for Hexafluoropropylene Oxide Dimer Acid and Its Ammonium Salt, Also Known as ‘GenX Chemicals.’”

[67] M. I. Gomis, R. Vestergren, D. Borg, and I. T. Cousins, “Comparing the toxic potency in vivo of long-chain perfluoroalkyl acids and fluorinated alternatives,” *Environ. Int.*, vol. 113, pp. 1–9, Apr. 2018, doi: 10.1016/J.ENVINT.2018.01.011.

[68] “Microtox ® Acute Toxicity Basic Test Procedures,” 1995.

[69] B. Lashuk, M. Pineda, S. AbuBakr, D. Boffito, and V. Yargeau, “Application of photocatalytic ozonation with a WO3/TiO2 catalyst for PFAS removal under UVA/visible light,” *Sci. Total Environ.*, vol. 843, no. June, 2022, doi: 10.1016/j.scitotenv.2022.157006.

[70] Y. Liu *et al.*, “Removal of perfluorooctanoic acid in simulated and natural waters with different electrode materials by electrocoagulation,” *Chemosphere*, vol. 201, pp. 303–309, Jun. 2018, doi: 10.1016/J.CHEMOSPHERE.2018.02.129.

[71] H. Lin, J. Niu, S. Ding, and L. Zhang, “Electrochemical degradation of perfluorooctanoic acid (PFOA) by Ti / SnO 2 e Sb , Ti / SnO 2 e Sb / PbO 2 and Ti / SnO 2 e Sb / MnO 2 anodes,” vol. 6, pp. 2–10, 2012, doi: 10.1016/j.watres.2012.01.053.

[72] A. Fath, F. Sacher, and J. E. Mccaskie, “Electrochemical decomposition of fluorinated wetting agents in plating industry waste water,” pp. 1659–1667, 2016, doi: 10.2166/wst.2015.650.

[73] H. Zhao, J. Gao, G. Zhao, J. Fan, Y. Wang, and Y. Wang, “Fabrication of novel SnO 2 - Sb / carbon aerogel electrode for ultrasonic electrochemical oxidation of perfluorooctanoate with high catalytic efficiency,” *"Applied Catal. B, Environ.*, vol. 136–137, pp. 278–286, 2013, doi: 10.1016/j.apcatb.2013.02.013.

[74] C. Fang, Z. Sobhani, J. Niu, and R. Naidu, “Removal of PFAS from aqueous solution using PbO2 from lead-acid battery,” *Chemosphere*, vol. 219, pp. 36–44, 2019, doi: 10.1016/j.chemosphere.2018.11.206.

[75] Y. Su *et al.*, “Potential-Driven Electron Transfer Lowers the Dissociation Energy of the C-F Bond and Facilitates Reductive Defluorination of Perfluorooctane Sulfonate (PFOS),” *ACS Appl. Mater. Interfaces*, vol. 11, no. 37, pp. 33913–33922, 2019, doi: 10.1021/acsami.9b10449.

[76] Á. Soriano, D. Gorri, and A. Urtiaga, “Efficient treatment of perfluorohexanoic acid by nanofiltration followed by electrochemical degradation of the NF concentrate,” *Water Res.*, vol. 112, pp. 147–156, 2017, doi: 10.1016/j.watres.2017.01.043.

[77] Q. Zhuo *et al.*, "Electrochemical oxidation of 1H,1H,2H,2H-perfluorooctane sulfonic acid (6:2 FTS) on DSA electrode: Operating parameters and mechanism," *J. Environ. Sci. (China)*, vol. 26, no. 8, pp. 1733–1739, 2014, doi: 10.1016/j.jes.2014.06.014.

[78] B. Gomez-Ruiz *et al.*, "Boron doped diamond electrooxidation of 6:2 fluorotelomers and perfluorocarboxylic acids. Application to industrial wastewaters treatment," *J. Electroanal. Chem.*, vol. 798, no. May, pp. 51–57, 2017, doi: 10.1016/j.jelechem.2017.05.033.

[79] A. Urtiaga, A. Soriano, and J. Carrillo-Abad, "BDD anodic treatment of 6:2 fluorotelomer sulfonate (6:2 FTSA). Evaluation of operating variables and by-product formation," *Chemosphere*, vol. 201, pp. 571–577, 2018, doi: 10.1016/j.chemosphere.2018.03.027.

[80] C. E. Schaefer, C. Andaya, A. Urtiaga, E. R. McKenzie, and C. P. Higgins, "Electrochemical treatment of perfluorooctanoic acid (PFOA) and perfluorooctane sulfonic acid (PFOS) in groundwater impacted by aqueous film forming foams (AFFFs)," *J. Hazard. Mater.*, vol. 295, pp. 170–175, 2015, doi: 10.1016/j.jhazmat.2015.04.024.

[81] B. Gomez-Ruiz *et al.*, "Efficient electrochemical degradation of poly- and perfluoroalkyl substances (PFASs) from the effluents of an industrial wastewater treatment plant," *Chem. Eng. J.*, vol. 322, pp. 196–204, 2017, doi: 10.1016/j.cej.2017.04.040.

[82] Y. Wang *et al.*, "Electroreductive Defluorination of Unsaturated PFAS by a Quaternary Ammonium Surfactant-Modified Cathode via Direct Cathodic Reduction," *Environ. Sci. Technol.*, 2022, doi: 10.1021/acs.est.2c08182.

[83] D. Ackerman Grunfeld *et al.*, "Electrochemical degradation of a C6-perfluoroalkyl substance (PFAS) using a simple activated carbon cathode," *Environ. Sci. Water Res. Technol.*, vol. 10, no. 1, pp. 272–287, Nov. 2023, doi: 10.1039/d3ew00543g.

[84] S. Barisci and R. Suri, "Degradation of emerging per- and polyfluoroalkyl substances (PFAS) using an electrochemical plug flow reactor," *J. Hazard. Mater.*, vol. 460, Oct. 2023, doi: 10.1016/j.jhazmat.2023.132419.

[85] N. Duinslaeger and J. Radjenovic, "Electrochemical degradation of per- and polyfluoroalkyl substances (PFAS) using low-cost graphene sponge electrodes," *Water Res.*, vol. 213, Apr. 2022, doi: 10.1016/j.watres.2022.118148.

[86] Y. Luo *et al.*, "Investigating the effect of polarity reversal of the applied current on electrochemical degradation of per-and polyfluoroalkyl substances," *J. Clean. Prod.*, vol. 433, Dec. 2023, doi: 10.1016/j.jclepro.2023.139691.

[87] K. Hughes, M. Pineda, S. Omanovic, and V. Yargeau, "Study on the importance of the reductive degradation of GenX in its overall electrochemical degradation process on different cathode materials," *Sci. Total Environ.*, p. 168415, Nov. 2023, doi: 10.1016/J.SCITOTENV.2023.168415.

[88] T. Mu, M. Park, and K. Y. Kim, "Energy-efficient removal of PFOA and PFOS in water using electrocoagulation with an air-cathode," *Chemosphere*, vol. 281, p. 130956, Oct. 2021, doi: 10.1016/J.CHEMOSPHERE.2021.130956.

[89] Y.-F. Li, C.-Y. Hu, Y.-C. Lee, and S.-L. Lo, "Effects of zinc salt addition on

perfluorooctanoic acid (PFOA) removal by electrocoagulation with aluminum electrodes," *Chemosphere*, p. 132665, Oct. 2021, doi: 10.1016/J.CHEMOSPHERE.2021.132665.

[90] Y. F. Li, C. Y. Ho, Y. J. Liu, Y. C. Lee, C. Y. Hu, and S. L. Lo, "Enhance electrocoagulation-flotation (ECF) removal efficiency perfluorohexanoic acid (PFHxA) by adding surfactants," *J. Environ. Chem. Eng.*, vol. 12, no. 1, p. 111773, 2024, doi: 10.1016/j.jece.2023.111773.

[91] B. Merchel Piovesan Pereira and I. Tagkopoulos, "Benzalkonium Chlorides: Uses, Regulatory Status, and Microbial Resistance," *Appl. Environ. Microbiol.*, vol. 85, no. 13, pp. 1–13, 2019.

[92] EU Reference Laboratories for Residues of Pesticides, "Analysis of Quaternary Ammonium Compounds (QACs) in Fruits and Vegetables using QuEChERS and LC-MS/MS," vol. 5. pp. 1–6, 2016. [Online]. Available: http://www.eurl-pesticides.eu/userfiles/file/EurlSRM/EurlSRM_meth_QAC_ShortMethod.pdf

[93] Editorial Team, "Active Ingredients of Lysol," *Homes Pursuit*, 2021. https://homespursuit.com/active-ingredients-of-lysol/ (accessed Jun. 01, 2022).

[94] Dettol, "Dettol Disinfectant Liquid Menthol Cool," *Reckitt Benckiser*, 2022. https://www.dettol.co.in/household-disinfection/disinfectant-liquid/dettol-disinfectant-liquid-menthol-cool-500ml/ (accessed Jun. 01, 2022).

[95] H. M. Dewey, J. M. Jones, M. R. Keating, and J. Budhathoki-Uprety, "Increased Use of Disinfectants During the COVID-19 Pandemic and Its Potential Impacts on Health and Safety," *ACS Chem. Heal. Saf.*, vol. 29, no. 1, pp. 27–38, 2022, doi: 10.1021/acs.chas.1c00026.

[96] US EPA, "Reregistration Eligibility Decision for Alkyl Dimethyl Benzyl Ammonium Chloride (ADBAC)," Washington D.C., 2006.

[97] B. M. P. Pereira and I. Tagkopoulos, "Benzalkonium chlorides: Uses, regulatory status, and microbial resistance," *Appl. Environ. Microbiol.*, vol. 85, no. 13, pp. 1–13, 2019, doi: 10.1128/AEM.00377-19.

[98] O. W. Barber and E. M. Hartmann, "Benzalkonium chloride: A systematic review of its environmental entry through wastewater treatment, potential impact, and mitigation strategies," *https://doi.org/10.1080/10643389.2021.1889284*, pp. 1–30, Mar. 2021, doi: 10.1080/10643389.2021.1889284.

[99] M. Tanada, T. Miyoshi, T. Nakamura, and S. Tanada, "Adsorption Removal of Benzalkonium Chloride by Granular Activated Carbon for Medical Waste Water Treatment," *Asia-Pacific J. Public Heal.*, vol. 5, no. 1, 1991.

[100] M. S. Fortunato *et al.*, "Biodegradability of Disinfectants in Surface Waters from Buenos Aires: Isolation of an Indigenous Strain Able to Degrade and Detoxify Benzalkonium Chloride," *Water. Air. Soil Pollut.*, vol. 229, no. 4, pp. 1–14, Apr. 2018, doi: 10.1007/S11270-018-3780-7/TABLES/2.

[101] S. Oh *et al.*, "Microbial community degradation of widely used quaternary ammonium disinfectants," *Appl. Environ. Microbiol.*, vol. 80, no. 19, pp. 5892–5900, 2014, doi:

10.1128/AEM.01255-14.

[102] E. Ertekin, J. K. Hatt, K. T. Konstantinidis, and U. Tezel, “Similar Microbial Consortia and Genes Are Involved in the Biodegradation of Benzalkonium Chlorides in Different Environments,” *Environ. Sci. Technol.*, vol. 50, no. 8, pp. 4304–4313, 2016, doi: 10.1021/acs.est.5b05959.

[103] I. Turku and T. Sainio, “Modeling of adsorptive removal of benzalkonium chloride from water with a polymeric adsorbent,” *Sep. Purif. Technol.*, vol. 69, no. 2, pp. 185–194, 2009, doi: 10.1016/j.seppur.2009.07.017.

[104] J. M. Hong, Y. F. Xia, Q. Zhang, and B. Y. Chen, “Oxidation of benzalkonium chloride in aqueous solution by S2O82−/Fe2+ process: Degradation pathway, and toxicity evaluation,” *J. Taiwan Inst. Chem. Eng.*, vol. 78, pp. 230–239, 2017, doi: 10.1016/j.jtice.2017.06.005.

[105] Q. Zhang, Y. F. Xia, and J. M. Hong, “Mechanism and toxicity research of benzalkonium chloride oxidation in aqueous solution by H2O2/Fe2+ process,” *Environ. Sci. Pollut. Res.*, vol. 23, no. 17, pp. 17822–17830, Sep. 2016, doi: 10.1007/S11356-016-6986-5/FIGURES/6.

[106] J. B. Carbajo *et al.*, “Ozonation as pre-treatment of activated sludge process of a wastewater containing benzalkonium chloride and NiO nanoparticles,” *Chem. Eng. J.*, vol. 283, pp. 740–749, Jan. 2016, doi: 10.1016/J.CEJ.2015.08.001.

[107] E. López Loveira, P. S. Fiol, A. Senn, G. Curutchet, R. Candal, and M. I. Litter, “TiO 2-photocatalytic treatment coupled with biological systems for the elimination of benzalkonium chloride in water,” *Sep. Purif. Technol.*, vol. 91, pp. 108–116, 2012, doi: 10.1016/j.seppur.2011.12.007.

[108] A. H. Khan, “Fate of Benzalkonium Chlorides in Natural Environment and Treatment Processes,” *Electron. Thesis Diss. Repos.*, no. December, 2016.

[109] D. R. Ryan, E. K. Maher, J. Heffron, B. K. Mayer, and P. J. McNamara, “Electrocoagulation-electrooxidation for mitigating trace organic compounds in model drinking water sources,” *Chemosphere*, vol. 273, p. 129377, 2021, doi: 10.1016/j.chemosphere.2020.129377.

[110] E. Hmani, Y. Samet, and R. Abdelhédi, “Electrochemical degradation of auramine-O dye at boron-doped diamond and lead dioxide electrodes,” *Diam. Relat. Mater.*, vol. 30, pp. 1–8, Nov. 2012, doi: 10.1016/J.DIAMOND.2012.08.003.

Appendix A Additional Information

Table A.1 Summary of Electrodegradation of PFAS from Literature

Compound	Anode	Cathode	Electrolyte	Main Conditions	Kinetics	Key findings	Ref
PFOA, PFOS	Magnéli phase Ti_4O_7	Stainless steel	0.10 M Na_2SO_4	10 mg/L PFAS 10 mA/cm^2 t = 180 mins	Pseudo 1st-order PFOA: k = 0.0226 min^{-1}, $t_{1/2}$ = 30.7 min PFOS: k = 0.0491 min^{-1}, $t_{1/2}$ = 14.1 min	96% removal of PFOA 98.9% removal of PFOS	[57]
PFOA	Ti/SnO_2–Sb, Ti/SnO_2–Sb/PbO_2, Ti/ SnO_2–Sb/MnO_2	Ti	0.01 M $NaClO_4$	100 mg/L PFAS 10 mA/cm^2 t = 90 mins	Pseudo 1st-order k = 0.064 min^{-1}, $t_{1/2}$ = 10.8 min	90.3%, 91.1%, 31.7% removal for respective anode materials	[71]
H_4PFOS, PFOS (mix of PFAS)	Platinised Ti, Pb	Pb	acidic PFAS + electroplating waste stream	1 – 20 mg/L 1–2 hrs 2 A/dm^2	Pseudo 1st-order	Effective decomposition of PFAS	[72]
PFOA, PFOS, PFBA, PFPeA, PFHxA, PFHpA, PFBS, PFHxS, PFHpS	BDD/Nb	Stainless steel	Different groundwater samples (Na_2SO_4)	0, 25 and 200 mA/cm^2 8 h	Pseudo 1st-order PFOA: k = 0.23 L/A h PFOS: k = 0.084 – 0.23 L/A h	BDD is able to defluoronate PFAAs	[12]

PFOA	BDD	Pt deposited Ti plate	0.01 M $NaClO_4$	0.04 – 1.2 mA/cm^2	Pseudo 1st-order, k = 0.024 dm^3/h	proposed mechanism is cleavage of COOH group from the molecule	[16]
PFOA, PFOS	BDD	W	1500 mg/L Na_2SO_4 (+ 167 mg/L NaCl)	15 mg/L PFOA, 10 mg/L PFOS 50, 15, 3 mA/cm^2	Pseudo 1st-order PFOA: k_{50} = 1.2 h^{-1} PFOS: k_{50} = 0.37 h^{-1}	Presence of $OH^{\bullet}$ didn't have significant effect on PFAS degradation implying direct oxidation on electrode surface	[62]
PFOA	SbO_2–Sb/CA, SnO_2-Sb/Ti	Ti	0.1 M Na_2SO_4	100 mg/L PFOA 20 mA/cm^2 5 h	Pseudo 1st-order, k = 0.52 h^{-1}	91% degradation with ultrasound, 47% degradation without	[73]
PFBS, PFHxS, PFOS	Nb/BDD	Nb/BDD	0.1 M Na_2SO_4	2.9 mg/L PFBS, 11 mg/L PFHxS, 15 mg/L PFOS 2.3 mA/cm^2 48 h	Pseudo 1st-order kinetics Rate constant increases with increasing PFAS chain length	45% PFBS, 91% PFHxS, 98% PFOS degradation	[24]
PFOA, PFOS, 6:2 FTS	PbO_2 from lead acid battery	Cathode panel from battery	0.01 M Na_2SO_4	50 mA/cm^2	Pseudo 1st-order, k = 0.0028 – 0.007 min^{-1}	>99% removal of PFAS	[74]
PFOS	Ti/Pt	Ti/Pt, graphite sheet	0.5 M $NaClO_4$	5 mg/L PFOA UV light	Not mentioned	Electron transfer by UV general electrons process without the addition of other	[75]

						chemicals is a promising technique for treating recalcitrant halogenated compounds	
PFHxA	p-Si/BDD	p-Si/BDD	Industrial water samples	870 mg/L PFHxA from nanofiltration 20, 50, 100 A/m^2	Pseudo 1st-order, k_{20} = 1.859 L/A h, k_{50} = 2.252 L/A h, k_{100} = 1.814 L/A h	98% degradation rate	[76]
GenX	BDD	Stainless steel	2475 mg/L Na_2SO_4 + 495 mg/L NaCl	4.98 mg/L GenX 50 mA/cm^2 4 h	Pseudo 1st-order Nanofiltrate: k = 0.0041 min^{-1}, $t_{1/2}$ = 169 min raw water: k = 0.0021 min^{-1}, $t_{1/2}$ = 330 min	Mechanism involves step-wise mineralisation of acid chain	[37]
6:2 FTS, PFOS	Ti/SnO_2–Sb_2O_5–Bi_2O_3	Ti	0.0114 M NaCl/ Na_2SO_4/ $NaClO_4$	1.42 – 6.80 mA/cm^2	Pseudo 1st-order, k = 0.074 h^{-1}	PFOS not degraded, ≤ 23.75% 6:2 FTS degradation	[77]
6:2 FTAB, 6:2 FTSA, 6:2 M4, PFCAs	BDD	Stainless steel	Industrial waste water	1111 µg/L 6:2 FTAB, 242.5 µg/L 6:2 FTSA, 34.4 µg/L 6:2 M4 50 mA/cm^2	Pseudo 1st-order 6:2 FTAB: k = 1.22 h^{-1} 6:2 FTSA: k = 0.35 h^{-1}	97.1% degradation of PFAS	[78]

				8 h			
6:2 FTSA	p-Si/BDD	p-Si/BDD	5 g/L Na_2SO_4, 3.5 g/L NaCl, 9.4 $NaClO_4$ g/L	100 mg/L 5 – 600 A/m^2	Pseudo 1st- order	Near 100% removal	[79]
PFOA, PFOS, other PFAAs	Ti/RuO_2	Stainless steel	100 mg/L NaCl + 1500 mg/L Na_2SO_4	5 mg/L 0 – 20 mA/cm^2 6 h	Pseudo 1st-order PFOA: k = 46 x 10^{-5} L/(mA/cm^2) min PFOS : k = 70 x 10^{-5} L/(mA/cm^2) min	PFOS and PFOA defluorinated, shorter chain PFAAs were more recalcitrant	[80]
Various PFAS	BDD	Stainless steel	Waste water treatment effluent	1652 µg/L 50 mA/cm^2 10 h	Pseudo 1st-order FTAB: k = 0.923 h^{-1} FTSA: k = 0.469 h^{-1}	99.7% PFAS removal	[81]
PFOA	Ti/SnO-Sb-Bi	Ti	1.4 g/L $NaClO_4$	0.1 – 20 mA/cm^2 3 h	Pseudo 1st-order k = 1.93 h^{-1}	>99% degradation	[30]
PFOA	BDD	Ti	1.4 g/L $NaClO_4$	20, 30, 50 mg/L 0.12 – 0.59 mA/cm^2 2 h	Pseudo 1st-order, $k_{3.0V}$ = 0.0134 min^{-1}, $k_{3.5V}$ = 0.0326 min^{-1}	97.48% removal	[31]
PFMeUPA	MWCNT-COOH	Quaternary ammonium surfactant-modified cathode (OTAB, CTAB,	0.05 M phosphate buffer (11.55 g/L $Na_2HPO_4 \cdot 12H_2O$, 2.77 g/L $NaH_2PO_4 \cdot 2H_2O$	5 mg/L -1.6 V vs Ag/AgCl 30°C	Pseudo 1st-order k_{OTAB} = 0.2158 h^{-1} k_{CTAB} = 0.0230 h^{-1} k_{TTAB} = 0.0096 h^{-1} k_{DTAB} = 0.0056 h^{-1}	99.81% removal efficiency, 78.67% defluorination efficiency on OTAB	[82]

		TTAB, DTAB)					
PFOA, PFOS, 6:2 FTSA	BDD/Nb	BDD/Nb	1.5, 7.85, 14.2 g/L Na_2SO_4 Wastewater	1, 5.5, 10 mg/L PFOA 2.3, 11.85, 21.4 mA/cm^2, 14.61 mA/cm^2 (wastewater) 2 cm electrode separation 1, 2.5, 4 h	Not mentioned	99.5% degradation efficiency	[56]
GenX,	BDD/Nb	Pt mesh	0.0025 – 0.015 M $NaClO_4$ 0.0025 – 0.015 M Na_2SO_4	15 mg/L GenX 5, 10, 20, 30 mA/cm^2 300 rpm 4 h	Pseudo 1st-order k = 0.0150 min^{-1}	Up to 97% degradation	[39]
PHHxA, PFHpA, PFOA, PFNA, PFBS, PFHxS, PFOS, 4:2 FTS, 6:2	Ti_4O_7 ceramic plate	304 stainless steel rod	0.02 M Na_2SO_4	0.005 - 0.5 µM PFAS 5 mA/cm^2 1 h	Pseudo 1^{st}-order	>99% degradation PFOS, PFOA, PFNA, 8:2 FTS >90% degradation PFHxS, 6:2 FTS	[43]

FTS, 8:2 FTS							
PFOA, PFBA, 6:2 FTCA, GenX	BDD	Stainless steel	0.1 – 10% w/v Na_2SO_4	0.2 – 200 mg/L PFOA 2-10 mA/cm^2 1-2 cm electrode separation 400 – 700 rpm	FTCA: k = 0.031 min^{-1} PFOA: k = 0.019 min^{-1} GenX: k = 0.013 min^{-1} PFBA: k = 0.008 min^{-1}	90.7% degradation of PFOA	[55]
PFMeUPA	GAC/stainless steel	GAC/stainless steel	0.1 M Na_2SO_4, 0.1 M $NaClO_4$	100 µM PFMeUPA	Pseudo 1st-order	Reduction rate increases with increasing temperature and decreasing reduction potential	[83]
PFOS, PFOA	Borophene-doped graphene, boron-doped graphene	Stainless steel sponge	0.1 M phosphate buffer UF-filtrated landfill leachate	0.2 µM PFAS 0.115 – 0.460 mA/cm^2	Not available	77% removal PFOS, 57% removal PFOA phosphate buffer 86% removal PFOS, 72% removal PFOA in UF-landfill leachate	[63]
GenX, 8:2 FTOH, PFECA, PFMDSF, PFO-1-ol, 6:2 FTS,	BDD	BDD	200 mg/L Na_2SO_4	100 µg/L PFAS 17.2 mA/cm^2	Pseudo 1st-order	68 – 100% degradation at 45.2 min of RT	[84]

PFOSA, PFEESA, Nafion byproduct 2							
PFBA, GenX, PFOA, 6:2 FTCA	BDD	Stainless steel	0.1% Na_2SO_4	20 mg/L PFAS 10 mA/cm^2 t = 120 mins	Psuedo 1st-order	97.9% degradation PFOA, 65.6% degradation PFBA, 84.9% degradation GenX, 99.4% degradation 6:2 FTCA	[38]
PFOS, PFOA, PFHxS, PFHxA, PFBS, PFBA	Boron-doped graphene sponge	Stainless steel sponge	0.01 M phosphate buffer (Na_2HPO_4/NaH_2PO_4)	0.2 µM PFAS 0.23 mA/cm^2	Not available	16.7-67% degradation. Graphene sponge anode capable of C-F bond cleavage	[85]
PFOA, PFOS, 6:2 FTS	Ti_4O_7	Ti_4O_7	0.14 M Na_2SO_4	50 µM PFAS t = 3 h	Pseudo 1st-order PFOA: k_{PR} = 0.20 min^{-1} k_{DC} = 0.22 min^{-1} PFOS: k = 0.014 min^{-1} 6:2 FTS: k = 0.022 min^{-1}	>95% removal PFOA, >99% removal PFOS and 6:2 FTS Polarity reversal increases defluorination, increasing energy efficiency and reduces fouling	[86]
PFOA, PFNA, PFDA	SnO_2−Sb−Ce	Ti	10 mM $NaClO_4$	0.25 mM PFAS	Pseudo 0th-order and pseudo 1st order	BDD:	[32]

	SnO_2−Sb/ Ce−PbO_2 BDD			t = 180 mins	kinetics for PFNA removal Pseudo 1st-order kinetics for PFDA removal	98.7 +/- 0.4% removal PFNA 96.0 +1.4% removal PFDA PbO_2: 97.1 +/- 1.0% removal PFNA 92.2 +/- 1.9% removal PFDA	
PFBA, PFPeA, PFHxA, PFHpA, PFOA	Ce-PbO_2	Ti	10 mM $NaClO_4$	100 mg/L PFAS 20 mA/cm^2 t = 90 mins	Pseudo 1st-order kinetics k_{PFBA} = 4.3 x 10^{-3} min^{-1} k_{PFPeA} = 5.9 x 10^{-3} min^{-1} k_{PFHxA} = 1.7 x 10^{-2} min^{-1} k_{PFHpA} = 4.1 x 10^{-2} min^{-1} k_{PFOA} = 3.7 x 10^{-2} min^{-1}	31.8 +/- 4.6% removal of PFBA 41.4 +/- 4.1% removal of PFPeA 78.2 +/- 3.2% removal of PFHxA 97.9 +/- 4.6% removal of PFHpA 96.7 +/- 3.0% removal of PFOA	[33]
GenX	BDD	Cu, Ti, Au	0.10 M Na_2SO_4 + 0.12 M NaCl	5 mg/L GenX	Pseudo 1st-order kinetics	76% removal on Cu	[87]

				t = 2 h 50 mA/cm^2	$k_{Cu} = 10.8 \times 10^{-3}$ min^{-1} $k_{Au} = 7.90 \times 10^{-3}$ min^{-1} $k_{Ti} = 7.88 \times 10^{-3}$ min^{-1}	63% removal on Au 61% removal on Ti	
PFOA, PFOS	BDD	Pt/Ti wire	10 mM Na_2SO_4	8 µg/L – 100 mg/L PFAS 8 – 40 mA/cm^2 t = 6 h	0th-order kinetics at low amperage 1st-order kinetics at higher amperage	`60% defluorination	[34]
GenX	BDD Fluorine doped tin oxide conductive glass (FTO) Pt	Graphene-Ni-foam	0.05 M K_2SO_4 + 0.2 mM Fe^{2+} catalyst	86.8 mg/L 8, 16 mA/cm^2 6 h Combined electro-Fenton process	Pseudo-1st order K = 0.0175 min^{-1}	92.2% mineralisation for EF	[40]

Table A.2 Summary of Electrocoagulation of PFAS from Literature

Compound	Electrodes	Filter	Electrolyte	Main Conditions	Key findings	Ref
PFBS, PFHxS, PFOS	Al-Zn	0.22 µm glass fibre	1 g/L NaCl Natural groundwater	1 mg/L PFAS 12 V pH 7 10 s reversal period	Synthetic water: 87.4% removal of PFBS 95.6 % removal of PFHxS 100% removal of PFOS Natural groundwater: 59.0% removal PFBS 88.2% removal PFHxS 100% removal PFOS	[44]
PFOA, PFOS	Zn-Air cathode	0.22 µm nylon	0.01 M NaCl	0.25 mM PFAS 45 min	99.8% removal PFOA 88.5% removal PFOS	[88]
PFOA	Fe-Fe	0.2 µm polyether sulphone	0.035 M NaCl	24 µM PFOA 80 mA/cm^2 6 h	100% removal PFOA	[46]
PFOA	Fe-Fe, Fe-Zn, Fe-Al, Al-Al, Zn-Zn, Al-Zn,	0.22 µm glass microfibre	2 g/L NaCl Natural groundwater	1 mg/L PFOA 9 V 500 rpm 10 s reversal	99.6% removal PFOA in synthetic water 79.4% removal in natural groundwater	[70]
PFHxS, PFOS, PFNA, PFOA, 6:2	Zn-SS	0.22 µm acetate	0.02 M Na_2SO_4	0.1 µM PFAS 1 mA/cm^2	>90% removal for PFOS and 6:2 FTS	[43]

FTS, PFHpA, 8:2 FTS, PFHxA, PFBA				2 h		
PFOA	Al-Al	0.22 µm PTFE	NaCl + ZnCl Natural wastewater	1 mM PFOA	~100% removal in synthetic water 90% removal in natural wastewater	[89]
PFOA, PFOS	Zn/Mg/Al/ Fe-SS	0.22 µm acetate	10 mM NaCl	1.5 µM – 0.5 mM PFAS	~100% removal	[48]
PFBA, PFPeA, PFHxA, PFHpA, PFOA, PFNA, PFDA, PFBS, PFHxS, PFOS	Al-Zn	0.22 µm glass fibre	2 g/L NaCl	1 mg/L PFAS 12 V	90.9% removal of PFBA 91.0% removal of PFBS 99.7% removal of PFOA: 100% removal of PFOS	[50]
PFBA, PFPeA, PFHxA, PFBS, PFPeS	Fe-Fe		2 g/L NaCl	1 mg/L PFAS 9 V 10 s reversal period	97 – 100% removal long chain PFAS Groundwater: 62.5% removal of PFBA 89% removal of PFPeA 96.4% removal of PFHxA 90% removal of PFBS 97.5% removal of PFPeS	[49]
PFHxA	Al-Al	0.45 µm	Not available	1 – 5 mM 0 – 60 V 0 – 6 A	Adding surfactants improves removal. Cationic surfactants	[90]

					are more efficient than anionic surfactants.	
HFPO-TA	Zn-SS		0.02 M NaCl	40 µM HFPO-TA 20 mA/cm^2 3 h	99.6% removal	[51]

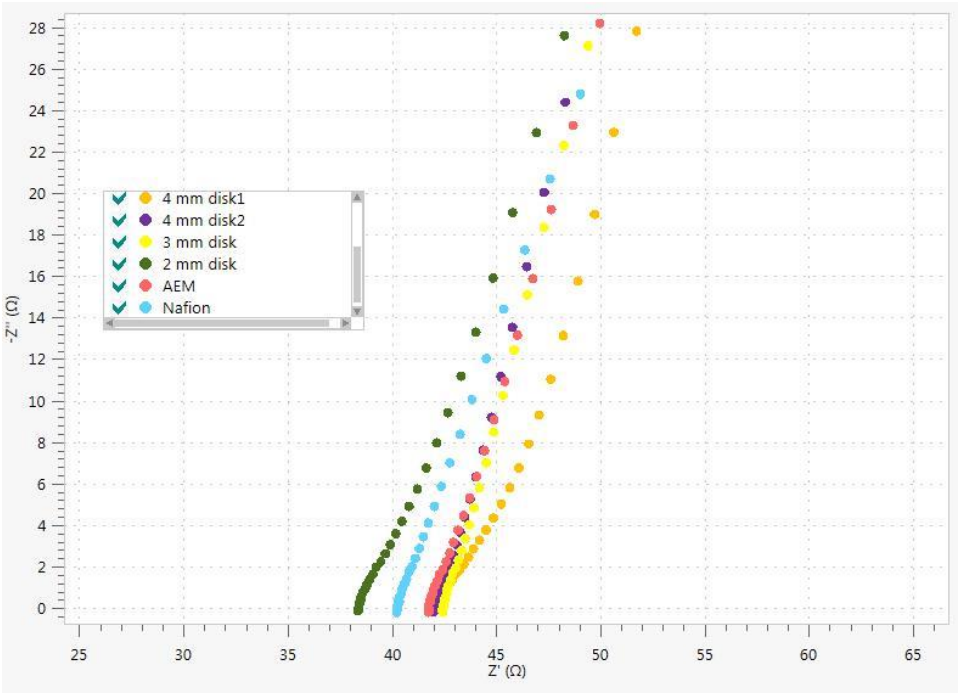

Figure A.1 Nyquist plot of different membranes in the divided cell recorded at a cell potential of 0 V.

Table A.3 Resistance of membrane in the divided cell

Membrane	**Ohmic Resistance (Ω)**
Nafion 117™	40.0
Anion Exchange Membrane	41.8
2 mm agar salt disk	38.0
3 mm agar salt disk	42.0
4 mm agar salt disk	42.3

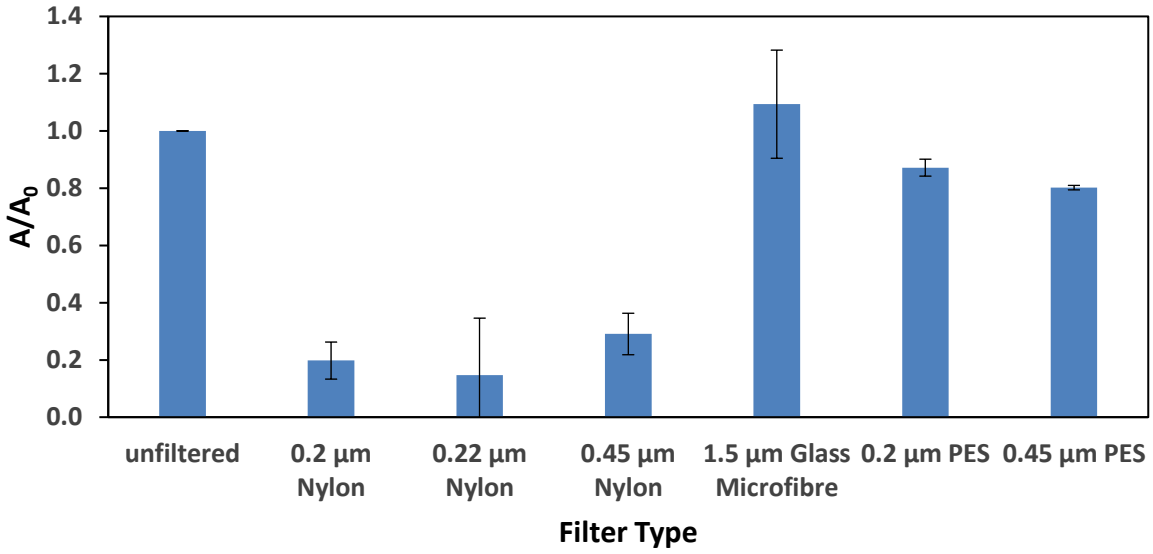

Figure A.2 Relative amount of GenX passed through different filters, n = 2

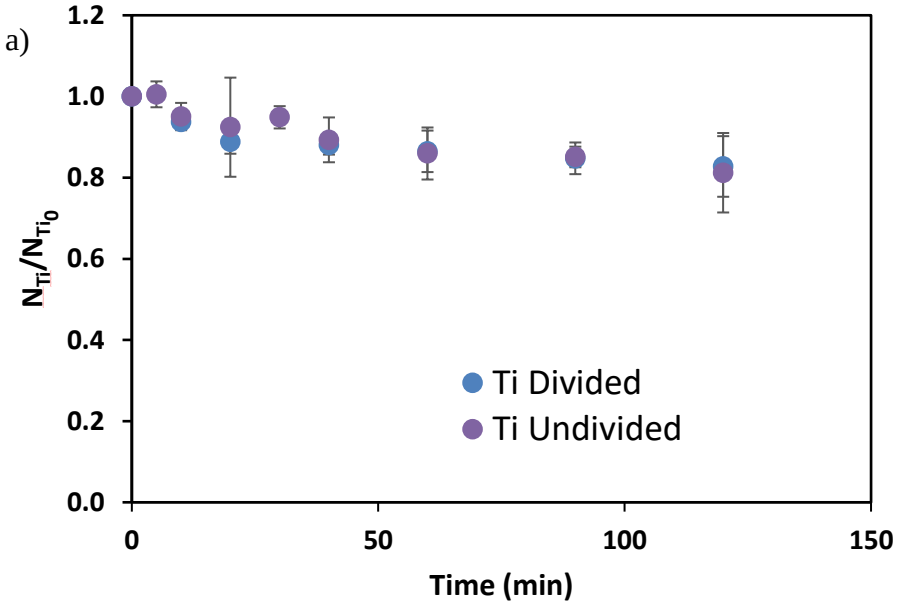

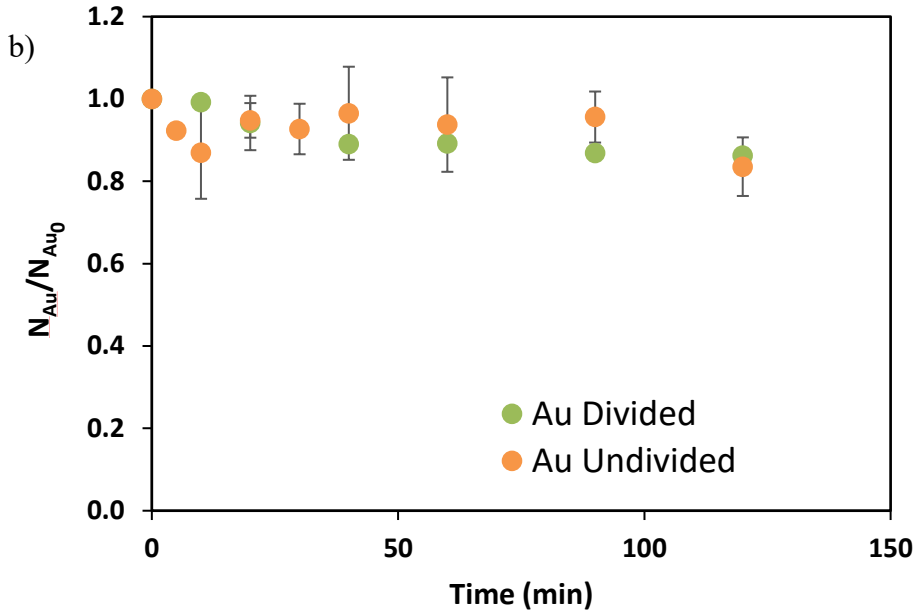

Figure A.3 Number of moles GenX degraded in undivided and divided cell at 13.5 mA/cm^2 a) Ti cathode b) Au cathode, n = 2, error bars = 1 standard deviation

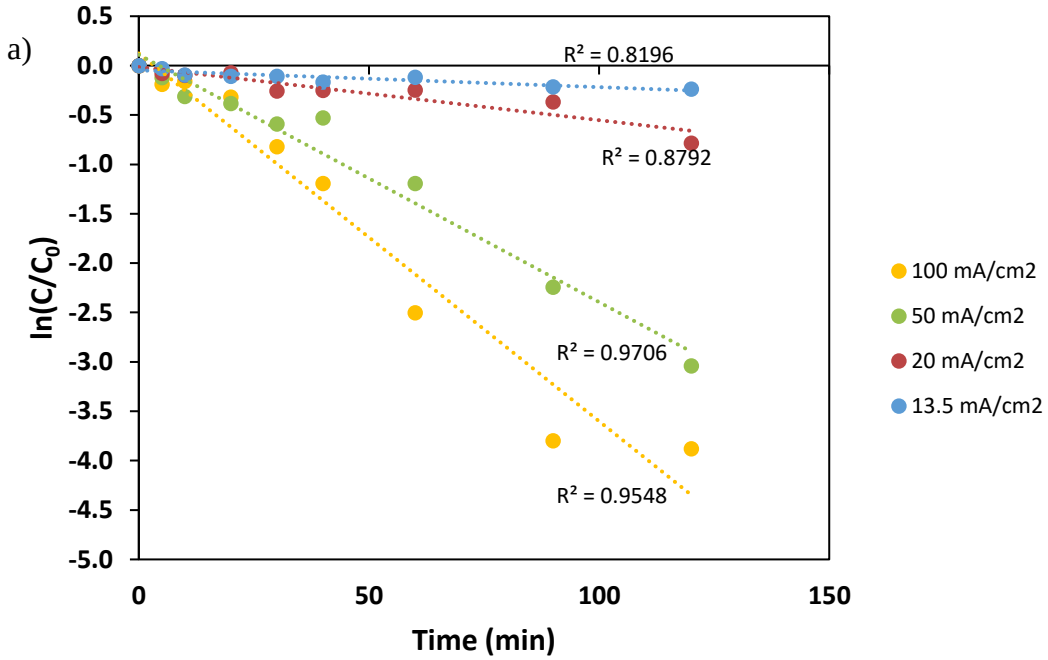

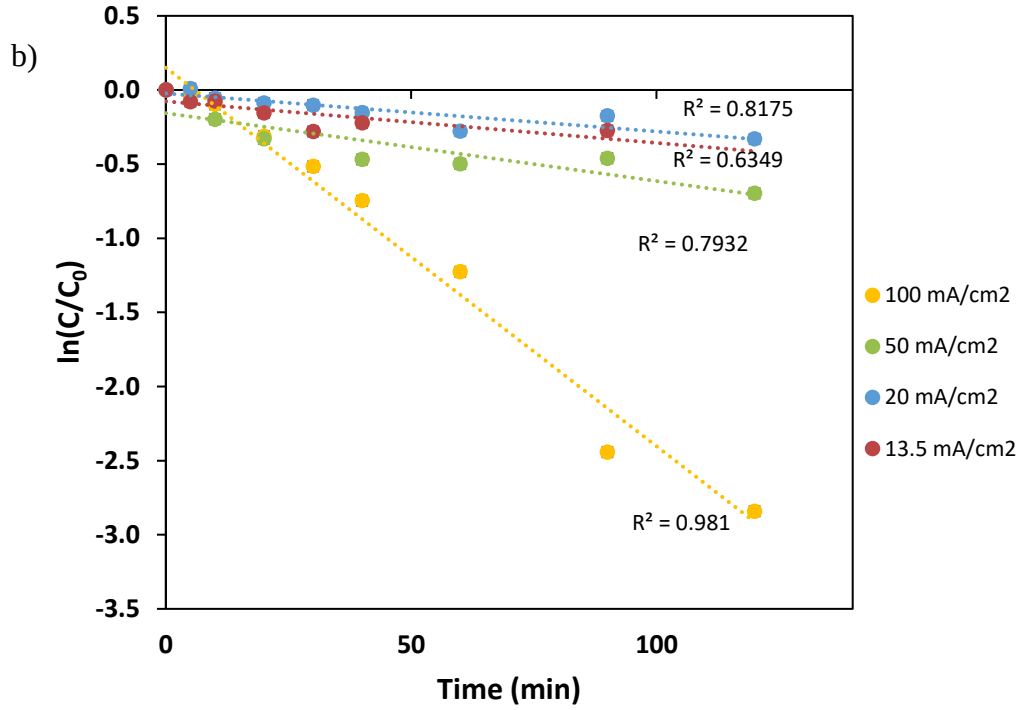

Figure A.4 Linearisation of GenX degradation curves at different current densities for a) oxidation and b) reduction in a divided cell

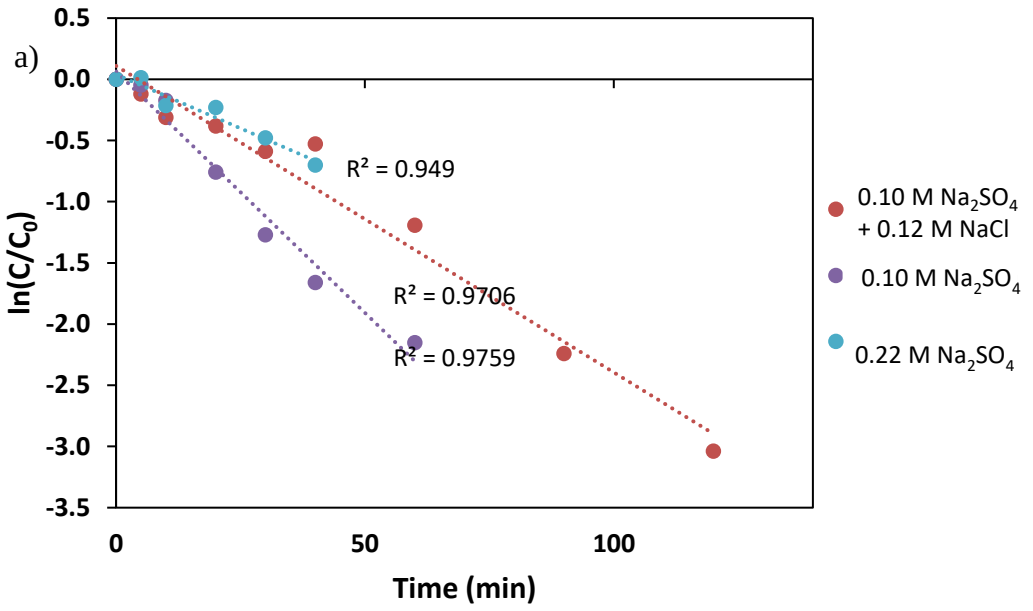

b)

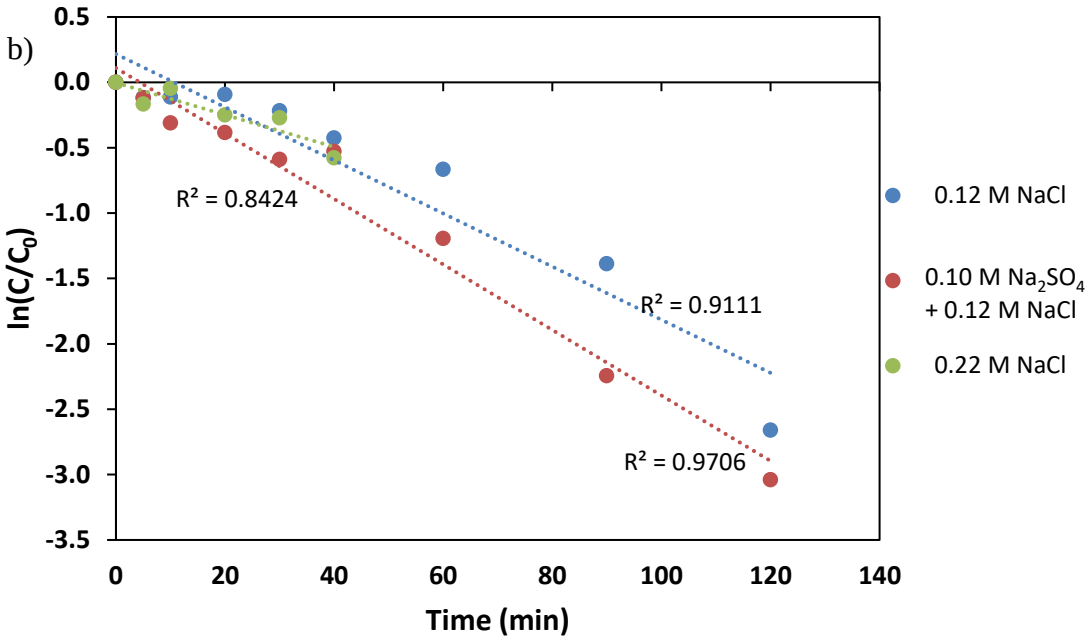
0.5
0.0
-0.5
-1.0
-1.5
-2.0
-2.5
-3.0
-3.5
ln(C/C0)
0
20
40
60
80
100
120
140
Time (min)
R² = 0.8424
R² = 0.9111
R² = 0.9706
0.12 M NaCl
0.10 M Na2SO4 + 0.12 M NaCl
0.22 M NaCl

c)

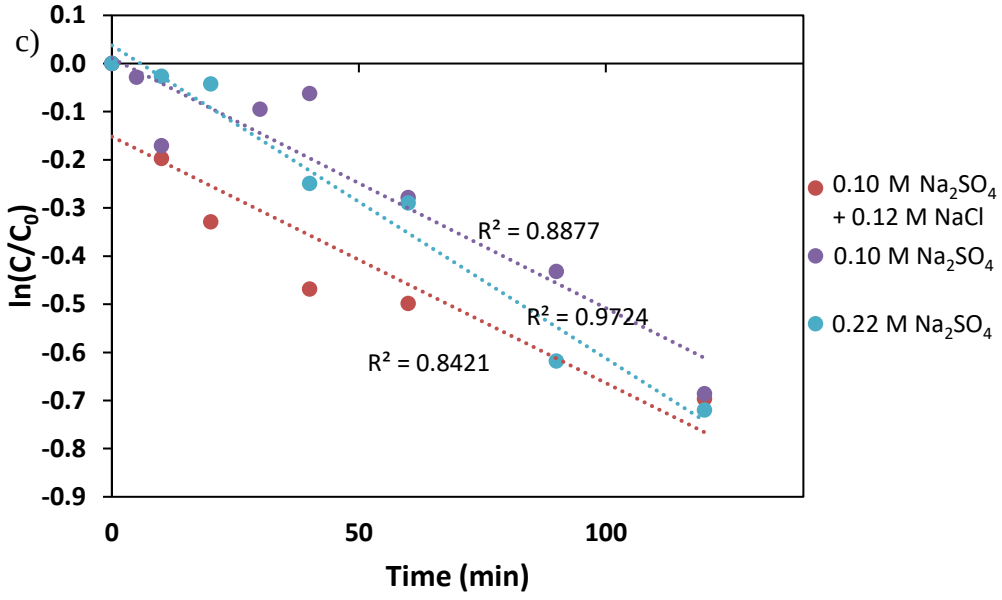
0.1
0.0
-0.1
-0.2
-0.3
-0.4
-0.5
-0.6
-0.7
-0.8
-0.9
ln(C/C0)
0
50
100
Time (min)
R² = 0.8877
R² = 0.9724
R² = 0.8421
0.10 M Na2SO4 + 0.12 M NaCl
0.10 M Na2SO4
0.22 M Na2SO4

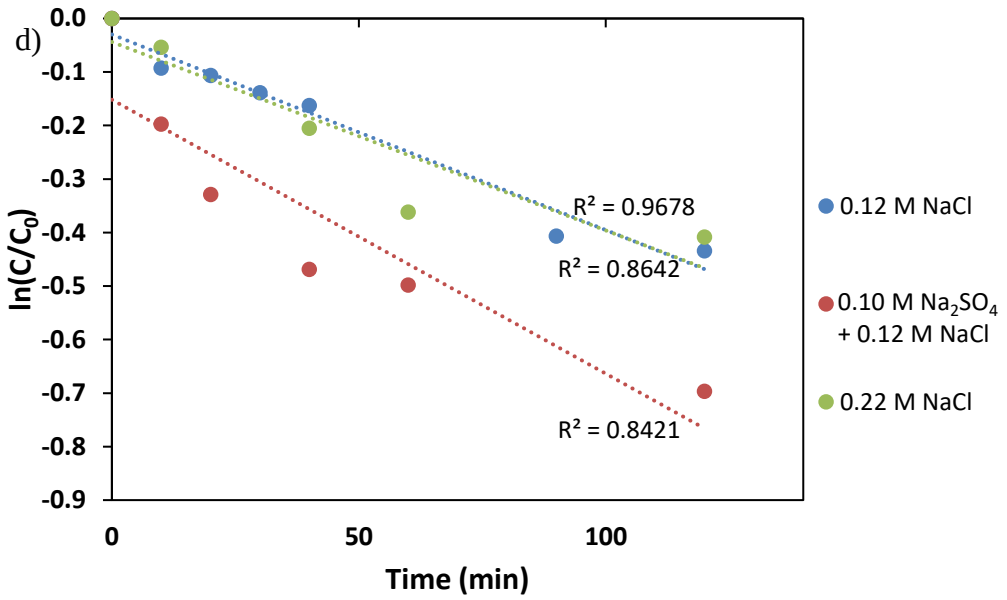

Figure A.5 Linearisation of GenX degradation curves in different electrolytes in a *divided* cell at 50 mA/cm^2: comparing different concentrations of a) Na_2SO_4 for oxidation, b) NaCl for oxidation, c) Na_2SO_4 for reduction and d) NaCl for reduction

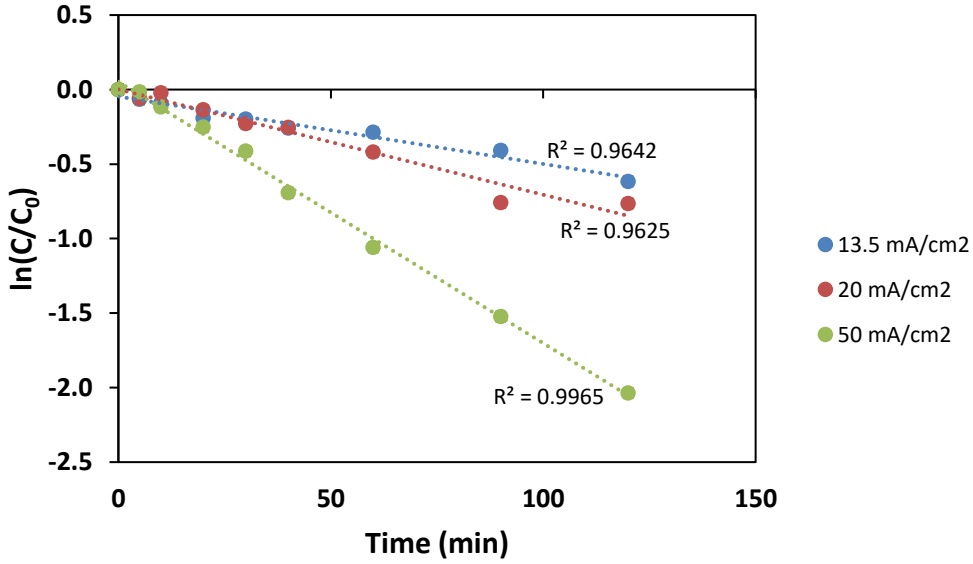

Figure A.6 Linearisation of GenX degradation curves in waste water at different current densities in an undivided cell

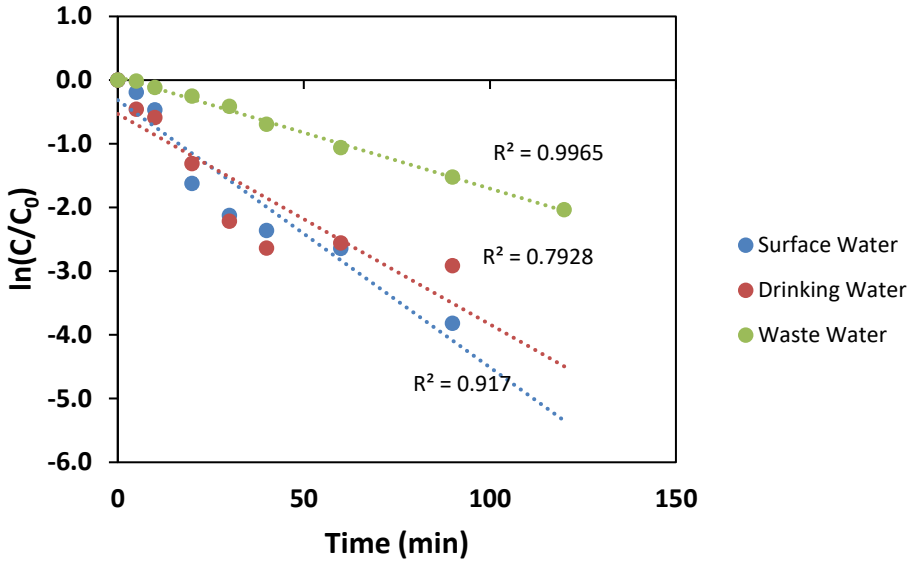

Figure A.7 Linearisation of GenX degradation curves in different water matrices at 50 mA/cm^2 different current densities in an undivided cell

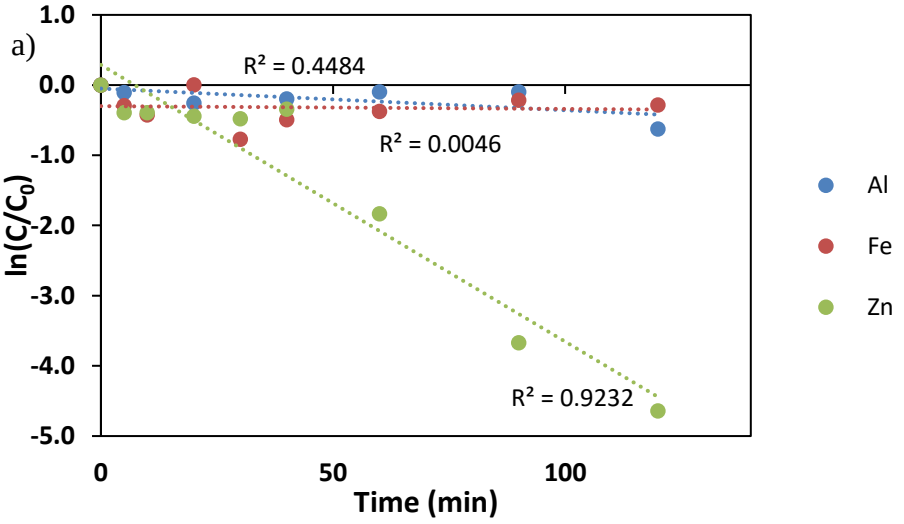

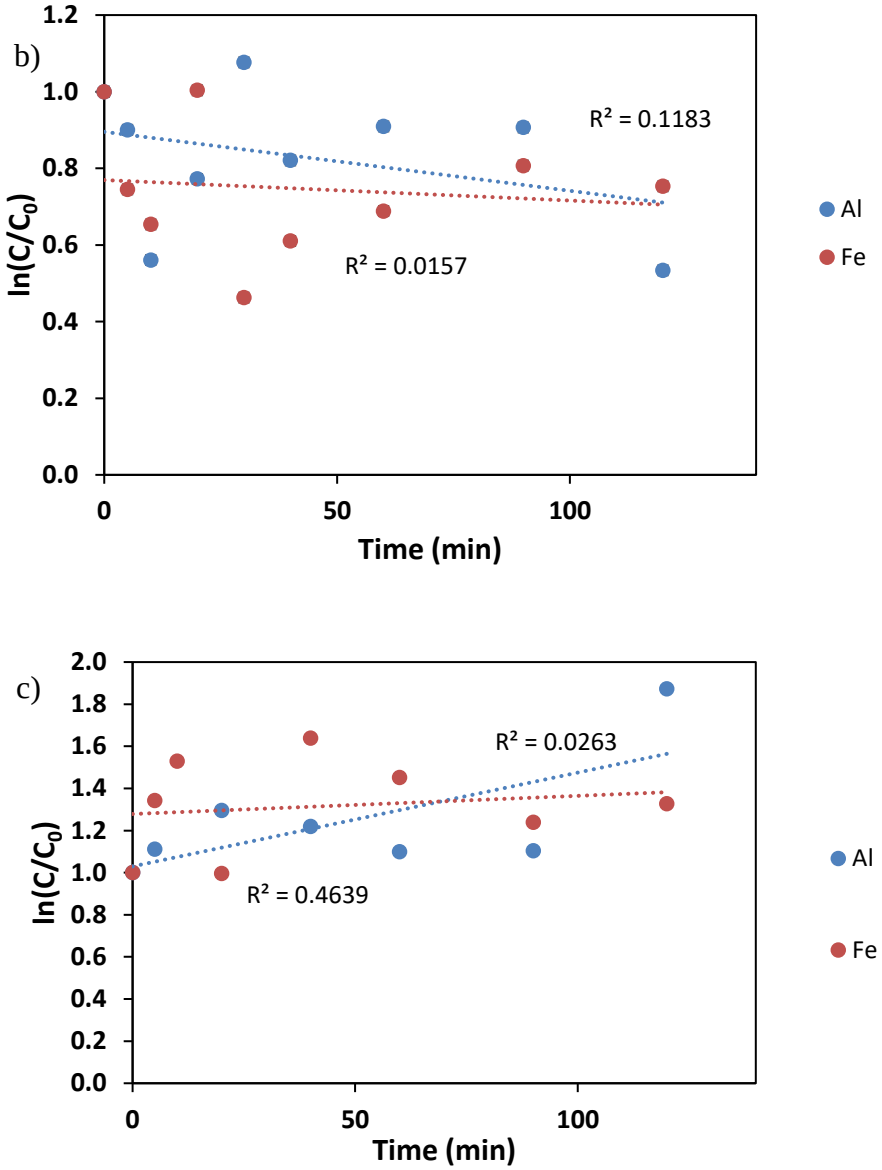

Figure A.8 Linearisation of GenX removal curves by electrocoagulation on different materials at 10 mA/cm^2 for the a) 1st order, b) 0th order and c) 2nd order rate equations

Table A.4 Summary of Microtox BiAssay Measurements

Chemical	Condition	Background Matrix	Cell Type	EC50*	Quenching
500 mg/L GenX	Untreated	0.10 M Na_2SO_4 + 0.12 M NaCl	N/A	2525 mg/L	Unquenched
N/A	Treated	0.10 M Na_2SO_4 + 0.12 M NaCl	Undivided	0.0644%	Unquenched
N/A	Treated	0.10 M Na_2SO_4 + 0.12 M NaCl	Divided – oxidation	0.1015%	Unquenched
N/A	Treated	0.10 M Na_2SO_4 + 0.12 M NaCl	Divided – reduction	Not toxic	Unquenched
20 g/L Bovine Serum Albumin	Untreated	--	-	21.308 g/L	--
0.12 M Dopamine chloride	Untreated	--	--	0.002631 M	--
N/A	Treated	0.10 M Na_2SO_4 + 0.12 M NaCl	Divided – oxidation	1.585%	0.05 M dopamine chloride
N/A	Treated	0.10 M Na_2SO_4 + 0.12 M NaCl	Undivided	2.28%	10 g/L Bovine Serum Albumin
N/A	Treated	0.10 M Na_2SO_4 + 0.12 M NaCl	Divided – oxidation	9.716%	10 g/L Bovine Serum Albumin
250 mg/L Catalase	Untreated	--	--	92.31 mg/L**	--

N/A	Treated	0.10 M Na_2SO_4 + 0.12 M NaCl	Undivided	0.1511%**	25 mg/L catalase
N/A	Treated	0.10 M Na_2SO_4 + 0.12 M NaCl	Divided – oxidation	0.2175%	25 mg/L catalase
N/A	Treated	0.10 M Na_2SO_4 + 0.12 M NaCl	Divided – reduction	Not toxic	25 mg/L catalase
N/A	Treated	0.10 M Na_2SO_4 + 0.12 M NaCl	Undivided	0.2905%**	50 mg/L catalase
N/A	Treated	0.10 M Na_2SO_4 + 0.12 M NaCl	Divided – oxidation	0.0781%	50 mg/L catalase
N/A	Treated	0.10 M Na_2SO_4 + 0.12 M NaCl	Divided – oxidation	1.23%	150 mg/L
N/A	Treated	0.10 M Na_2SO_4 + 0.12 M NaCl	Undivided	2794%	2500 mg/L $Na_2S_2O_3$
N/A	Treated	0.10 M Na_2SO_4 + 0.12 M NaCl	Divided – oxidation	0.3375%	7500 mg/L $Na_2S_2O_3$
N/A	Treated	0.10 M Na_2SO_4 + 0.12 M NaCl	Undivided	40.13%	5000 mg/L $Na_2S_2O_3$
N/A	Treated	0.10 M Na_2SO_4 + 0.12 M NaCl	Divided – oxidation	1.105%	9000 mg/L $Na_2S_2O_3$
N/A	Treated	0.10 M Na_2SO_4	Undivided	Not toxic	Unquenched
N/A	Treated	0.10 M Na_2SO_4	Divided – oxidation	0.006152%	Unquenched
N/A	Treated	0.10 M Na_2SO_4	Divided – reduction	Not toxic	Unquenched
N/A	Treated	0.10 M Na_2SO_4	Divided – oxidation	0.09792%	100 mg/L $Na_2S_2O_3$
N/A	Treated	0.10 M Na_2SO_4	Divided – oxidation	0.3317%	500 mg/L $Na_2S_2O_3$

N/A	Treated	0.10 M Na_2SO_4	Divided – oxidation	0.3925%	1000 mg/L $Na_2S_2O_3$
N/A	Treated	0.10 M Na_2SO_4	Divided – oxidation	Not toxic	2000 mg/L $Na_2S_2O_3$
GenX	Treated	0.10 M Na_2SO_4	Undivided	Not toxic	Unquenched
GenX	Treated	0.10 M Na_2SO_4	Divided – oxidation	23.26%	2000 mg/L $Na_2S_2O_3$
GenX	Treated	0.10 M Na_2SO_4	Divided – reduction	Not toxic	Unquenched
12,310 GenX	Untreated	--	--	2438 mg/L	Unquenched
12,310 GenX	Untreated	--	--	2238 mg/L	Unquenched

* The EC50 values after 15 minutes were reported
**The EC50 value after 5 minutes was used

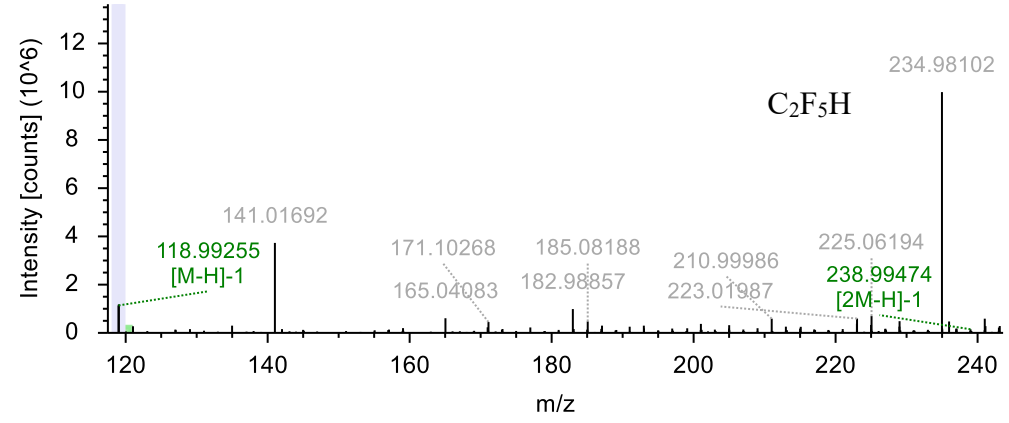
Intensity [counts] (10^6)
12
10
8
6
4
2
0
120
140
160
180
200
220
240
m/z
234.98102
C2F5H
141.01692
118.99255
[M-H]-1
171.10268
165.04083
185.08188
182.98857
210.99986
223.01987
225.06194
238.99474
[2M-H]-1

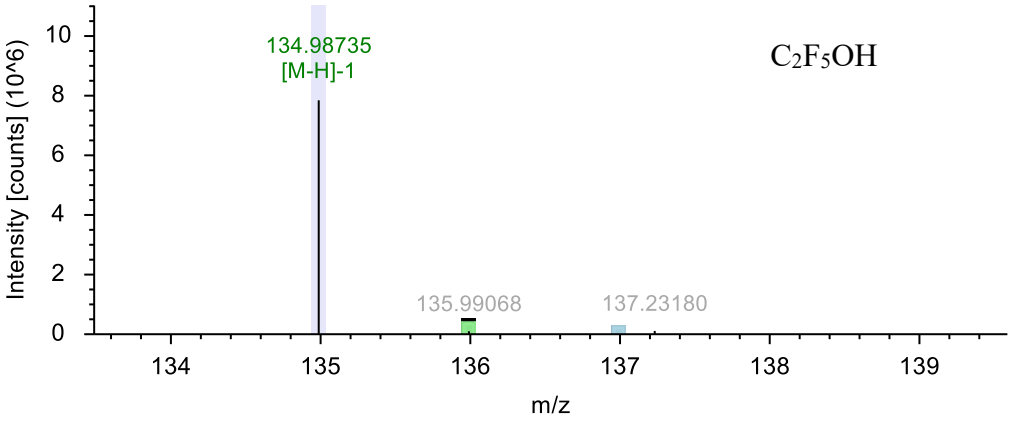
Intensity [counts] (10^6)
10
8
6
4
2
0
134
135
136
137
138
139
m/z
134.98735
[M-H]-1
C2F5OH
135.99068
137.23180

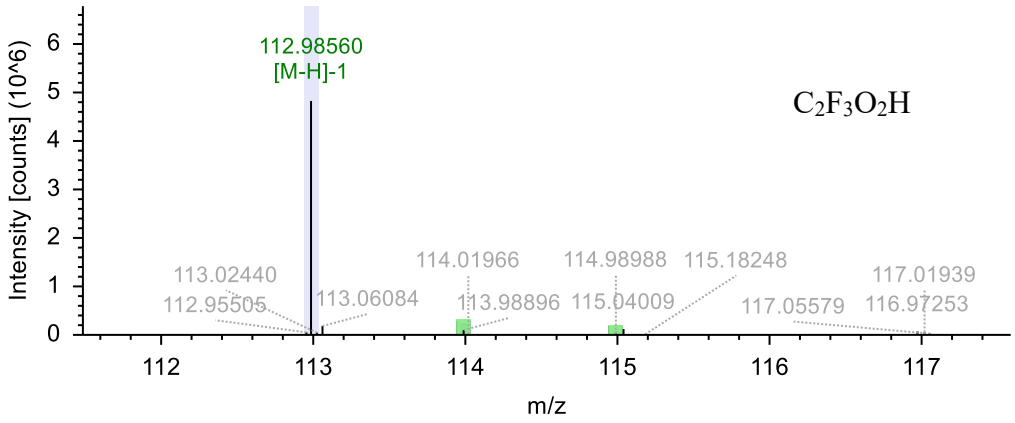
Intensity [counts] (10^6)
6
5
4
3
2
1
0
112
113
114
115
116
117
m/z
112.98560
[M-H]-1
C2F3O2H
113.02440
112.95505
113.06084
114.01966
113.98896
114.98988
115.04009
115.18248
117.05579
117.01939
116.97253

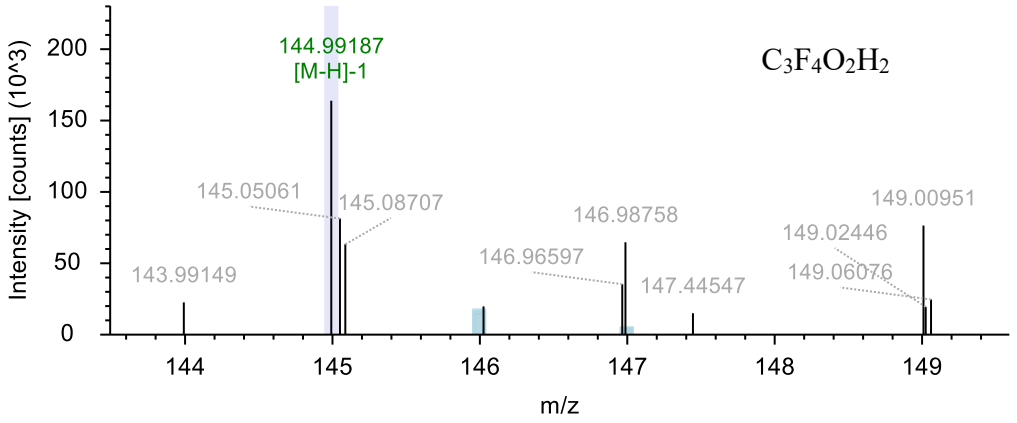
144.99187
[M-H]-1
$C_3F_4O_2H_2$
Intensity [counts] (10^3)
200
150
100
50
0
145.05061
145.08707
143.99149
146.98758
146.96597
147.44547
149.00951
149.02446
149.06076
144
145
146
147
148
149
m/z

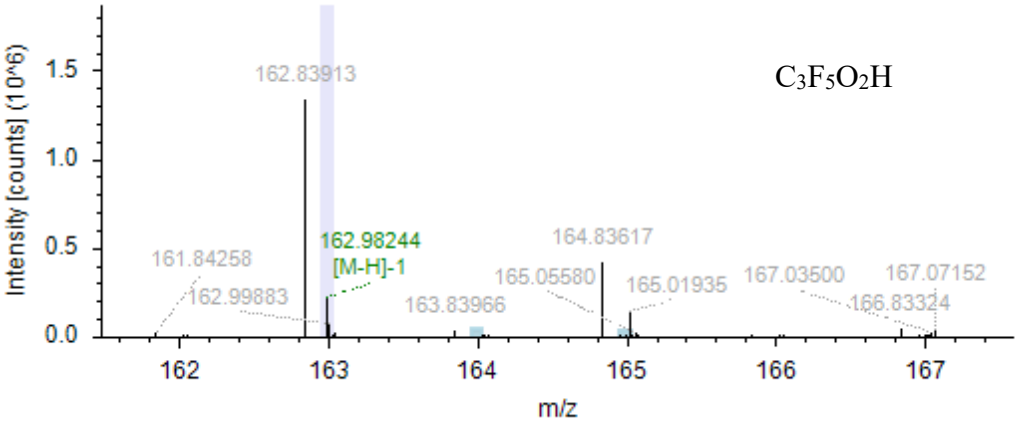
162.83913
$C_3F_5O_2H$
Intensity [counts] (10^6)
1.5
1.0
0.5
0.0
162.98244
[M-H]-1
161.84258
162.99883
163.83966
164.83617
165.05580
165.01935
167.03500
167.07152
166.83324
162
163
164
165
166
167
m/z

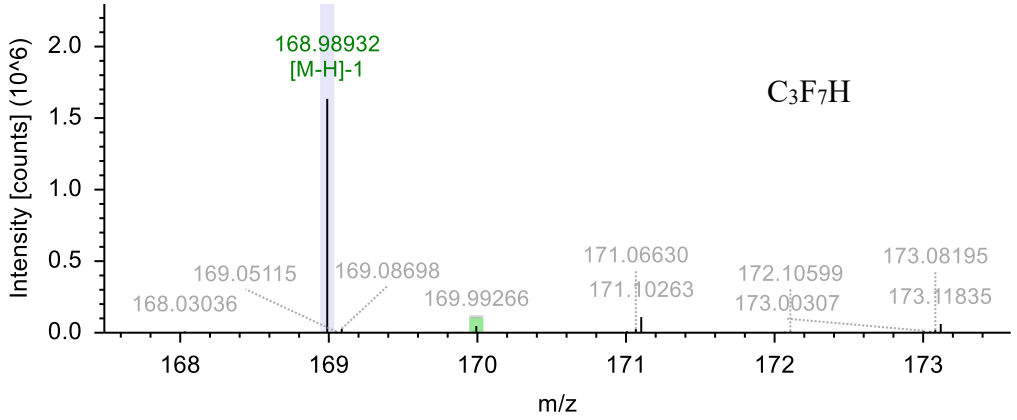
168.98932
[M-H]-1
C_3F_7H
Intensity [counts] (10^6)
2.0
1.5
1.0
0.5
0.0
169.05115
168.03036
169.08698
169.99266
171.06630
171.10263
172.10599
173.00307
173.08195
173.11835
168
169
170
171
172
173
m/z

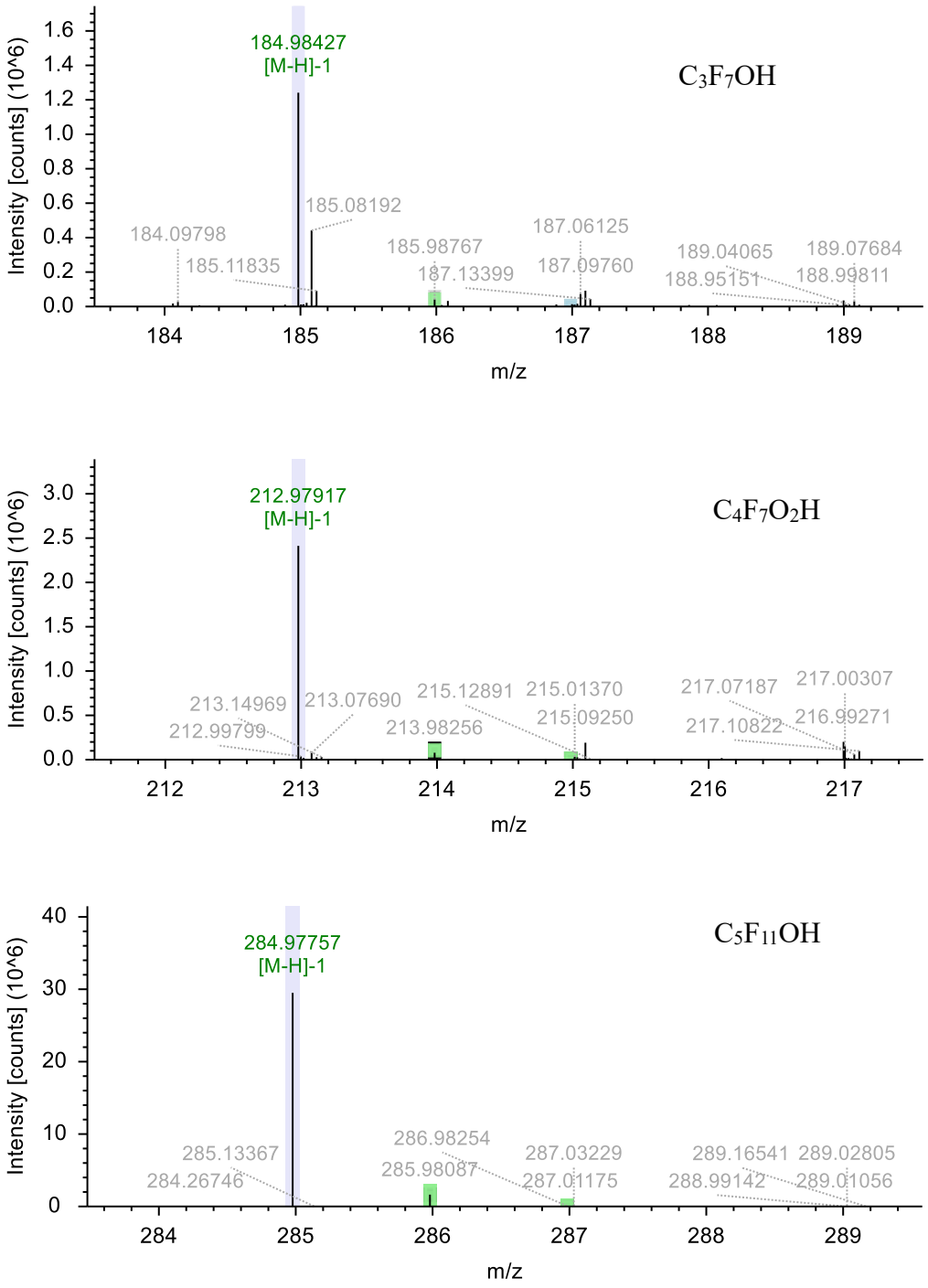

Figure A.9 MS1 chromatograms of GenX transformation products from HRMS

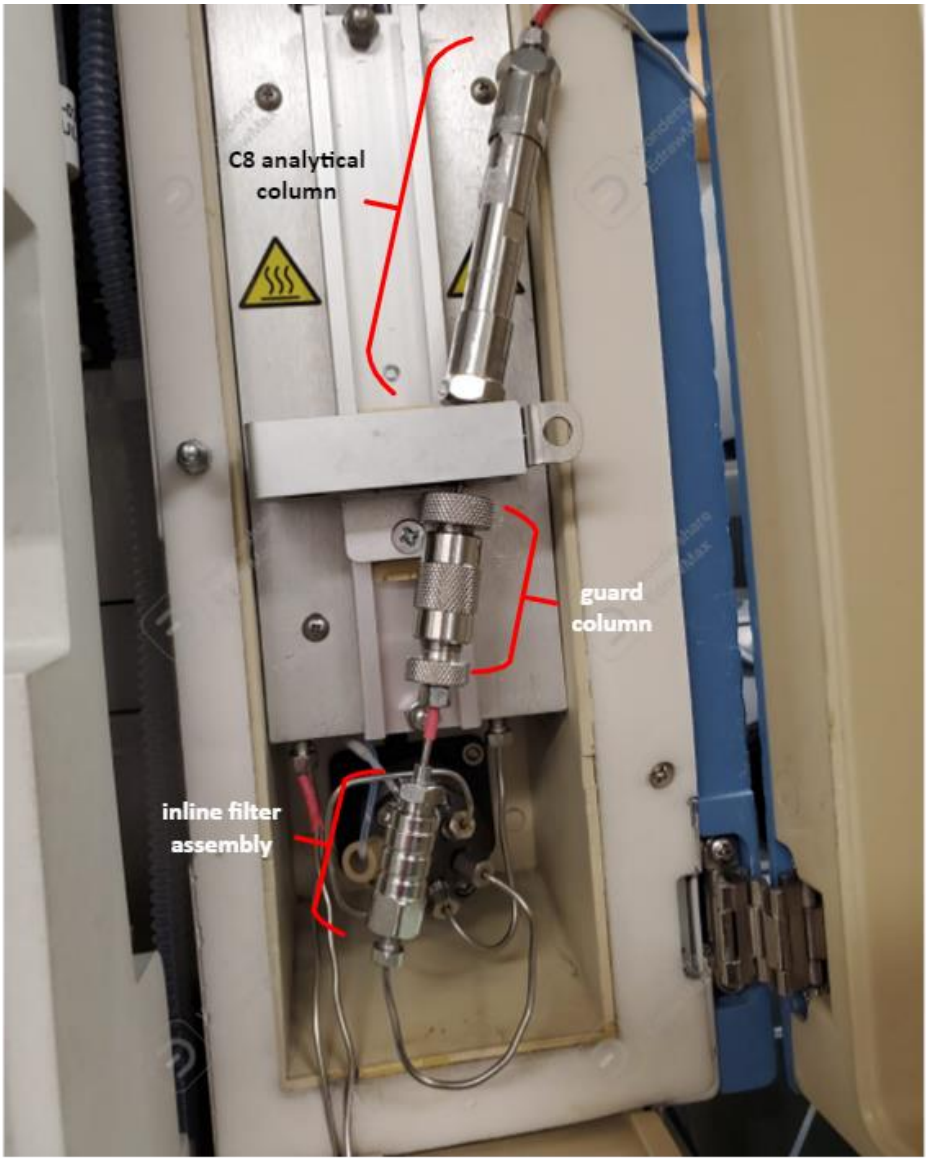

Figure A.10 LCMS column assembly used for analysis

Fabrication of the Agar Membrane

The agar membrane used for the divided cell was made from 1 g agar mixed with 5 g potassium nitrate in 50 mL water. The mixture was heated until small bubbles appeared. The mixture was poured into 3D printed moulds (2 mm thickness; ID 150 mm) and stored in saturated potassium nitrate aqueous solution until use.

Appendix B Statistical Tests

Table B.1 ANOVA results comparing the performance in the oxidation compartment of the divided cell for the different electrode pairings

Tukey's multiple comparisons test	Mean Diff.	95.00% CI of diff.	Below threshold?	Summary	Adjusted P Value
Adosrption Control vs. BDD-SS	0.000505	-0.0009557 to 0.001966	No	ns	0.9697
Adosrption Control vs. BDD-Ti	0.0002	-0.001261 to 0.001661	No	ns	>0.9999
Adosrption Control vs. BDD-Cu	0.001029	-0.0004317 to 0.002490	No	ns	0.3769
Adosrption Control vs. BDD-Sn	0.000531	-0.0009297 to 0.001992	No	ns	0.9593
Adosrption Control vs. BDD-Au	-0.0006	-0.002061 to 0.0008611	No	ns	0.9203
Adosrption Control vs. BDD-Graphite	-0.00029	-0.001755 to 0.001167	No	ns	0.9992
Adosrption Control vs. Ni40Co60-BDD	-0.00074	-0.002197 to 0.0007248	No	ns	0.7882
BDD-SS vs. BDD-Ti	-0.00031	-0.001855 to 0.001245	No	ns	0.9993
BDD-SS vs. BDD-Cu	0.000524	-0.001026 to 0.002074	No	ns	0.9735
BDD-SS vs. BDD-Sn	0.000026	-0.001524 to 0.001576	No	ns	>0.9999
BDD-SS vs. BDD-Au	-0.00111	-0.002655 to 0.0004445	No	ns	0.3606
BDD-SS vs. BDD-Graphite	-0.0008	-0.002349 to 0.0007505	No	ns	0.7667
BDD-SS vs. Ni40Co60-BDD	-0.00124	-0.002791 to 0.0003082	No	ns	0.2172
BDD-Ti vs. BDD-Cu	0.000829	-0.0007205 to 0.002379	No	ns	0.7297
BDD-Ti vs. BDD-Sn	0.000331	-0.001219 to 0.001881	No	ns	0.9988
BDD-Ti vs. BDD-Au	-0.0008	-0.002350 to 0.0007495	No	ns	0.7655
BDD-Ti vs. BDD-Graphite	-0.00049	-0.002044 to 0.001056	No	ns	0.9816
BDD-Ti vs. Ni40Co60-BDD	-0.00094	-0.002486 to 0.0006132	No	ns	0.5853

BDD-Cu vs. BDD-Sn	-0.0005	-0.002048 to 0.001052	No	ns	0.9806
BDD-Cu vs. BDD-Au	-0.00163	-0.003179 to -7.950e-005	Yes	*	0.0322
BDD-Cu vs. BDD-Graphite	-0.00132	-0.002873 to 0.0002265	No	ns	0.1532
BDD-Cu vs. Ni40Co60-BDD	-0.00177	-0.003315 to -0.0002158	Yes	*	0.0144
BDD-Sn vs. BDD-Au	-0.00113	-0.002681 to 0.0004185	No	ns	0.3299
BDD-Sn vs. BDD-Graphite	-0.00083	-0.002375 to 0.0007245	No	ns	0.7348
BDD-Sn vs. Ni40Co60-BDD	-0.00127	-0.002817 to 0.0002822	No	ns	0.1951
BDD-Au vs. BDD-Graphite	0.000306	-0.001244 to 0.001856	No	ns	0.9993
BDD-Au vs. Ni40Co60-BDD	-0.00014	-0.001686 to 0.001413	No	ns	>0.9999
BDD-Graphite vs. Ni40Co60-BDD	-0.00044	-0.001992 to 0.001107	No	ns	0.9909

Table B.2 ANOVA results comparing the performance in the reduction compartment of the divided cell for the different electrode pairings

Tukey's multiple comparisons test	**Mean Diff.**	**95.00% CI of diff.**	**Below threshold?**	**Summary**	**Adjusted P Value**
Adosrption Control vs. BDD-SS	0.001156	-0.0001790 to 0.002490	No	ns	0.1409
Adosrption Control vs. BDD-Ti	0.002187	0.0008520 to 0.003521	Yes	****	<0.0001
Adosrption Control vs. BDD-Cu	0.001947	0.0006120 to 0.003281	Yes	***	0.0005
Adosrption Control vs. BDD-Sn	0.001177	-0.0001580 to 0.002511	No	ns	0.1259
Adosrption Control vs. BDD-Au	0.002287	0.0009520 to 0.003621	Yes	****	<0.0001
Adosrption Control vs. BDD-Graphite	0.00115	-0.0001850 to 0.002484	No	ns	0.1454

Adosrption Control vs. Ni40Co60-BDD	-7.3E-05	-0.001408 to 0.001261	No	ns	>0.9999
BDD-SS vs. BDD-Ti	0.001031	-0.0003845 to 0.002447	No	ns	0.3326
BDD-SS vs. BDD-Cu	0.000791	-0.0006245 to 0.002207	No	ns	0.6817
BDD-SS vs. BDD-Sn	0.000021	-0.001395 to 0.001437	No	ns	>0.9999
BDD-SS vs. BDD-Au	0.001131	-0.0002845 to 0.002547	No	ns	0.2201
BDD-SS vs. BDD-Graphite	-6E-06	-0.001422 to 0.001410	No	ns	>0.9999
BDD-SS vs. Ni40Co60-BDD	-0.00123	-0.002644 to 0.0001868	No	ns	0.1388
BDD-Ti vs. BDD-Cu	-0.00024	-0.001656 to 0.001176	No	ns	0.9998
BDD-Ti vs. BDD-Sn	-0.00101	-0.002426 to 0.0004055	No	ns	0.3599
BDD-Ti vs. BDD-Au	0.0001	-0.001316 to 0.001516	No	ns	>0.9999
BDD-Ti vs. BDD-Graphite	-0.00104	-0.002453 to 0.0003785	No	ns	0.3251
BDD-Ti vs. Ni40Co60-BDD	-0.00226	-0.003675 to -0.0008442	Yes	***	0.0001
BDD-Cu vs. BDD-Sn	-0.00077	-0.002186 to 0.0006455	No	ns	0.7119
BDD-Cu vs. BDD-Au	0.00034	-0.001076 to 0.001756	No	ns	0.9972
BDD-Cu vs. BDD-Graphite	-0.0008	-0.002213 to 0.0006185	No	ns	0.6729
BDD-Cu vs. Ni40Co60-BDD	-0.00202	-0.003435 to -0.0006042	Yes	***	0.0008
BDD-Sn vs. BDD-Au	0.00111	-0.0003055 to 0.002526	No	ns	0.2413
BDD-Sn vs. BDD-Graphite	-2.7E-05	-0.001443 to 0.001389	No	ns	>0.9999
BDD-Sn vs. Ni40Co60-BDD	-0.00125	-0.002665 to 0.0001658	No	ns	0.1248
BDD-Au vs. BDD-Graphite	-0.00114	-0.002553 to 0.0002785	No	ns	0.2143
BDD-Au vs. Ni40Co60-BDD	-0.00236	-0.003775 to -0.0009442	Yes	****	<0.0001
BDD-Graphite vs. Ni40Co60-BDD	-0.00122	-0.002638 to 0.0001928	No	ns	0.143

Table B.3 ANOVA results comparing the degradation of GenX using different cathodes in an undivided cell at 50 mA/cm^2

Tukey's multiple comparisons test	Mean Diff.	95.00% CI of diff.	Below threshold?	Summary	Adjusted P Value
Ti vs. Au	0.000424	-0.0007277 to 0.001576	No	ns	0.6336
Ti vs. Cu	0.003221	0.002069 to 0.004373	Yes	****	<0.0001
Au vs. Cu	0.002797	0.001645 to 0.003949	Yes	****	<0.0001

Table B.4 ANOVA results comparing the degradation of GenX at different current densities in an undivided and divided cell

Šídák's multiple comparisons test	Mean Diff.	95.00% CI of diff.	Below threshold?	Summary	Adjusted P Value
13.5 mA/cm^2 Oxidation vs. 13.5 mA/cm^2 ReductionMake	0.000118	-0.005207 to 0.005443	No	ns	>0.9999
13.5 mA/cm^{2}Oxidation vs. 20 mA/cm^{2}Oxidation	0.003848	-0.001276 to 0.008972	No	ns	0.3737
13.5 mA/cm^{2}Oxidation vs. 50 mA/cm^{2}Oxidation	0.025	0.02015 to 0.02984	Yes	****	<0.0001
13.5 mA/cm^{2}Oxidation vs. 100 mA/cm^{2}Oxidation	0.03598	0.03116 to 0.04080	Yes	****	<0.0001
13.5 mA/cm^2 Reduction vs. 20 mA/cm^2 Reduction	0.000476	-0.004648 to 0.005600	No	ns	>0.9999
13.5 mA/cm^2 Reduction vs. 50 mA/cm^2 Reduction	0.004636	-0.0001847 to 0.009457	No	ns	0.0716
13.5 mA/cm^2 Reduction vs. 100 mA/cm^2 Reduction	0.01636	0.01154 to 0.02118	Yes	****	<0.0001

13.5 mA/cm^2 Undivided vs. 20 mA/cm^2 Undivided	0.002359	-0.002296 to 0.007014	No	ns	0.9301
13.5 mA/cm^2 Undivided vs. 50 mA/cm^2 Undivided	0.008111	0.003513 to 0.01271	Yes	****	<0.0001
20 mA/cm^{2}Oxidation vs. 50 mA/cm^{2}Oxidation	0.02115	0.01652 to 0.02577	Yes	****	<0.0001
20 mA/cm^{2}Oxidation vs. 100 mA/cm^{2}Oxidation	0.03213	0.02753 to 0.03673	Yes	****	<0.0001
20 mA/cm^2 Reduction vs. 50 mA/cm^2 Reduction	0.00416	-0.0004377 to 0.008758	No	ns	0.1186
20 mA/cm^2 Reduction vs. 100 mA/cm^2 Reduction	0.01588	0.01128 to 0.02048	Yes	****	<0.0001
20 mA/cm^2 Undivided vs. 50 mA/cm^2 Undivided	0.005752	0.001433 to 0.01007	Yes	**	0.0013
50 mA/cm^{2}Oxidation vs. 100 mA/cm^{2}Oxidation	0.01098	0.006693 to 0.01527	Yes	****	<0.0001
50 mA/cm^2 Reduction vs. 100 mA/cm^2 Reduction	0.01172	0.007465 to 0.01598	Yes	****	<0.0001
20 mA/cm^{2}Oxidation vs. 20 mA/cm^2 Reduction	-0.00325	-0.008169 to 0.001661	No	ns	0.6023
50 mA/cm^{2}Oxidation vs. 50 mA/cm^2 Reduction	-0.02024	-0.02453 to -0.01596	Yes	****	<0.0001
100 mA/cm^{2}Oxidation vs. 100 mA/cm^2 Reduction	-0.0195	-0.02376 to -0.01524	Yes	****	<0.0001
50 mA/cm^2 Undivided vs. TOC - 50 mA/cm^2 Undivided	-0.00168	-0.007225 to 0.003875	No	ns	0.9999

Table B.5 ANOVA results comparing the degradation of GenX at different charge densities in a divided cell

Tukey's multiple comparisons test	Mean Diff.	95.00% CI of diff.	Below threshold?	Summary	Adjusted P Value
100 mA/cm^{2}Oxidation vs. 100 mA/cm^{2}Reduction	-0.01216	-0.06770 to 0.04338	No	ns	0.9978
100 mA/cm^{2}Oxidation vs. 50 mA/cm^{2}Oxidation	0.0786	0.02494 to 0.1323	Yes	***	0.0003
100 mA/cm^{2}Oxidation vs. 50 mA/cm^{2}Reduction	-0.0029	-0.05656 to 0.05076	No	ns	>0.9999
100 mA/cm^{2}Oxidation vs. 20 mA/cm^{2}Oxidation	0.1056	0.04767 to 0.1635	Yes	****	<0.0001
100 mA/cm^{2}Oxidation vs. 20 mA/cm^{2}Reduction	0.0185	-0.03943 to 0.07643	No	ns	0.9779
100 mA/cm^{2}Oxidation vs. 13.5 mA/cm^{2}Oxidation	0.0462	-0.01544 to 0.1078	No	ns	0.3049
100 mA/cm^{2}Oxidation vs. 13.5 mA/cm^{2}Reduction	0.0532	-0.008443 to 0.1148	No	ns	0.1483
100 mA/cm^{2}Reduction vs. 50 mA/cm^{2}Oxidation	0.09076	0.03478 to 0.1467	Yes	****	<0.0001
100 mA/cm^{2}Reduction vs. 50 mA/cm^{2}Reduction	0.00926	-0.04672 to 0.06524	No	ns	0.9996
100 mA/cm^{2}Reduction vs. 20 mA/cm^{2}Oxidation	0.1178	0.05767 to 0.1779	Yes	****	<0.0001

100 mA/cm^{2}Reduction vs. 20 mA/cm^{2}Reduction	0.03066	-0.02943 to 0.09075	No	ns	0.7765
100 mA/cm^{2}Reduction vs. 13.5 mA/cm^{2}Oxidation	0.05836	-0.005316 to 0.1220	No	ns	0.0996
100 mA/cm^{2}Reduction vs. 13.5 mA/cm^{2}Reduction	0.06536	0.001684 to 0.1290	Yes	*	0.0395
50 mA/cm^{2}Oxidation vs. 50 mA/cm^{2}Reduction	-0.0815	-0.1356 to -0.02738	Yes	***	0.0002
50 mA/cm^{2}Oxidation vs. 20 mA/cm^{2}Oxidation	0.027	-0.03136 to 0.08536	No	ns	0.8522
50 mA/cm^{2}Oxidation vs. 20 mA/cm^{2}Reduction	-0.0601	-0.1185 to -0.001741	Yes	*	0.0383
50 mA/cm^{2}Oxidation vs. 13.5 mA/cm^{2}Oxidation	-0.0324	-0.09444 to 0.02964	No	ns	0.7551
50 mA/cm^{2}Oxidation vs. 13.5 mA/cm^{2}Reduction	-0.0254	-0.08744 to 0.03664	No	ns	0.9168
50 mA/cm^{2}Reduction vs. 20 mA/cm^{2}Oxidation	0.1085	0.05014 to 0.1669	Yes	****	<0.0001
50 mA/cm^{2}Reduction vs. 20 mA/cm^{2}Reduction	0.0214	-0.03696 to 0.07976	No	ns	0.9527
50 mA/cm^{2}Reduction vs. 13.5 mA/cm^{2}Oxidation	0.0491	-0.01294 to 0.1111	No	ns	0.2384
50 mA/cm^{2}Reduction	0.0561	-0.005945 to 0.1181	No	ns	0.1096

vs. 13.5 mA/cm^{2}Reduction					
20 mA/cm^{2}Oxidation vs. 20 mA/cm^{2}Reduction	-0.0871	-0.1494 to -0.02479	Yes	***	0.0007
20 mA/cm^{2}Oxidation vs. 13.5 mA/cm^{2}Oxidation	-0.0594	-0.1252 to 0.006375	No	ns	0.1105
20 mA/cm^{2}Oxidation vs. 13.5 mA/cm^{2}Reduction	-0.0524	-0.1182 to 0.01338	No	ns	0.2307
20 mA/cm^{2}Reduction vs. 13.5 mA/cm^{2}Oxidation	0.0277	-0.03808 to 0.09348	No	ns	0.9045
20 mA/cm^{2}Reduction vs. 13.5 mA/cm^{2}Reduction	0.0347	-0.03108 to 0.1005	No	ns	0.7452
13.5 mA/cm^{2}Oxidation vs. 13.5 mA/cm^{2}Reduction	0.007	-0.06207 to 0.07607	No	ns	>0.9999

Table B.6 ANOVA results comparing the overall degradation of GenX at different current densities in an undivided and divided cell

Tukey's multiple comparisons test	**Mean Diff.**	**95.00% CI of diff.**	**Below threshold?**	**Summary**	**Adjusted P Value**
20 mA/cm^2 Divided vs. 20 mA/cm^2 Undivided	0.000207	-0.005189 to 0.005603	No	ns	0.9996
20 mA/cm^2 Divided vs. 50 mA/cm^2 Divided	0.005904	0.0005747 to 0.01123	Yes	*	0.0236

20 mA/cm^2 Divided vs. 50 mA/cm^2 Undivided	0.005404	7.947e-006 to 0.01080	Yes	*	0.0495
20 mA/cm^2 Undivided vs. 50 mA/cm^2 Divided	0.005697	0.0006910 to 0.01070	Yes	*	0.0189
20 mA/cm^2 Undivided vs. 50 mA/cm^2 Undivided	0.005197	0.0001200 to 0.01027	Yes	*	0.0427
50 mA/cm^2 Divided vs. 50 mA/cm^2 Undivided	-0.0005	-0.005506 to 0.004506	No	ns	0.9938

Table B.7 ANOVA results comparing the overall degradation of GenX in an undivided and divided cell at 13.5 mA/cm^2 using different cathodes

Tukey's multiple comparisons test	**Mean Diff.**	**95.00% CI of diff.**	**Below threshold?**	**Summary**	**Adjusted P Value**
Ti (Divided) vs. Cu (Divided)	0.000608	-0.001038 to 0.002254	No	ns	0.8774
Ti (Divided) vs. Au (Divided)	0.00004	-0.001606 to 0.001686	No	ns	>0.9999
Ti (Divided) vs. Ti (Undivided)	0.00049	-0.001062 to 0.002042	No	ns	0.9329
Ti (Divided) vs. Cu (Undivided)	0.000776	-0.0007756 to 0.002328	No	ns	0.6705
Ti (Divided) vs. Au (Undivided)	-0.00056	-0.002116 to 0.0009870	No	ns	0.8841
Cu (Divided) vs. Au (Divided)	-0.00057	-0.002214 to 0.001078	No	ns	0.905
Cu (Divided) vs. Ti (Undivided)	-0.00012	-0.001670 to 0.001434	No	ns	>0.9999
Cu (Divided) vs. Cu (Undivided)	0.000168	-0.001384 to 0.001720	No	ns	0.9995
Cu (Divided) vs. Au (Undivided)	-0.00117	-0.002724 to 0.0003790	No	ns	0.2349

Au (Divided) vs. Ti (Undivided)	0.00045	-0.001102 to 0.002002	No	ns	0.9525
Au (Divided) vs. Cu (Undivided)	0.000736	-0.0008156 to 0.002288	No	ns	0.7173
Au (Divided) vs. Au (Undivided)	-0.0006	-0.002156 to 0.0009470	No	ns	0.8514
Ti (Undivided) vs. Cu (Undivided)	0.000286	-0.001165 to 0.001737	No	ns	0.9913
Ti (Undivided) vs. Au (Undivided)	-0.00106	-0.002506 to 0.0003968	No	ns	0.2735
Cu (Undivided) vs. Au (Undivided)	-0.00134	-0.002792 to 0.0001108	No	ns	0.085

Table B.8 ANOVA results comparing the cell potential in a divided cell at 13.5 mA/cm^2 using different cathodes

Tukey's multiple comparisons test	**Mean Diff.**	**95.00% CI of diff.**	**Below threshold?**	**Summary**	**Adjusted P Value**
BDD(Ti) vs. Ti	-0.00692	-0.01121 to -0.002629	Yes	***	0.0001
BDD(Ti) vs. BDD (Cu)	-0.00071	-0.005006 to 0.003578	No	ns	0.9967
BDD(Ti) vs. Cu	-0.00804	-0.01233 to -0.003744	Yes	****	<0.0001
BDD(Ti) vs. BDD (Au)	-0.00022	-0.004512 to 0.004072	No	ns	>0.9999
BDD(Ti) vs. Au	-0.00693	-0.01085 to -0.003015	Yes	****	<0.0001
Ti vs. BDD(Cu)	0.006207	0.001915 to 0.01050	Yes	***	0.0008
Ti vs. Cu	-0.00112	-0.005407 to 0.003177	No	ns	0.9745
Ti vs. BDD(Au)	0.006701	0.002409 to 0.01099	Yes	***	0.0002

Ti vs. Au	-1.2E-05	-0.003930 to 0.003906	No	ns	>0.9999
BDD(Cu) vs. Cu	-0.00732	-0.01161 to -0.003030	Yes	****	<0.0001
BDD(Cu) vs. BDD(Au)	0.000494	-0.003798 to 0.004786	No	ns	0.9994
BDD(Cu) vs. Au	-0.00622	-0.01014 to -0.002301	Yes	***	0.0002
Cu vs. BDD(Au)	0.007816	0.003524 to 0.01211	Yes	****	<0.0001
Cu vs. Au	0.001103	-0.002815 to 0.005021	No	ns	0.9639
BDD(Au) vs. Au	-0.00671	-0.01063 to -0.002795	Yes	****	<0.0001

Table B.9 ANOVA results comparing the performance of GenX degradation in wastewater to the laboratory electrolyte at 13.5 mA/cm^2

Tukey's multiple comparisons test	Mean Diff.	95.00% CI of diff.	Below threshold?	Summary	Adjusted P Value
Control vs. Milli-Q	0.00288	0.0008823 to 0.004878	Yes	**	0.0028
Control vs. Wastewater	0.003054	0.001056 to 0.005052	Yes	**	0.0015
Milli-Q vs. Wastewater	0.000174	-0.001239 to 0.001587	No	ns	0.9529

Table B.10 ANOVA results comparing the performance of GenX degradation in wastewater to the laboratory electrolyte at 20 mA/cm^2

Tukey's multiple comparisons test	Mean Diff.	95.00% CI of diff.	Below threshold?	Summary	Adjusted P Value
Control vs. Milli-Q	0.000829	-0.001414 to 0.003072	No	ns	0.6477
Control vs. Wastewater	0.00351	0.001395 to 0.005625	Yes	***	0.0006
Milli-Q vs. Wastewater	0.002681	0.001009 to 0.004353	Yes	***	0.0009

Table B.11 ANOVA results comparing the performance of GenX degradation in different water matrices at 50 mA/cm^2

Tukey's multiple comparisons test	Mean Diff.	95.00% CI of diff.	Below threshold?	Summary	Adjusted P Value
Control vs. Milli-Q	0.00554	1.595e-005 to 0.01106	Yes	*	0.049
Control vs. Wastewater	0.007284	0.002076 to 0.01249	Yes	**	0.0017
Control vs. Surface Water	0.01056	0.005352 to 0.01577	Yes	****	<0.0001
Control vs. Drinking Water	0.01003	0.004822 to 0.01524	Yes	****	<0.0001
Milli-Q vs. Wastewater	0.001744	-0.002373 to 0.005861	No	ns	0.7649
Milli-Q vs. Surface Water	0.00502	0.0009026 to 0.009137	Yes	**	0.0087
Milli-Q vs. Drinking Water	0.00449	0.0003726 to 0.008607	Yes	*	0.0253
Wastewater vs. Surface Water	0.003276	-0.0004067 to 0.006959	No	ns	0.1056
Wastewater vs. Drinking Water	0.002746	-0.0009367 to 0.006429	No	ns	0.2409
Surface Water vs. Drinking Water	-0.00053	-0.004213 to 0.003153	No	ns	0.9945

Table B.12 ANOVA results comparing the performance of GenX degradation in electrolytes at 50 mA/cm^2

Tukey's multiple comparisons test	Mean Diff.	95.00% CI of diff.	Below threshold?	Summary	Adjusted P Value
Both Oxidation vs. Both Reduction	-0.02024	-0.02631 to -0.01418	Yes	****	<0.0001
Both Oxidation vs. 0.22 M $NaSO_4$ Oxidation	0.01177	0.005226 to 0.01831	Yes	****	<0.0001
Both Oxidation vs. 0.22 M Na_2SO_4 Reduction	-0.02119	-0.02773 to -0.01464	Yes	****	<0.0001
Both Oxidation vs. 0.22 M NaCl Oxidation	0.01048	0.003936 to 0.01702	Yes	****	<0.0001
Both Oxidation vs. 0.22 M NaCl Reduction	-0.02345	-0.02999 to -0.01690	Yes	****	<0.0001

Both Oxidation vs. 0.10 M Na_2SO_4 Oxidation	0.00225	-0.004294 to 0.008794	No	ns	0.9847
Both Oxidation vs. 0.10 M Na_2SO_4 Reduction	-0.02188	-0.02842 to -0.01533	Yes	****	<0.0001
Both Oxidation vs. 0.12 M NaCl Oxidation	-0.00902	-0.01556 to -0.002476	Yes	***	0.0007
Both Oxidation vs. 0.12 M NaCl Reduction	-0.02324	-0.02978 to -0.01669	Yes	****	<0.0001
Both Reduction vs. 0.22 M Na_2SO_4 Oxidation	0.03201	0.02551 to 0.03852	Yes	****	<0.0001
Both Reduction vs. 0.22 M Na_2SO_4 Reduction	-0.00095	-0.007450 to 0.005560	No	ns	>0.9999
Both Reduction vs. 0.22 M NaCl Oxidation	0.03072	0.02422 to 0.03723	Yes	****	<0.0001
Both Reduction vs. 0.22 M NaCl Reduction	-0.00321	-0.009710 to 0.003300	No	ns	0.8607
Both Reduction vs. 0.10 M Na_2SO_4 Oxidation	0.02249	0.01599 to 0.02900	Yes	****	<0.0001
Both Reduction vs. 0.10 M Na_2SO_4 Reduction	-0.00164	-0.008142 to 0.004868	No	ns	0.9985
Both Reduction vs. 0.12 M NaCl Oxidation	0.01122	0.004717 to 0.01773	Yes	****	<0.0001
Both Reduction vs. 0.12 M NaCl Reduction	-0.00299	-0.009499 to 0.003511	No	ns	0.9035
0.22 M Na_2SO_4 Oxidation vs. 0.22 M Na_2SO_4 Reduction	-0.03296	-0.03991 to -0.02600	Yes	****	<0.0001
0.22 M Na_2SO_4 Oxidation vs. 0.22 M NaCl Oxidation	-0.00129	-0.008244 to 0.005664	No	ns	0.9999
0.22 M Na_2SO_4 Oxidation vs. 0.22 M NaCl Reduction	-0.03522	-0.04217 to -0.02826	Yes	****	<0.0001

0.22 M Na_2SO_4 Oxidation vs. 0.10 M Na_2SO_4 Oxidation	-0.00952	-0.01647 to -0.002566	Yes	***	0.0007
0.22 M Na_2SO_4 Oxidation vs. 0.10 M Na_2SO_4 Reduction	-0.03365	-0.04060 to -0.02670	Yes	****	<0.0001
0.22 M Na_2SO_4 Oxidation vs. 0.12 M NaCl Oxidation	-0.02079	-0.02774 to -0.01384	Yes	****	<0.0001
0.22 M Na_2SO_4 Oxidation vs. 0.12 M NaCl Reduction	-0.03501	-0.04196 to -0.02805	Yes	****	<0.0001
0.22 M Na_2SO_4 Reduction vs. 0.22 M NaCl Oxidation	0.03167	0.02471 to 0.03862	Yes	****	<0.0001
0.22 M Na_2SO_4 Reduction vs. 0.22 M NaCl Reduction	-0.00226	-0.009214 to 0.004694	No	ns	0.9897
0.22 M Na_2SO_4 Reduction vs. 0.10 M Na_2SO_4 Oxidation	0.02344	0.01648 to 0.03039	Yes	****	<0.0001
0.22 M Na_2SO_4 Reduction vs. 0.10 M Na_2SO_4 Reduction	-0.00069	-0.007646 to 0.006262	No	ns	>0.9999
0.22 M Na_2SO_4 Reduction vs. 0.12 M NaCl Oxidation	0.01217	0.005213 to 0.01912	Yes	****	<0.0001
0.22 M Na_2SO_4 Reduction vs. 0.12 M NaCl Reduction	-0.00205	-0.009003 to 0.004905	No	ns	0.995
0.22 M NaCl Oxidation vs. 0.22 M NaCl Reduction	-0.03393	-0.04088 to -0.02697	Yes	****	<0.0001
0.22 M NaCl Oxidation vs. 0.10 M Na_2SO_4 Oxidation	-0.00823	-0.01518 to -0.001276	Yes	**	0.0074
0.22 M NaCl Oxidation vs. 0.10 M Na_2SO_4 Reduction	-0.03236	-0.03931 to -0.02541	Yes	****	<0.0001
0.22 M NaCl Oxidation vs. 0.12 M NaCl Oxidation	-0.0195	-0.02645 to -0.01255	Yes	****	<0.0001
0.22 M NaCl Oxidation vs. 0.12 M NaCl Reduction	-0.03372	-0.04067 to -0.02676	Yes	****	<0.0001

0.22 M NaCl Reduction vs. 0.10 M Na_2SO_4 Oxidation	0.0257	0.01874 to 0.03265	Yes	****	<0.0001
0.22 M NaCl Reduction vs. 0.10 M Na_2SO_4 Reduction	0.001568	-0.005386 to 0.008522	No	ns	0.9994
0.22 M NaCl Reduction vs. 0.12 M NaCl Oxidation	0.01443	0.007473 to 0.02138	Yes	****	<0.0001
0.22 M NaCl Reduction vs. 0.12 M NaCl Reduction	0.000211	-0.006743 to 0.007165	No	ns	>0.9999
0.10 M Na_2SO_4 Oxidation vs. 0.10 M Na_2SO_4 Reduction	-0.02413	-0.03108 to -0.01718	Yes	****	<0.0001
0.10 M Na_2SO_4 Oxidation vs. 0.12 M NaCl Oxidation	-0.01127	-0.01822 to -0.004316	Yes	****	<0.0001
0.10 M Na_2SO_4 Oxidation vs. 0.12 M NaCl Reduction	-0.02549	-0.03244 to -0.01853	Yes	****	<0.0001
0.10 M Na_2SO_4 Reduction vs. 0.12 M NaCl Oxidation	0.01286	0.005905 to 0.01981	Yes	****	<0.0001
0.10 M Na_2SO_4 Reduction vs. 0.12 M NaCl Reduction	-0.00136	-0.008311 to 0.005597	No	ns	0.9998
0.12 M NaCl Oxidation vs. 0.12 M NaCl Reduction	-0.01422	-0.02117 to -0.007262	Yes	****	<0.0001

Table B.13 ANOVA results comparing the performance of GenX electrocoagulation on different electrodes at 10 mA/cm^2

Tukey's multiple comparisons test	**Mean Diff.**	**95.00% CI of diff.**	**Below threshold?**	**Summary**	**Adjusted P Value**
Al vs. Fe	-0.00125	-0.004929 to 0.002439	No	ns	0.6945
Al vs. Zn	0.006099	0.002467 to 0.009731	Yes	***	0.0005
Fe vs. Zn	0.007344	0.003712 to 0.01098	Yes	****	<0.0001

Appendix C Additional Publication Not Related to Thesis

Electrochemical oxidation of the increasingly-used disinfectant benzalkonium chloride

Kara Hughes*, Weiqi Han, Viviane Yargeau, Sasha Omanovic

Department of Chemical Engineering, McGill University
Montreal, Quebec, Canada

*Corresponding author: kara.hughes2@mail.mcgill.ca

Abstract

Benzalkonium chloride (BAC) is a key ingredient in many cleaning and disinfectant products due to it being an effective antiviral and biocidal agent. Because of its prolific use, especially following the recent global COVID pandemic, increased levels of BAC have been found in the environment, in particular wastewater, where it has negative impacts due to its toxicity. This necessitates an effective treatment for BAC in wastewater to reduce its toxicity. In this work, electrochemical oxidation of BAC on a boron doped diamond anode was studied to successfully remove BAC. The electrochemical measurements performed at different current densities confirmed that BAC was completely oxidized within 20 mins of treatment at 50 mA/cm^2. However, chemical oxygen demand (COD) measurements showed that around 50% of the initial BAC was completely mineralized after one hour of degradation at 50 mA/cm^2, while the remaining electrooxidation of BAC resulted in the production of transformation products.

Keywords: benzalkonium chloride, electrochemical degradation, water treatment

1 INTRODUCTION

Benzalkonium chloride (BAC), also known as alkyl dimethyl benzyl ammonium chloride, is a mixture of alkylbenzyl dimethylammonium chlorides with different even-numbered alkyl chain lengths, ranging from C8 to C18, Figure 1.[[91], [92]]

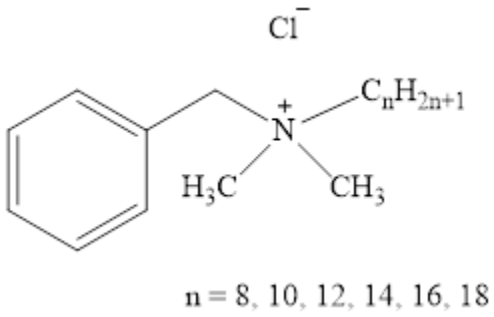

FIGURE 1 Schematic of BAC Molecule

BAC is a quaternary ammonium compound (QAC) which is primarily used as an active ingredient in disinfectants and as a biocide in agricultural, industrial, clinical and domestic areas due to its antimicrobial activity.[[91]] In addition, due to its antiviral properties, some common applications include hand sanitizer and disinfectants such as Lysol® and Dettol spray and wipes.[[93], [94]] In recent years, the fear of COVID-19 spread has led to more frequent use of disinfectants in public facilities, hospitals, and even private households. This has resulted in increased direct exposure of humans to BAC and increased presence in the environment, in particular through the discharge of wastewater.[[95]]

BACs are classified by the Environmental Protection Agency (EPA) in the toxicity category II based on the oral and inhalation routes, and toxicity category III *via* the dermal route.[[96]] In addition, in a 2006 report, the EPA recommended not to release BAC into water bodies, such as rivers, lakes and oceans, due to the toxicity of BAC to the aquatic ecosystem.[[97]] Despite that, BAC has been commonly detected in the wastewater influent, surface water and groundwater. Once BAC enters the environment, it can invoke antimicrobial resistance and can be lethal to aquatic organisms such as fish, oyster, shrimp and invertebrates.[[98]] A study of European hospital wastewaters demonstrates that the concentration of BAC in the hospitals' effluent is proportional to the use of BAC. Considering that wastewater

treatment plants have not been designed to remove BAC, the treatment train might not be sufficient to prevent the release of BAC through the disposal of biosolids or the discharge of treated wastewater in receiving streams. BAC has slow degradation kinetics in the solid phase and it is highly adsorptive, which means that if specific treatment measures are not present in the wastewater treatment sequence, it is likely that BAC can remain in the effluent or in biosolids, the latter of which can lead to leaching and groundwater contamination if landfilled.[98] Additionally, the presence of other disinfectants in the wastewater can lower the effect of bacterial degradation of BAC.[99] Therefore it is important that effective treatment be employed to degrade BAC.

Limited work has been done on the targeted removal of BAC during wastewater treatment. One method reported in literature is based on the use of *Pseudomonas* strains to biodegrade BAC in wastewater containing a high BAC concentration.[98], [100] One indigenous *Pseudomonas* isolated from Punta Lara was capable to degrade 100 mg/L of BAC in 10 h.[100] It was found that *Pseudomonas nitroreducens* encoded at least one key enzyme responsible for BAC dealkylation[101] and can also biodegrade BAC under aerobic batch-fed conditions. In addition to *Pseudomonas*, *Achromobacter sp.* is another effective alternative to biodegrade BAC.[102]

In addition to biodegradation, there are other methods of BAC treatment and removal that have been studied. Adsorptive removal of BAC was studied on granular active carbon (GAC) and Amberlite XAD-16 by Tanada et al.[99] and Turku et al.,[103] respectively. They were able to completely remove the BAC from the water stream and, in the case of the Amberlite XAD-16, using aqueous ethanol as a desorbent improved the regeneration of the sorption material. However these methods involve disposing of the contaminated adsorbent material and are limited to the transfer of the contaminant from one phase to another.[103] Some advanced oxidation processes, such as persulphate oxidation and the Fenton process, have been reported for BAC degradation.[104], [105] For persulphate oxidation, over 90% BAC was degraded after an hour, and an increase in the biodegradability of the degradation products being reported by Hong et al. Effective degradation (>80%) using the Fenton process was also reported by Zhang et al. Other processes such as ozonation and heterogenous photocatalysis have been investigated as pre-treatments for biological degradation, with both Carbajo et al, 2016 and López et al, 2012,

presenting complete BAC removal but with limited mineralisation.[106], [107] However, López et al, reported that below 100 mg/L the heterogenous photocatalysis was not working properly and Carbajo et al reported that the addition of ozone increased the toxicity of the final treated wastewater.

Electrochemical treatment, such as electrooxidation, is considered a potentially viable wastewater treatment option due to its mild conditions, lack of waste generation, efficiency, modularity and possibility to degrade very toxic and biorefractory compounds.[108] However, very little research has been done on BAC electrochemical degradation. The only study available in literature using electrodegradation focussed on using electrocoagulation-electrooxidation to mitigate BAC-C10 in model groundwaters and surface waters.[109] However, so far, no research has been reported in the scientific literature on degrading BAC solely by electrooxidation. Consequently, here we report our findings on the electrochemical oxidation of BAC in a batch electrochemical reactor employing a boron-doped diamond (BDD) anode. We demonstrate that BAC can be efficiently oxidized in a short time, employing the said system. However, more research is needed in order to optimize the BAC electrooxidation conditions and investigate transformation products, which is an ongoing effort in our laboratory and will be reported in a separate manuscript.

2 METHODOLOGY

Benzalkonium chloride (purity ≥ 95.0%) and anhydrous sodium thiosulphate (purity ≥ 98.0%) were procured from Sigma Aldrich, and anhydrous sodium sulphate (purity 99+%) was obtained from Acros Organics. All solutions were made using MilliQ water (resistivity of 18.2 MΩ cm).

The electrolyte used for the degradation experiments was 100 mg/L BAC + 0.5 M Na_2SO_4. The electrochemical batch cell consisted of a vessel that housed a BDD anode (20 cm^2 exposed to the electrolyte) and a 316 L stainless steel cathode (50 cm^2 exposed to the electrolyte). 150 mL of the electrolyte was used, and the electrodes were positioned 1 cm apart from each other. The current was provided by B&K Precision 1760A Power Supply. During the experiment, the electrolyte was mixed using a magnetic stirrer at 300 rpm. All the experiments were conducted at 22±1°C, and at current densities of 10, 20 and 50 mA/cm^2 (with respect to the BDD anode surface area).

1 mL of the electrolyte containing BAC was collected from the cell at specific time points (over 2 hrs of degradation) to monitor the kinetics of BAC oxidation. Upon collection, 2 µL of 250 µg/L $Na_2S_2O_3$ was added to quench OH radicals that could be present in solution, and prevent further degradation of BAC. The samples were diluted with 0.5 M Na_2SO_4 and analyzed by UV-visible spectroscopy (Thermo Scientific Evolution 220 UV-Visible Spectrophotometer). Chemical oxygen demand (COD) measurements were made using a standard method provided by CHEMetrics using a Hach DRB 200 COD Reactor and Hach DREL/2400 Spectrophotometer with LR COD vials from CHEMetrics.

3 RESULT AND DISCUSSION

Figure 2a shows the BAC degradation curves recorded at various current densities. The results demonstrate that BAC can completely be oxidized relatively quickly under the experimental conditions employed. While at 10 mA/cm^2 it took close to 90 minutes to decrease

the BAC concentration in the reactor to the point where it was undetectable by UV-vis spectroscopy, by increasing the degradation current density to 50 mA/cm^2 the degradation time decreased to 20 minutes. Assuming BAC is oxidized predominantly by hydroxyl radicals generated at the BDD electrode surface, this increase in the degradation rate is due to the increased production of hydroxyl radicals at the BDD electrode surface at higher currents.[[110]]

However, an increase in current applied to the cell might not necessarily lead to the proportional increase in BAC degradation kinetics because oxygen evolution occurs in parallel with the BAC oxidation. This affects the faradaic efficiency for oxidation of the targeted molecule (BAC). Namely, in most cases of electrochemical degradation of organic molecules, the fraction of current for the unwanted oxygen evolution reaction increases with current density, which results in a decrease in faradaic efficiency for the oxidation of the targeted organic molecules. To check if this is the case for the BAC degradation, the data in Figure 2a s presented in Figure 2b as a function of charge passed through the electrochemical cell. As evidenced, all three degradation curves are close one to each other, confirming that the faradaic efficiency for BAC degradation remains the same under the experimental conditions employed. This is of practical importance since, referring to Figure 2a, it would be beneficial to work at higher current densities to shorten the time of BAC degradation.

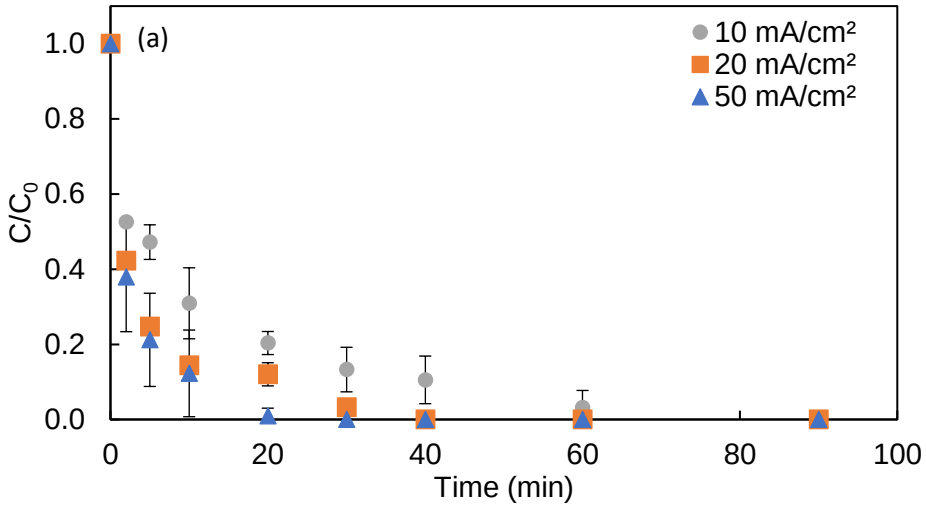
(a)
10 mA/cm²
20 mA/cm²
50 mA/cm²
C/C0
1.0
0.8
0.6
0.4
0.2
0.0
0
20
40
60
80
100
Time (min)

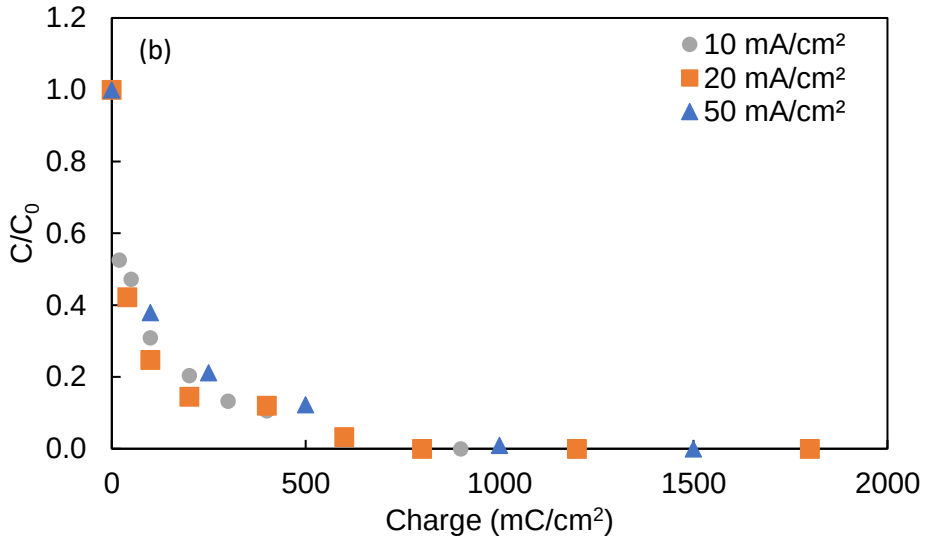
(b)
10 mA/cm²
20 mA/cm²
50 mA/cm²
C/C0
1.2
1.0
0.8
0.6
0.4
0.2
0.0
0
500
1000
1500
2000
Charge (mC/cm²)

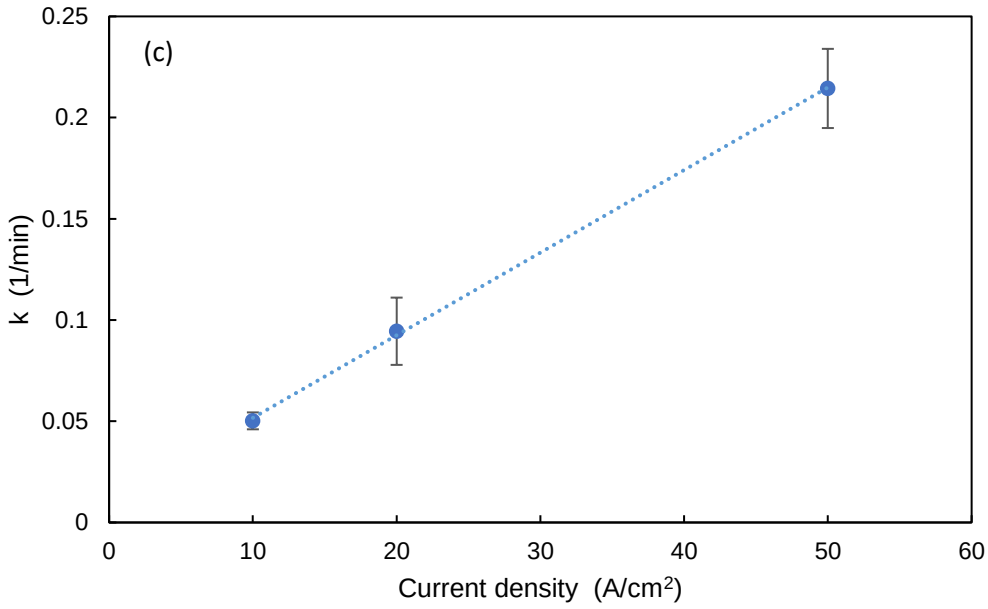

FIGURE 2 (a) Dependence of normalized BAC concentration on time recorded during the treatment at various current densities. (b) The data from plot (a) presented as a function of charge passed through the electrochemical cell. (c) Dependence of the apparent reaction rate constant for degradation of BAC at different current densities calculated from the data in plot (a). Error bars: standard deviation of 3 replicates.

A pseudo-first-order kinetic model was employed to analyze the data in Figure 2a (the R^2 values for the 10, 20 and 50 mA/cm^2 data are 0.960, 0.890 and 0.976, respectively), and the corresponding apparent rate constants are presented in Figure 2c. With an increase in current density, the apparent rate constant increases, which is to be expected since current represents a reaction rate of an electrochemical reaction. However, this increase is linear, which agrees with the conclusions obtained from the data presented in Figure 2b. Namely, since the fraction of current used to degrade BAC (vs. that one for oxygen evolution) does not change within the current density range investigated, the increase in current leads to the proportional (linear) increase in the BAC degradation apparent rate constant.

Figure 2a the removal of BAC degradation over time, but it does not provide information on the extent of BAC mineralization. BAC is a complex organic molecule (Figure 1) and it is unlikely that it can completely be degraded under the conditions tested. To estimate the degree of

mineralization of BAC during the two-hour treatment time, chemical oxygen demand (COD) measurements were performed for the experiment conducted at the highest current density tested, 50 mA/cm^2, corresponding to the highest removal level. The results presented in Figure 3 show that although BAC completely disappeared after only ca. 20 minutes of treatment (right axis), the COD data (left axis) evidence that BAC was not completely mineralized even after two hours of treatment. Taking into account that the COD of the background electrolyte was 8 mg/L, Figure 3 demonstrates that about 50% of the initial BAC was completely mineralized after 2 hours, and the residual COD can be associated with the formation of transformation products of BAC.

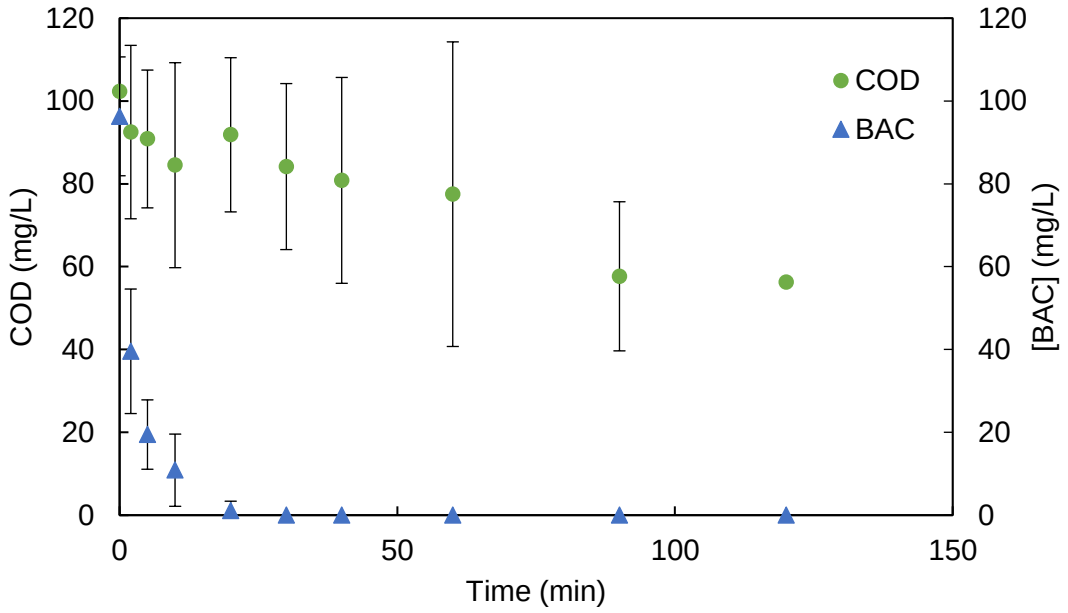

FIGURE 3 Variation of COD (left axis, circles) and BAC concentration (right axis, triangles) as a function of time during the electrochemical treatment of BAC at 50 mA/cm^2. Error bars: standard deviation of 3 replicates.

4 CONCLUSION AND RECOMMENDATIONS

Due to the prevalence of the chemical as an active ingredient in many disinfectants and its environmental toxicity, it is important that an effective treatment be implemented for wastewater that may be contaminated with BAC. The results of the present study demonstrate that electrooxidation is a promising treatment method to successfully degrade benzalkonium chloride.

Further studies on the degradation of BAC to expand the investigation to other electrodes than BDD (eg. dimensionally stable anodes / mixed metal oxide electrodes) in order to lower the cost of the treatment, are recommended. Considering the low level of mineralization, it is also recommended to investigate the degradation pathway to better understand and optimise the process, especially at more environmentally relevant concentrations.

Acknowledgement

Grateful acknowledgment is made to the McGill University through the McGill Engineering Doctoral Award (MEDA) program, and to the Natural Sciences and Engineering Research Council of Canada (NSERC).

5 REFERENCES

(1) Merchel Piovesan Pereira, B.; Tagkopoulos, I. Benzalkonium Chlorides: Uses, Regulatory Status, and Microbial Resistance. *Appl. Environ. Microbiol.* **2019**, *85* (13), 1–13.

(2) EU Reference Laboratories for Residues of Pesticides. Analysis of Quaternary Ammonium Compounds (QACs) in Fruits and Vegetables Using QuEChERS and LC-MS/MS. 2016, pp 1–6. http://www.eurl-pesticides.eu/userfiles/file/EurlSRM/EurlSRM_meth_QAC_ShortMethod.pdf.

(3) Editorial Team. *Active Ingredients of Lysol*. Homes Pursuit. https://homespursuit.com/active-ingredients-of-lysol/ (accessed 2022-06-01).

(4) Dettol. *Dettol Disinfectant Liquid Menthol Cool*. Reckitt Benckiser. https://www.dettol.co.in/household-disinfection/disinfectant-liquid/dettol-disinfectant-liquid-menthol-cool-500ml/ (accessed 2022-06-01).

(5) Dewey, H. M.; Jones, J. M.; Keating, M. R.; Budhathoki-Uprety, J. Increased Use of Disinfectants During the COVID-19 Pandemic and Its Potential Impacts on Health and Safety. *ACS Chem. Heal. Saf.* **2022**, *29* (1), 27–38. https://doi.org/10.1021/acs.chas.1c00026.

(6) US EPA. *Reregistration Eligibility Decision for Alkyl Dimethyl Benzyl Ammonium Chloride (ADBAC)*; Washington D.C., 2006.

(7) Pereira, B. M. P.; Tagkopoulos, I. Benzalkonium Chlorides: Uses, Regulatory Status, and Microbial Resistance. *Appl. Environ. Microbiol.* **2019**, *85* (13), 1–13. https://doi.org/10.1128/AEM.00377-19.

(8) Barber, O. W.; Hartmann, E. M. Benzalkonium Chloride: A Systematic Review of Its Environmental Entry through Wastewater Treatment, Potential Impact, and Mitigation Strategies. *https://doi.org/10.1080/10643389.2021.1889284* **2021**, 1–30. https://doi.org/10.1080/10643389.2021.1889284.

(9) Tanada, M.; Miyoshi, T.; Nakamura, T.; Tanada, S. Adsorption Removal of Benzalkonium Chloride by Granular Activated Carbon for Medical Waste Water Treatment. *Asia-Pacific J. Public Heal.* **1991**, *5* (1).

(10) Fortunato, M. S.; Baroni, S.; González, A. J.; Álvarez Roncancio, J. D.; Papalia, M.;

Martinefsky, M.; Trípodi, V.; Planes, E.; Gallego, A.; Korol, S. E. Biodegradability of Disinfectants in Surface Waters from Buenos Aires: Isolation of an Indigenous Strain Able to Degrade and Detoxify Benzalkonium Chloride. *Water. Air. Soil Pollut.* **2018**, *229* (4), 1–14. https://doi.org/10.1007/S11270-018-3780-7/TABLES/2.

(11) Oh, S.; Kurt, Z.; Tsementzi, D.; Weigand, M. R.; Kim, M.; Hatt, J. K.; Tandukar, M.; Pavlostathis, S. G.; Spain, J. C.; Konstantinidis, K. T. Microbial Community Degradation of Widely Used Quaternary Ammonium Disinfectants. *Appl. Environ. Microbiol.* **2014**, *80* (19), 5892–5900. https://doi.org/10.1128/AEM.01255-14.

(12) Ertekin, E.; Hatt, J. K.; Konstantinidis, K. T.; Tezel, U. Similar Microbial Consortia and Genes Are Involved in the Biodegradation of Benzalkonium Chlorides in Different Environments. *Environ. Sci. Technol.* **2016**, *50* (8), 4304–4313. https://doi.org/10.1021/acs.est.5b05959.

(13) Turku, I.; Sainio, T. Modeling of Adsorptive Removal of Benzalkonium Chloride from Water with a Polymeric Adsorbent. *Sep. Purif. Technol.* **2009**, *69* (2), 185–194. https://doi.org/10.1016/j.seppur.2009.07.017.

(14) Hong, J. M.; Xia, Y. F.; Zhang, Q.; Chen, B. Y. Oxidation of Benzalkonium Chloride in Aqueous Solution by S2O82−/Fe2+ Process: Degradation Pathway, and Toxicity Evaluation. *J. Taiwan Inst. Chem. Eng.* **2017**, *78*, 230–239. https://doi.org/10.1016/j.jtice.2017.06.005.

(15) Zhang, Q.; Xia, Y. F.; Hong, J. M. Mechanism and Toxicity Research of Benzalkonium Chloride Oxidation in Aqueous Solution by H2O2/Fe2+ Process. *Environ. Sci. Pollut. Res.* **2016**, *23* (17), 17822–17830. https://doi.org/10.1007/S11356-016-6986-5/FIGURES/6.

(16) Carbajo, J. B.; Petre, A. L.; Rosal, R.; Berná, A.; Letón, P.; García-Calvo, E.; Perdigón-Melón, J. A. Ozonation as Pre-Treatment of Activated Sludge Process of a Wastewater Containing Benzalkonium Chloride and NiO Nanoparticles. *Chem. Eng. J.* **2016**, *283*, 740–749. https://doi.org/10.1016/J.CEJ.2015.08.001.

(17) López Loveira, E.; Fiol, P. S.; Senn, A.; Curutchet, G.; Candal, R.; Litter, M. I. TiO 2-Photocatalytic Treatment Coupled with Biological Systems for the Elimination of Benzalkonium Chloride in Water. *Sep. Purif. Technol.* **2012**, *91*, 108–116.

https://doi.org/10.1016/j.seppur.2011.12.007.

(18) Khan, A. H. Fate of Benzalkonium Chlorides in Natural Environment and Treatment Processes. *Electron. Thesis Diss. Repos.* **2016**, No. December.

(19) Ryan, D. R.; Maher, E. K.; Heffron, J.; Mayer, B. K.; McNamara, P. J. Electrocoagulation-Electrooxidation for Mitigating Trace Organic Compounds in Model Drinking Water Sources. *Chemosphere* **2021**, *273*, 129377. https://doi.org/10.1016/j.chemosphere.2020.129377.

(20) Hmani, E.; Samet, Y.; Abdelhédi, R. Electrochemical Degradation of Auramine-O Dye at Boron-Doped Diamond and Lead Dioxide Electrodes. Diam. Relat. Mater. 2012, 30, 1–8. https://doi.org/10.1016/J.DIAMOND.2012.08.003.